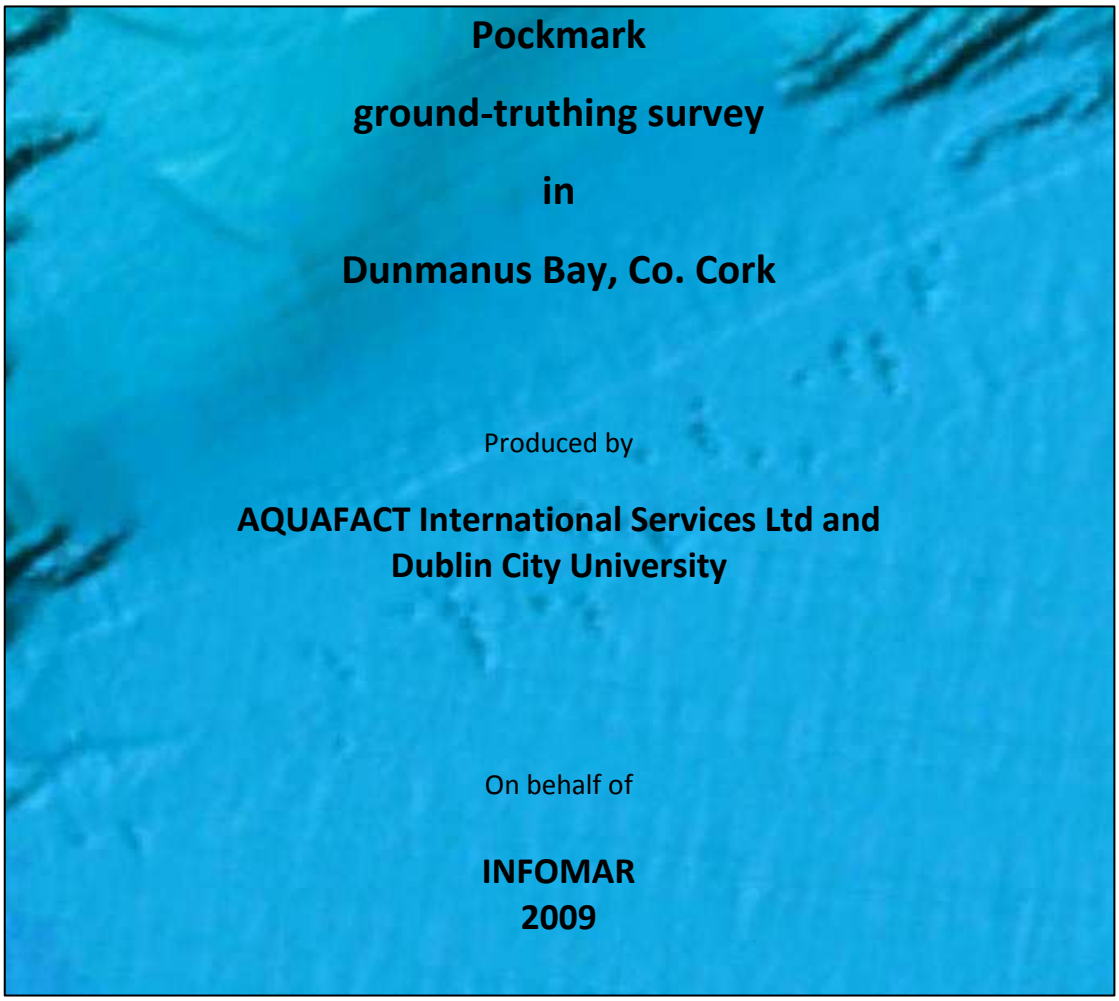

Pockmark ground-truthing survey in Dunmanus Bay, Co. Cork

Produced by

AQUAFACT International Services Ltd and Dublin City University

On behalf of

INFOMAR 2009

Dr Brendan O'Connor,
AQUAFACT INTERNATIONAL SERVICES ltd
12 KILKERRIN park
TUAM rd
GALWAY city
www.aquafact.ie
info@aquafact.ie
tel +353 (0) 91 756812
fax +353 (0) 91 756888

Michal Szpak andBrian Kelleher,
School of Chemical Science,
Dublin City University,
Glasnevein,
Dublin 9.
E-mail: brian.kelleher@dcu.ie
Tel: 01 7005134
Fax: 01 7005133

Table of Contents

List of Appendices

Abstract

AQUAFACT International Services Ltd. and Dublin City University (DCU) were grant aided by INFOMAR to carry out a ground-truthing survey of pockmark areas in Dunmanus Bay, Co. Cork. Ship-time on board the *Celtic Voyager* was also awarded to DCU by the Marine Institute for a survey of Dunmanus Bay from April 22nd to April 28th, 2009. Before the transit to west Cork, mobilisation, testing and training was carried out in Cork Harbour. Gravity cores, box cores and day grabs were recovered from the seabed with video footage from selected sites. In all, over 5 days of 24 hour operations, 132 sampling stations and 12 gravity core stations were covered. The leg ended in demobilisation in Castletownbere. A multidisciplinary approach is now being taken to gain an insight into the nature of the seabed in the area and close to pockmarks and involves geophysical (GSI), biological (Aquafact), geochemical (DCU, TCD and UL) and microbiological (Queens University Belfast) investigations.

Initial results include evidence for a potential source of land-based material at the sea bottom in Dunmanus bay. This is corroborated by unusual gradients in the cores that do not suggest simple diagenetic depth profiles Straight sulphate profiles indicate a high methane flux and that anaerobic oxidation of methane is a dominating process in the deeper sections of the sediment. We are also finding evidence for anaerobic methane oxidation through the presence of a consortia consisting mainly of archaea in the bottom section of cores. Furthermore, different catabolic gene clusters for anaerobic benzoate degradation have been found in the top sections of Dunmanus Bay cores. An abundance of terrestrial lipids, confirmed by stable isotope data, have been found in grab and core smaples. There are also indications of a higher plant input and signals derived from microalgae and phytoplankton. The results of faunal analyses, particle size distribution, combined faunal and sediment analyses show the area sampled in Dunmanus to be quite uniform throughout with no discernable differences between pockmark and non-pockmark areas. However, there appears to be a difference in methane concentrations in bottom water that may be an indication of seepage from the pockmark area. Analysis is continuing, as well as analysis of other pockmark areas in Dublin Bay and the Malin Shelf. The next year will be spent collecting and interpreting data that will allow us to gain a clearer insight into pockmark formation and their role in the cycling of carbon.

1. Introduction

1.1 What are pockmarks?

Pockmarks are a specific type of geological setting resembling craters or pits (Figure 1). These recently discovered geological facies are hard to observe because they are predominantly found in inaccessible aquatic environments on Earth (Judd and Howland, 2007). The pockmarked seafloor is often compared to the lunar surface. According to Schumm (1970) some lunar surface features could have been formed in the same way as terrestrial pockmarks. Similarly, high resolution data obtained from the Mars Global Surveyor satellite revealed pockmark-like features on Mars (Komatsu et al., 2000). Generally, terrestrial pockmarks can be described as shallow depressions usually formed in the soft, fine-grained seafloor surface (Hovland and Judd, 1988).

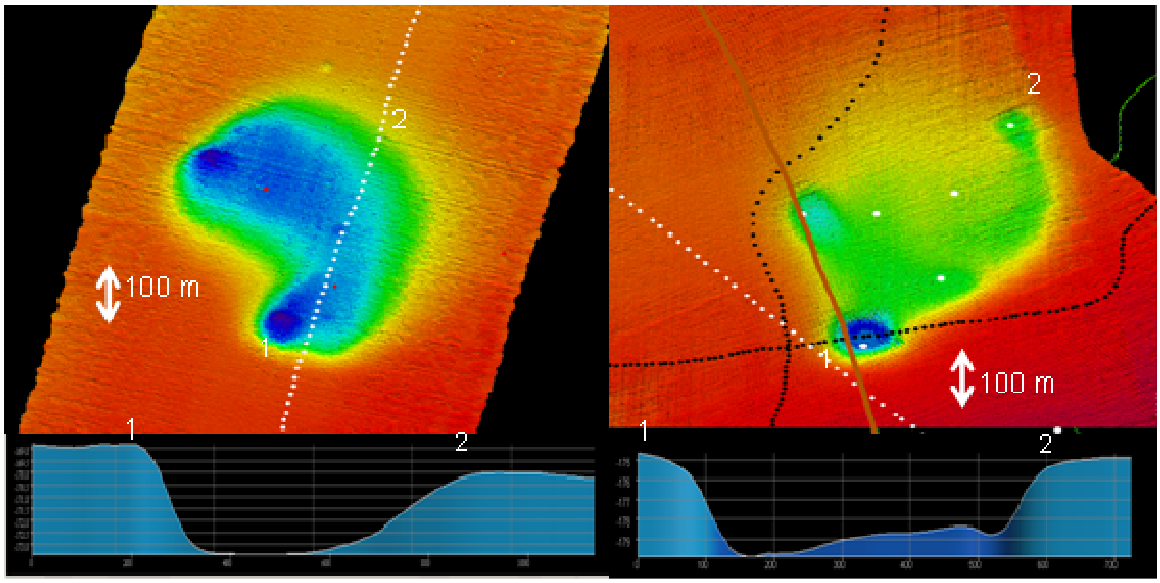

Figure 1. Bathymetry image and depth profiles of pockmark features of the Malin Sea. Dotted lines depict transect lines of the vessel, red and white dots depict sampling sites. Image courtesy to Xavier Monteys, GSI, Ireland

Pockmarks are usually sub-circular but can be elongated by currents and resemble ellipsoidal craters (Josenhans et al., 1978; Boe et al., 1998) or composite when two or more pockmarks merge (Stoker, 1981). Asymmetric, elongated and trough-like pockmarks have also been reported (Hovland and Judd, 1988). Pockmarks are widespread and have been reported in a variety of aquatic environments such as lakes or deltas as well as in oceans, seas and estuaries (MacDonald et al., 1994; Danto et al., 1991; Taylor, 1992; Berkson and Clay, 1973; Hovland et al., 1997). At present, no differences have been identified between freshwater,

seawater and estuarine pockmarks. They can be found isolated, occurring in groups referred to as "pockmark fields" (which may exceed 1000 km^2) (Fader, 1991, Kelley et al., 1994) or as large chains of craters known as "pockmark trains" (Pilcher and Argent, 2007). With diameters of up to 2000 m and depths reaching 45 m pockmarks comprise an interesting and important component of the seabed's morphology.

1.2 Formation of pockmarks

Since their discovery, numerous formation theories have been proposed. It has been suggested that terrestrial pockmarks may be sub-glacial or permafrost features, meteorite impact craters, World War II bomb craters, wrecks sites or even the nests of bottom-dwelling creatures including dinosaurs (Judd, 1981; Hovland et al., 1984; Judd and Hovland, 2007). In more recent years these theories have been revised in favour of the fluid migration theory proposed by King and MacLean (1970) in their pioneering work. Although not conclusive, this theory is still the most popular and has been supported by a large volume of evidence provided by various authors (McQuillin and Fannin, 1979; Josenhans et al., 1978; Judd, 1981; Hovland, 1981; 1981a; 1982; 2003) (Figure 2). It suggests that three types of fluid are involved in the formation process of the majority of pockmarks: 1. groundwater springs; 2. hydrocarbon gas and 3. hydrothermal gas. Increased pore fluid pressure creates dome-like deformation of the sediment surface (A). This process is accompanied by multiple fractures and cracks in the seabed structure. Eventually a hydraulic connection is established between the over pressurized fluid and the water column. In such a system high pressure gradient becomes main driving force of a violent release of the over pressurized fluid. (B). These escaping fluids entrain bottom sediment and lift the fine grained material into the water column. Suspended fine sediment is carried away by currents while coarser grains settle within or close to the pockmark (C). As the material is removed the side walls of pockmarks slump because fine sediments typical of pockmark areas can support only a very gentle slope and a new crater is formed. It is worth mentioning that initial fluid escape through undisturbed seafloor may be violent, and the blow-out characteristics may be subsequently repeated through mild venting events. Nevertheless once the hydraulic connection is established it is likely to be used by the migrating fluids in future (Hovland, 2007). Some authors suggest that too few attempts have been made to verify this hypothesis and evidence of active fluid venting, even in systematically studied pockmark areas, has not been found. Therefore, other mechanisms may be responsible.

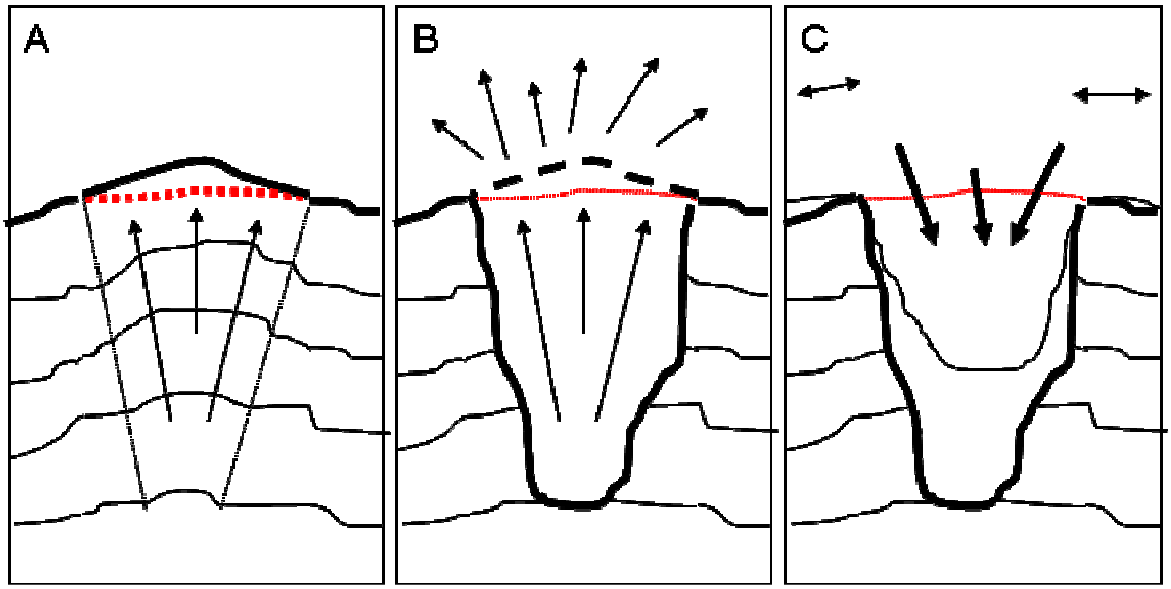

Figure 2. Suspected pockmark formation mechanism. A - seabed doming caused by increasing fluid pressure; B - blow-out of the gas charged sediment and creation of the sediment plume in the water column; C - sedimentation of the coarse material and the fine grains, joint with side walls slumping. Red dotted curve depicts initial seabed profile. Concept after Hovland and Judd, 1988.

Paull et al., 2002 suggested a *"freshwater ice rafting"* mechanism, where periodically freezing freshwater can bind and eventually float the sediment away resulting in shallow pockmark formation. Permafrost can reduce sediment permeability and therefore create favourable conditions for gas entrapment. The accumulated gas can be released violently when the ice seal melts and the permeability of the sediment is restored (Bondarev et al. 2002 and Kvenvolden et al., 1993). Boulton et al, 1993 reported cases of ice sheets induced groundwater discharges which could be linked to pockmark formation. In such a system stress imposed by ice sheets increases pore water pressure which escapes through the sediment collapsing the seabed. The above mentioned theories are plausible and have been attributed to at least some of documented pockmarks.

1.3 Historical background

Elusive to the scientific community which regarded them as geological curiosities, pockmarks were finally uncovered thanks to the development of the side-scan sonar and towed photographic cameras in the mid 1960s. New technology made high-resolution seafloor mapping possible and along with existing discoveries of pockmarks and hydrothermal vents have enabled the pace of research and development in this field to increase progressively. Shortly after the first pockmark had been explored by a manned

submersible dive offshore Nova Scotia (1969), the first scientific paper related to pockmarks by King and MacLean (1970) was published. In the next decade marine scientists reported pockmarks in numerous locations in different parts of the world. With the use of modern high quality 3D seismic technology, scientists have been able to confirm that pockmarks are not recent features but rather an expression of continuous processes in the Earth's crust. Cole *et al.* (2000) reported large pockmarks in the North Sea of Palaeogene age hidden under the contemporary seabed. These erosive features were located beneath the pockmarked Witch Ground Basin which strongly suggests historical continuity of pockmark formation processes. Solheim and Elverhoi, (1993) also reported relict features in the Barents Sea created at the end of the last glacial period when retreating ice sheets triggered rapid methane hydrate dissociation resulting in an explosive pockmark formation.

There is also evidence of fluid flow in historical records, some dating 2000 years ago. Petroleum products from areas where hydrocarbon seeps frequently occurred were often utilized by local communities. Native Americans impregnated their boats with tar, which was also used to fuel torches and lamps, insulate huts, baskets as well as improving hunting weapons (Judd and Howland, 2007). Natural hydrocarbon deposits were also an inspiration to myths, legends and even religions. In Pitch Lake at La Brea, in southwest Trinidad, the largest natural asphalt deposit was for local tribes a manifestation of God's power and has been included in Arawak tribal mythology. Natural eternal flames of gas seeps were crucial in ancient Persian beliefs and are central to the Zoroastrian faith. Furthermore, a number of gas vents were reported in ancient times in the Olympos valley on the south coast of Turkey. The area known as the Yanartaş area or 'Flaming Rock' and its spontaneously ignited gas was used as a reference point by sailors and fire cults and led to the erection of a temple devoted to Hephaestus, divine protector of fire. Olympus flaming rocks are also a source to the first ever Olympic fire (Hakan Hosgörmez, 2006). Evidence for submarine groundwater discharges, observed in ancient times, has been collected and published by Taniguchi *et al*. (2002). These non-petroleum seepages have been reported as far as 2000 years ago: submarine spring offshore from Latakia, Syria in the Mediterranean which was used as a source of freshwater for the city; discharging groundwater in the Black Sea coastal; coastal springs used by the Etruscans for "hot baths" are mentioned (Judd and Howland, 2007).

Here we report on an on-going multidisciplinary analysis of a pockmark area in Dunmanus Bay. This study is part of a larger attempt to investigate and understand the geochemical, microbiological and geophysical characteristics of pockmark areas around the coast of

Ireland including the Malin Shelf and Dublin Bay. By studying these parameters we hope to understand the mechanisms and dynamics of pockmark formation and how they contribute to carbon cycling.

1.4. Dunmanus Bay Geophysical data.

The pockmarks were identified from an INFOMAR multibeam survey of the Bay in 2007. Figure 3 shows the survey area, located approximately 650m east of Dooneen Point and approximately 2.4km west of Carbery Island. Figure 4 provides an overview of the pockmarks and sampling locations while Figure 5 provides a bathymetry image of the

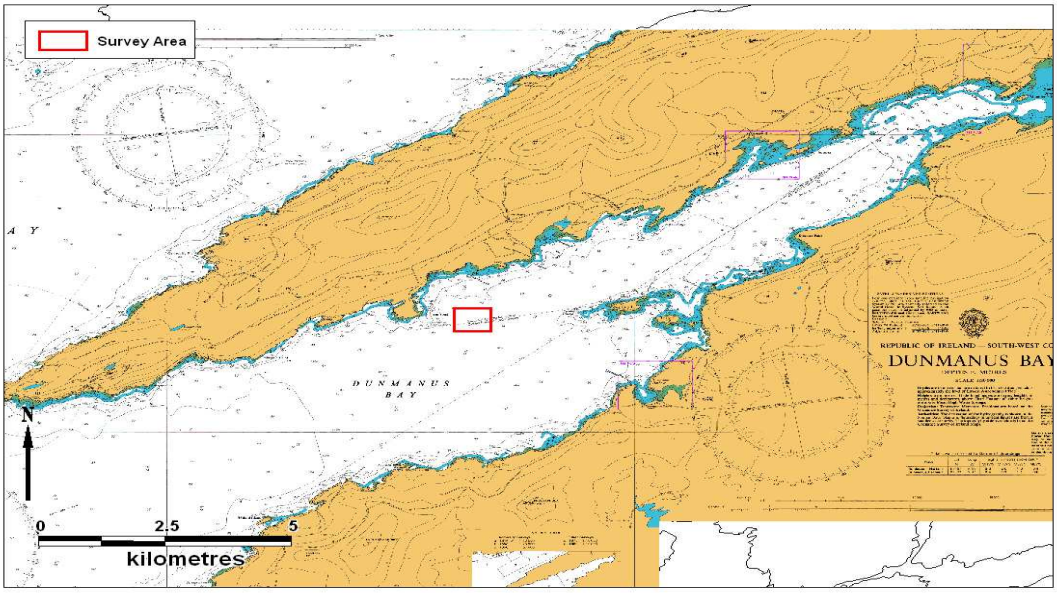

Figure 3: Location of the survey area within Dunmanus Bay, Co. Cork.

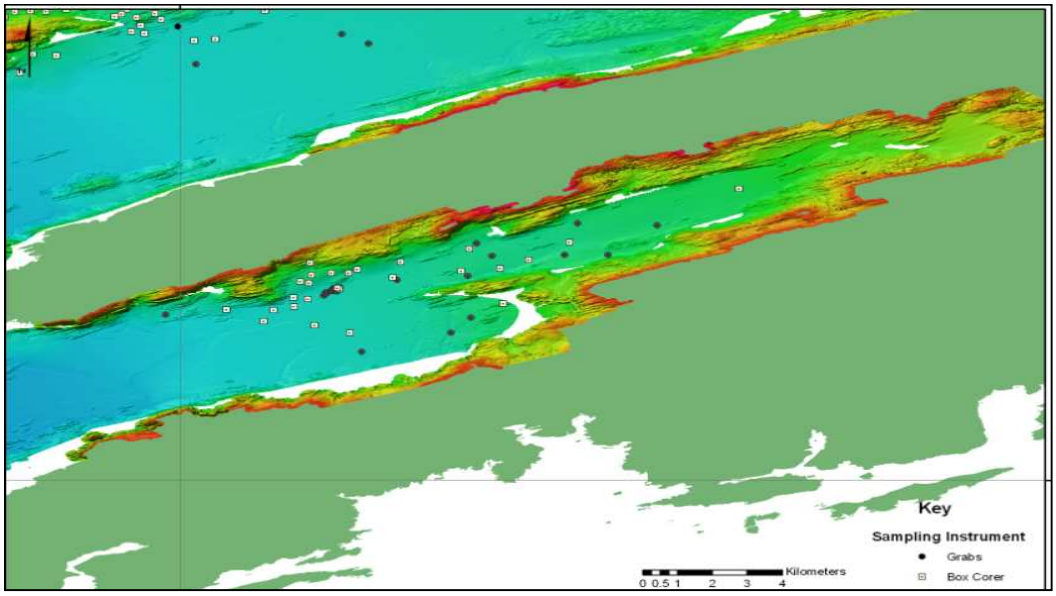

Figure 4. Overview of sampling in Dunmanus Bay, April 2009.

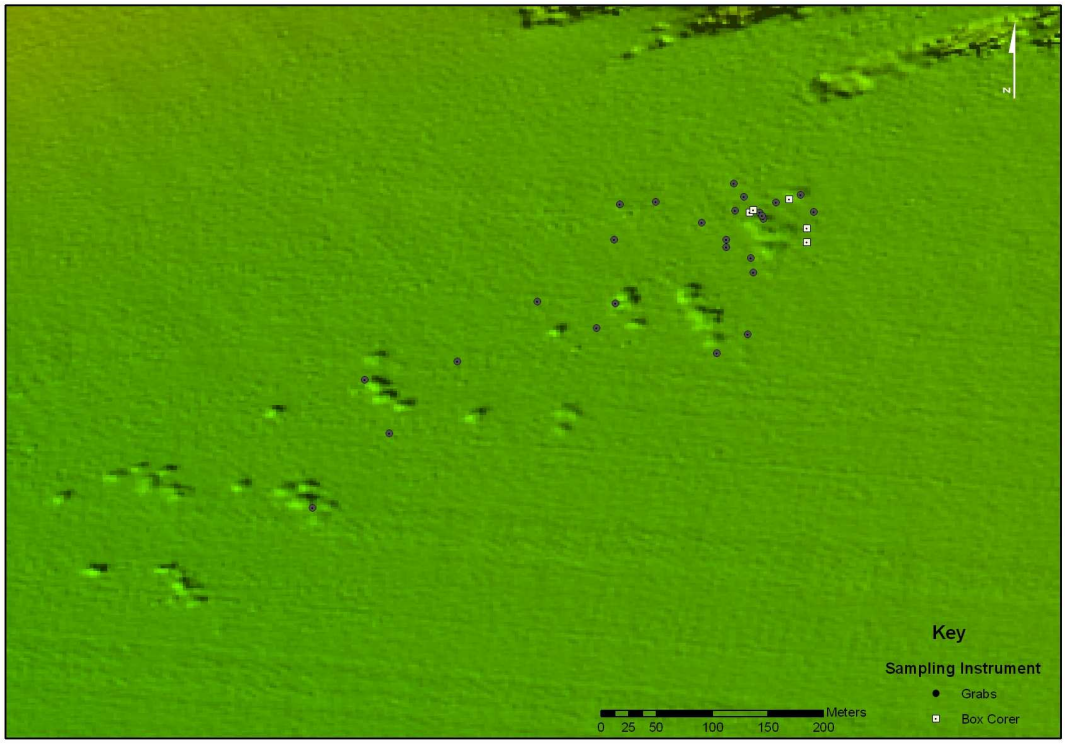

Figure 5. Bathymetry image of Dunmanus Bay highlighting pockmark areas and samples (black dots) taken in April 2009

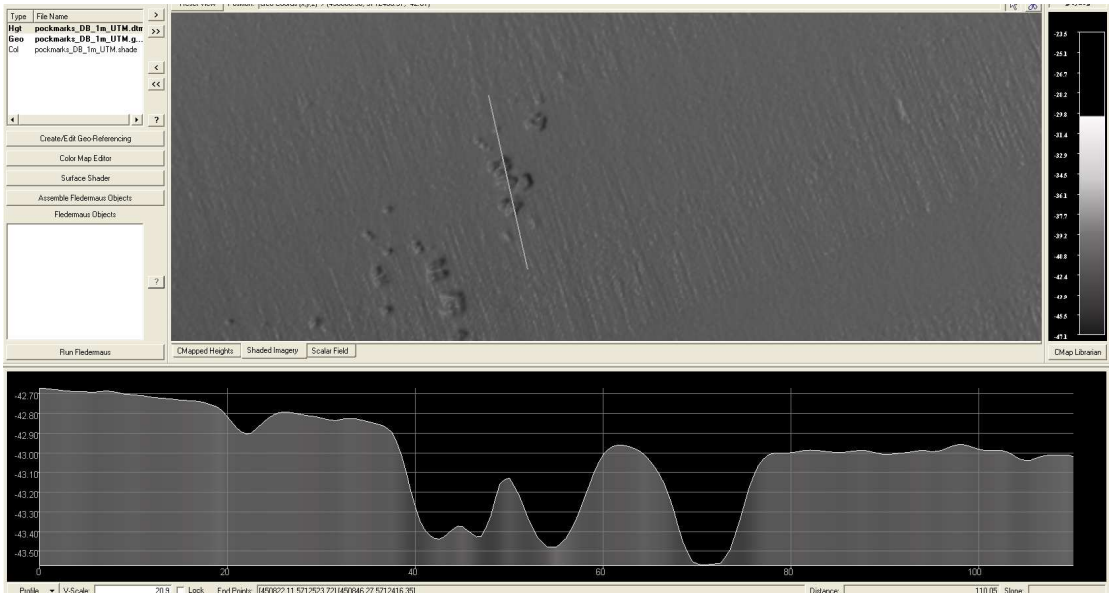

Figure 6. Bathymetry image of Dunmanus Bay highlighting several pockmark. Typically, pockmarks are up to 20m in diammeter, and between 0.3m to 0.8m deep.

2. Biology

This chapter outlines the biological results produced by AQUAFACT International Services Ltd. who were grant aided by INFOMAR to carry out a biological ground-truthing survey of pockmarked areas in Dunmanus Bay, Co. Cork.

2.1 Methodology

2.1.1 Grab Sampling Procedure & Processing

To carry out the ground-truthing survey of the pockmarks in Dunmanus Bay, AQUAFACT International Services Ltd. sampled 10 stations in the location of the pockmarks. The station locations can be seen in Figure 6. The accompanying coordinates for these stations can be seen in Table 1. The locations of Stations 16 and 40 were specifically chosen as they are outside the area of pockmark activity.

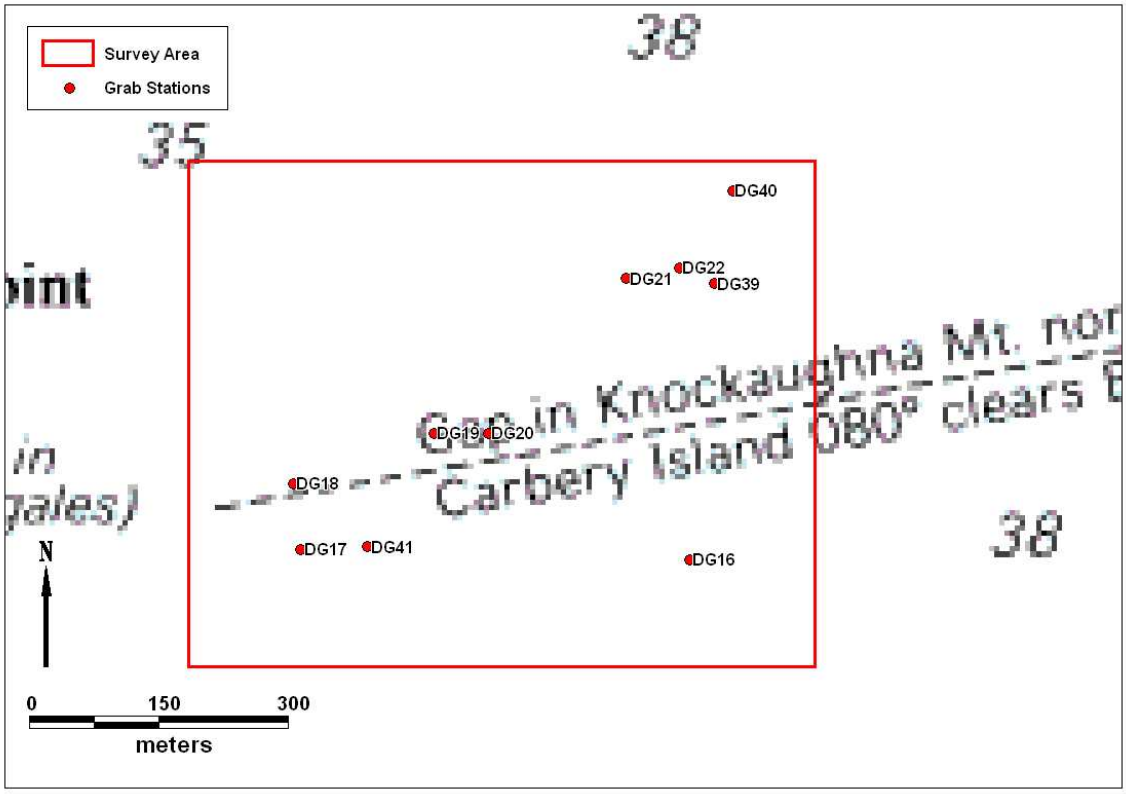

Figure 6: Grab station locations in Dunmanus Bay.

Table 1: Grab station coordinates

Station	Longitude		Latitude	
	Degrees	Decimal Minutes	Degrees	Decimal Minutes
DG39	9	42.5963	51	33.6174
DG22	9	42.6311	51	33.6273
DG21	9	42.6842	51	33.6208
DG20	9	42.8229	51	33.5239
DG19	9	42.8781	51	33.5236
DG18	9	43.0197	51	33.4923
DG17	9	43.0119	51	33.4511
DG16	9	42.621	51	33.4446
DG40	9	42.5777	51	33.6758
DG41	9	42.9447	51	33.453

Sampling in Dunmanus Bay took place on the 24th and 25th April 2009 from the *R.V. Celtic Voyager*. Stations were located using DGPS and this positioning method is accurate to within c. 1m. A 0.1m^2 Day Grab was used to collect the benthic samples. Five replicate samples were taken at each of the 10 stations.

Measurements of sediment depth were taken in a diagonal transect across the grab surface using a clean plexiglass ruler. Data on each sample, e.g. station number, date, time, depth of sediment, surface features and visible macrofauna were logged in a field notebook. The data for each station can be seen in Appendix I. Each grab sample was photographed and a 5cm diameter Perspex core was inserted to a depth of 10cm into the grab sample to remove a meiofaunal sample. This was bunged at the surface and bottom and removed from the grab sample. This sub-sample was washed with freshwater and fixed with 10% buffered formalin. The remaining grab content was sieved on a 1 mm mesh sieve for macrofaunal and fixed with 10% buffered formalin.

On returning to the laboratory, the meiofaunal samples were sieved on a 1mm mesh sieve to remove the macrofaunal species and the portion that passed through the sieve was retained for meiofaunal analysis. All meiofaunal and macrofaunal amples were then sorted under a microscope (x 10 magnification), into four main groups: Polychaeta, Mollusca, Crustacea and others. The 'others' group consisted of echinoderms, nematodes, nemerteans, cnidarians and other lesser phyla. The taxa were then identified to species level where possible.

An additional sample was taken at each station and used for granulometric analyses. The sediment samples were taken through the opening on the top of the grab. The sediment samples were collected using a plastic spoon and placed in labeled plastic bags. All samples were stored immediately in a cold room on board the vessel and were frozen at –20^{o}C on return to the lab.

Particle size analysis was carried out using the traditional granulometric approach, which involved the dry sieving of approximately 100g of sediment using a series of Wentworth graded sieves. The process involved the separation of the sediment fractions by passing them through a series of sieves. Each sieve retained a fraction of the sediment, which were later weighed and a percentage of the total was calculated. Table 2 shows the classification of sediment particle ranges into size classes. Sieves, which corresponded to the range of particle size (Table 2) were used in the analyses.

Table 2: The classification of sediment particle size ranges into size classes (adapted from Buchanan, 1984).

Range of Particle Size	Classification	Phi Unit
<63 µm	Silt/Clay	>4 Ø
63-125 µm	Very Fine Sand	4 Ø, 3.5 Ø
125-250 µm	Fine Sand	3 Ø, 2.5 Ø
250-500 µm	Medium Sand	2 Ø, 1.5 Ø
500-1000 µm	Coarse Sand	1 Ø, 0.5 Ø
1000-2000 µm	Very Coarse Sand	0 Ø, -0.5 Ø
>2000 µm	Gravel	-1 Ø, -1.5 Ø, -2 Ø, -3 Ø, -4 Ø

2.1.2 SPI Sampling Procedure & Processing

In order to examine the nature of the seafloor, Sediment Profile Imagery (SPI) was employed. AQUAFACT International Services Ltd. sampled 10 stations in the location of the pockmarks. The station locations can be seen in Figure 7. The accompanying coordinates for these stations can be seen in Table 3.

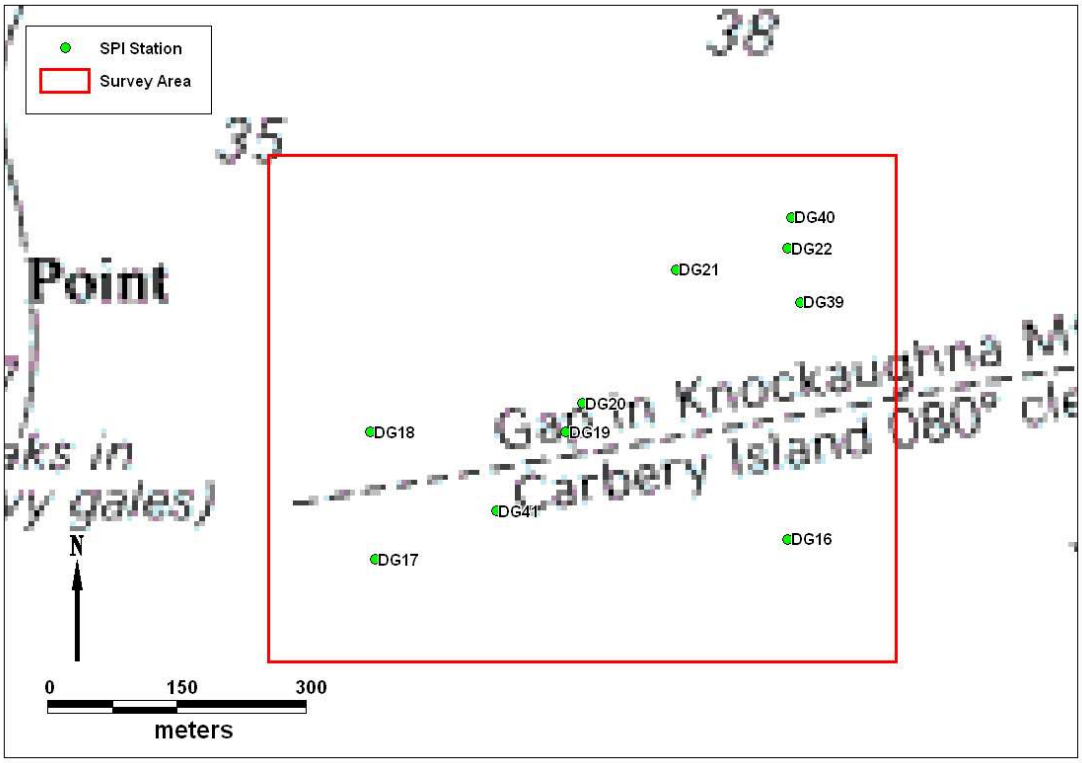

Figure 7: SPI stations samples in Dunmanus Bay.

Table 3: coordinates of the 10 SPI stations sampled in Dunmanus Bay.

Station	Longitude		Latitude	
	Degrees	Decimal Minutes	Degrees	Decimal Minutes
DG21	9	42.7152	51	33.624
DG16	9	42.6024	51	33.456
DG39	9	42.5904	51	33.6
DG22	9	42.6024	51	33.636
DG40	9	42.5988	51	33.654
DG17	9	43.0176	51	33.444
DG18	9	43.0224	51	33.522
DG41	9	42.8958	51	33.474
DG19	9	42.8262	51	33.522
DG20	9	42.8094	51	33.54

Sampling in Dunmanus Bay took place on the 25th April 2009 from the *R.V. Celtic Voyager*. Stations were located using DGPS and this positioning method is accurate to within c. 1m. AQUAFACT's SPI camera was used to take images at each station. Five replicate SPI images were obtained from five separate deployments of the SPI machine at each sampling location. Using SPI, one can deduce the dynamics of biological and physical seafloor processes from imaged structures. The SPI camera differs from other underwater cameras in

that it effects a vertical profile of the sediment water interface and obtains a photographic image of that profile (see Figure 4 and Appendix II). Since the SPI camera obtains images of the undisturbed sediment *in situ*, it delivers information on benthic processes that is not readily available using many conventional sampling tools (Rosenberg & Diaz, 1993). Furthermore, as the object being photographed is directly against the faceplate of the camera assembly, water turbidity is never a limiting factor.

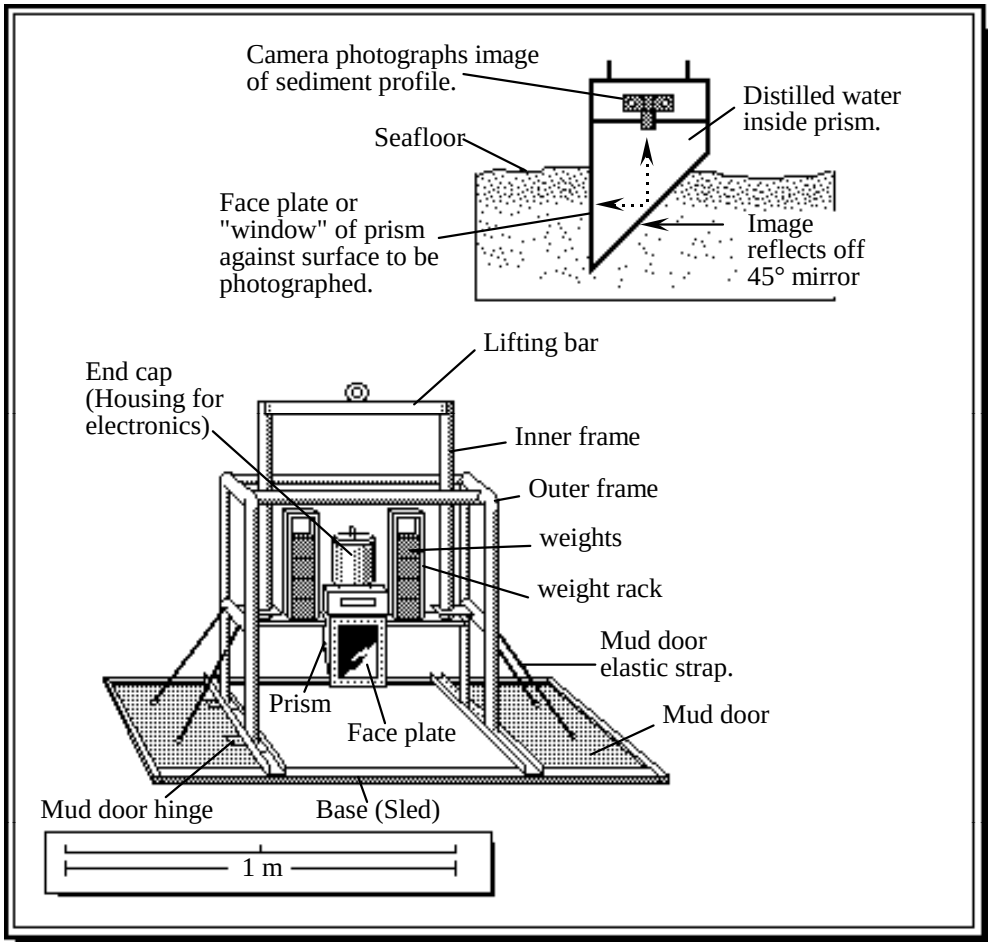

Figure 8: Representation of the SPI apparatus.

SPI can remotely identify the successional status of the seafloor and also has the potential to document its maintenance, development and/or destruction over time. With experience, both the physical and biological forces responsible for maintaining or driving a succession (e.g. bottom erosion or deposition, changes in substratum type, relative changes in levels of dissolved oxygen, organic decomposition processes, etc.) can also be detected with confidence. This also applies to chemical driving forces where sensing probes are used in conjunction with the SPI instrument. A great deal of information about benthic processes is available from sediment profile images and while certain features (e.g. deep-living infaunal

forms) may escape direct observation on the SPI images, their presence can typically be inferred from their impacts on the sediment structure (Appendix II).

Images were analysed using a dedicated image analysis system. Appendix II outlines the rationale and methods of analyses of SPI. The SPI parameters measured from each image include:

1. sediment type measured from the upper 5 cm sediment layer
2. prism penetration depth which gives an indication of relative sediment compaction
3. sediment boundary roughness which indicates the degree of physical disturbance or biotic activity at the sediment water boundary
4. sediment apparent redox potential discontinuity depth (ARPD) assesses the depth of oxygenated sediment on the bottom
5. infaunal successional status which qualifies the type of animals living in the bottom
6. additional parameters such as the presence of mud clasts, epifauna (surface living animals), infaunal burrows and tubes, outgassing of sediments (due to production of hydrogen sulphide and ammonia as by-products of anaerobic metabolism) etc. were also assessed
7. calculation of a benthic habitat quality index (BHQ value) which integrates the information gained from the other parameters measured into a single index which is indicative of the health status of the location under investigation (see Appendix II).

2.1.3 Grab Data Processing

2.1.3.1 Fauna

All meiofaunal and macrofaunal abundances were combined to give a total abundance for each sample. All faunal replicates were then combined to give a total for each station. Data matrices of all the faunal data were compiled and later used for statistical analyses using the Primer® (Plymouth Routines in Multivariate Ecological Research) programme.

Univariate statistics in the form of diversity indices were calculated. The following diversity indices were calculated:

1. Margalef's species richness index (D), (Margalef, 1958).

$$D = \frac{S-1}{\log_2 N}$$

where: N is the number of individuals

S is the number of species

2. Pielou's Evenness index (J), (Pielou, 1977).

$$J = \frac{H' (observed)}{H'_{max}}$$

where: H'_{max} is the maximum possible diversity, which could be achieved if all species were equally abundant (= $\log_2 S$)

1. Shannon-Wiener diversity index (H'), (Pielou, 1977).

$$H' = -\sum_{i=1}^{S} p_i (\log_2 p_i)$$

where: p_l is the proportion of the total count accounted for by the i^{th} taxa

Species richness is a measure of the total number of species present for a given number of individuals. Evenness is a measure of how evenly the individuals are distributed among different species. The diversity index incorporates both of these parameters. Richness ranges from 0 (low richness) to 12 (high richness), evenness ranges from 0 (low evenness) to 1 (high evenness), diversity ranges from 0 (low diversity) to 5 (high diversity).

The PRIMER ® programme (Clarke & Warwick, 2001) was used to carry out multivariate analyses on the station-by-station faunal data. This was done for all surveys individually and on the combined survey data. All species/abundance data were fourth root transformed and used to prepare a Bray-Curtis similarity matrix in PRIMER ®. The fourth root transformation was used in order to down-weigh the importance of the highly abundant species and to allow the mid-range and rarer species to play a part in the similarity calculation. The similarity matrix was then used in classification/cluster analysis. This aim of this analysis was to find "natural groupings' of samples, i.e. samples within a group that are more similar to each other, than they are similar to samples in different groups (Clarke & Warwick, *loc. cit.*). The PRIMER ® programme CLUSTER carried out this analysis by successively fusing the samples into groups and the groups into larger clusters, beginning with the highest mutual similarities then gradually reducing the similarity level at which groups are formed. The result is represented graphically in a dendrogram, the x-axis representing the full set of

samples and the y-axis representing similarity levels at which two samples/groups are said to have fused.

The Bray-Curtis similarity matrix was also subjected to a non-metric multi-dimensional scaling (MDS) algorithm (Kruskal & Wish, 1978), using the PRIMER ® programme MDS. This programme produces an ordination, which is a map of the samples in two- or three-dimensions, whereby the placement of samples reflects the similarity of their biological communities, rather than their simple geographical location (Clarke & Warwick, 2001). With regard to stress values, they give an indication of how well the multi-dimensional similarity matrix is represented by the two-dimensional plot. They are calculated by comparing the interpoint distances in the similarity matrix with the corresponding interpoint distances on the 2-d plot. Perfect or near perfect matches are rare in field data, especially in the absence of a single overriding forcing factor such as an organic enrichment gradient. Stress values increase, not only with the reducing dimensionality (lack of clear forcing structure), but also with increasing quantity of data (it is a sum of the squares type regression coefficient). Clarke and Warwick (*loc. cit*.) have provided a classification of the reliability of MDS plots based on stress values, having compiled simulation studies of stress value behaviour and archived empirical data. This classification generally holds well for 2-d ordinations of the type used in this study. Their classification is given below:

Stress value < 0.05: Excellent representation of the data with no prospect of misinterpretation.
Stress value < 0.10: Good representation, no real prospect of misinterpretation of overall structure, but very fine detail may be misleading in compact subgroups.
Stress value < 0.20: This provides a useful 2-d picture, but detail may be misinterpreted particularly nearing 0.20.
Stress value 0.20 to 0.30: This should be viewed with scepticism, particularly in the upper part of the range, and discarded for a small to moderate number of points such as < 50.
Stress values > 0.30: The data points are close to being randomly distributed in the 2-d ordination and not representative of the underlying similarity matrix.

Each stress value must be interpreted both in terms of its absolute value and the number of data points. In the case of this study, the moderate number of data points indicates that the

stress value can be interpreted more or less directly. While the above classification is arbitrary, it does provide a framework that has proved effective in this type of analysis.

2.1.3.2 Sediment

A procedure similar to multi-dimensional scaling (MDS) was carried out on the sediment data. The procedure is known as principal component analysis (PCA) and it is a 2D/3D ordination. Like MDS, it is based on an underlying (dis)similarity matrix; however in this case it is a Euclidean distance dissimilarity matrix not a Bray-Curtis similarity matrix. The data matrix used for PCA included the sediment particle size percentage distributions (% sand, %silt-clay etc). This dataset was transformed to prevent any outliers having a disproportionate influence on the results. The sediment particle size percentage distributions were square-root transformed. If any significant (pairwise correlation >0.95) correlations existed between variables, only one variable from that correlated group was included in the analysis, to prevent the correlation being exaggerated in the analysis. Following the transformations, the data were normalised to equalise the variance and standardise the contributory importance of each variable. The resulting data matrix was subjected to a correlation based PCA using the PRIMER® program PCA (Clarke & Warwick, 1994), to identify the parameters that accounted for a large proportion of the variance in the original data set. The variances of the principal components (eigen values), the proportion and cumulative proportion of the total variance, explained by each principal component, and the coefficients for each principal component (eigen vectors) were calculated. A two-dimensional PCA ordination of the data was constructed. The PCA plot defined the positions of samples in relation to each axes, which represented the full set of variables. Each station acquired a place on this graph and the location depended on a number of variables significant to that station and which set it apart from all the rest.

2.1.4 SPI Data Processing

All images were analysed as outlined in Appendix II.

2.2 Results

2.2.1 Fauna

The taxonomic identification of the benthic infauna across all 10 stations sampled in Dunmanus Bay yielded a total count of 122 species, comprising 8865 individuals, ascribed to 12 phyla. A complete listing of these species abundance is provided in Appendix III. Of the 122 species enumerated, 57 were polychaetes 25 were crustaceans, 13 were molluscs and 8 species were echinoderms. Eight phyla were grouped as others; this group consisted of cnidarians, plathyhelminthes, nemerteans, nematodes,priapulids, sipunculids, oligochaetes and phoronids .

2.2.2 Univariate Analyses

Univariate statistical analyses were carried out on the combined replicate station-by-station faunal data. The following parameters were calculated and can be seen in Table 4; species numbers, number of individuals, richness, evenness and diversity. Species numbers ranged from 23 (DG21) to 77 (DG16). Number of individuals ranged from 382 (DG20) to 1878 (DG19). Richness ranged from 3.47 (DG21) to 11.16 (DG16). Evenness ranged from 0.35 (DG21) to 0.61 (DG20). Diversity ranged from 1.6 (DG21) to 3.66 (DG16).

Table 4: Diversity Indices for the Dunmanus Bay samples.

Station	Species	Individuals	Richness	Evenness	Diversity
DG16	77	908	11.16	0.58	3.66
DG17	46	632	6.98	0.57	3.14
DG18	39	1462	5.21	0.37	1.96
DG19	43	1878	5.57	0.37	2.01
DG20	34	382	5.55	0.61	3.09
DG21	23	568	3.47	0.35	1.60
DG22	43	786	6.30	0.36	1.94
DG39	35	929	4.98	0.42	2.17
DG40	32	741	4.69	0.40	2.02
DG41	41	579	6.29	0.60	3.19

2.2.3 Multivariate Analyses

The dendrogram and the MDS plot can be seen in Figures 8 and 9 respectively. Stations DG18 and DG19 were the most similar, grouping at a similarity level of 73.94%. This was

followed by the grouping of stations DG17 and DG41, which grouped at a similarity level of 71.15%. All four of these stations grouped at a similarity level of 70.33%. The next most similar stations were DG20 and DG22 grouping at a similarity level of 69.1%. All six of these stations grouped at a similarity level of 66.37%. Station DG39 grouped with these stations at a similarity level of 65.4%, followed by Station DG40 at 59.92%, DG21 at 555.49% and lastly by Station DG16 at 47.35%.

These delineations were also preserved in the MDS plot. The stress value of the MDS ordination is 0.05; this is an excellent representation of the data with no prospect of misinterpretation of the overall structure. Station DG16 grouped separately from the other stations. Stations DG18, DG19, DG17, DG41, DG20 and DG22 formed a central group with stations DG39, DG40 and DG21 at varying distances from the central group.

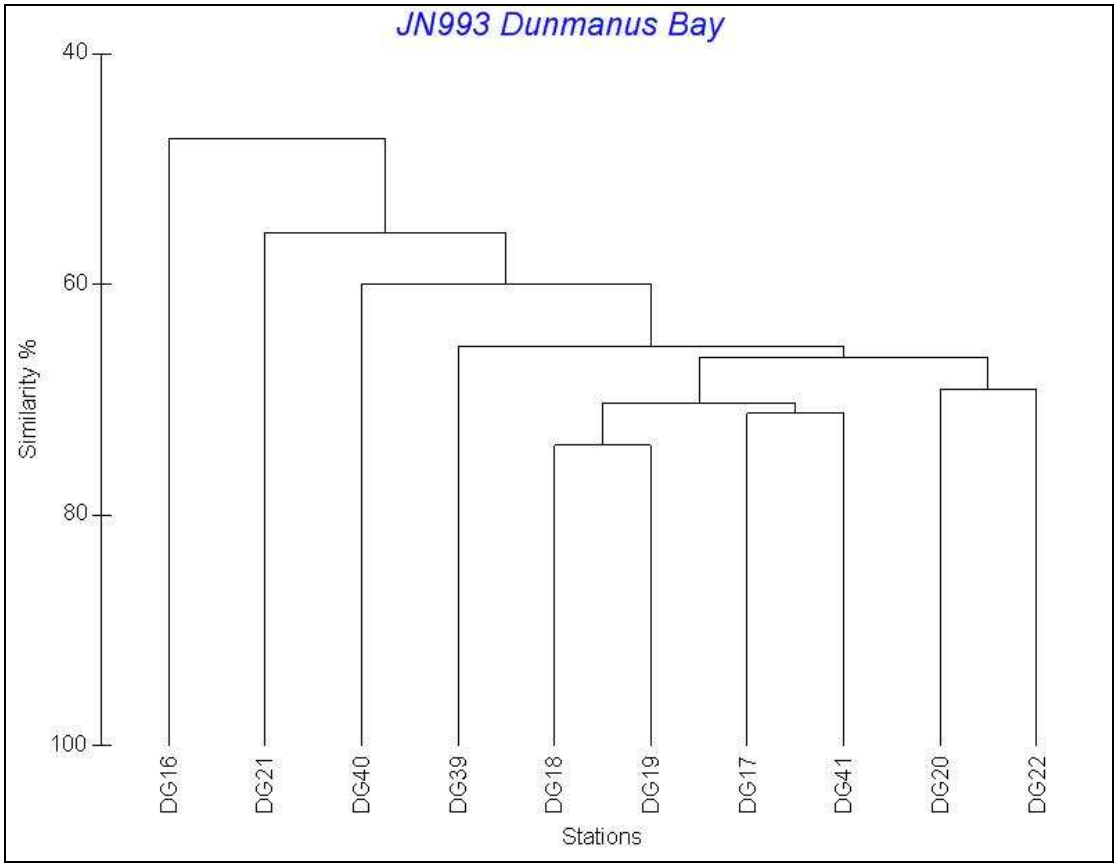

Figure 8: Dendrogram of all 10 Dunmanus Bay stations.

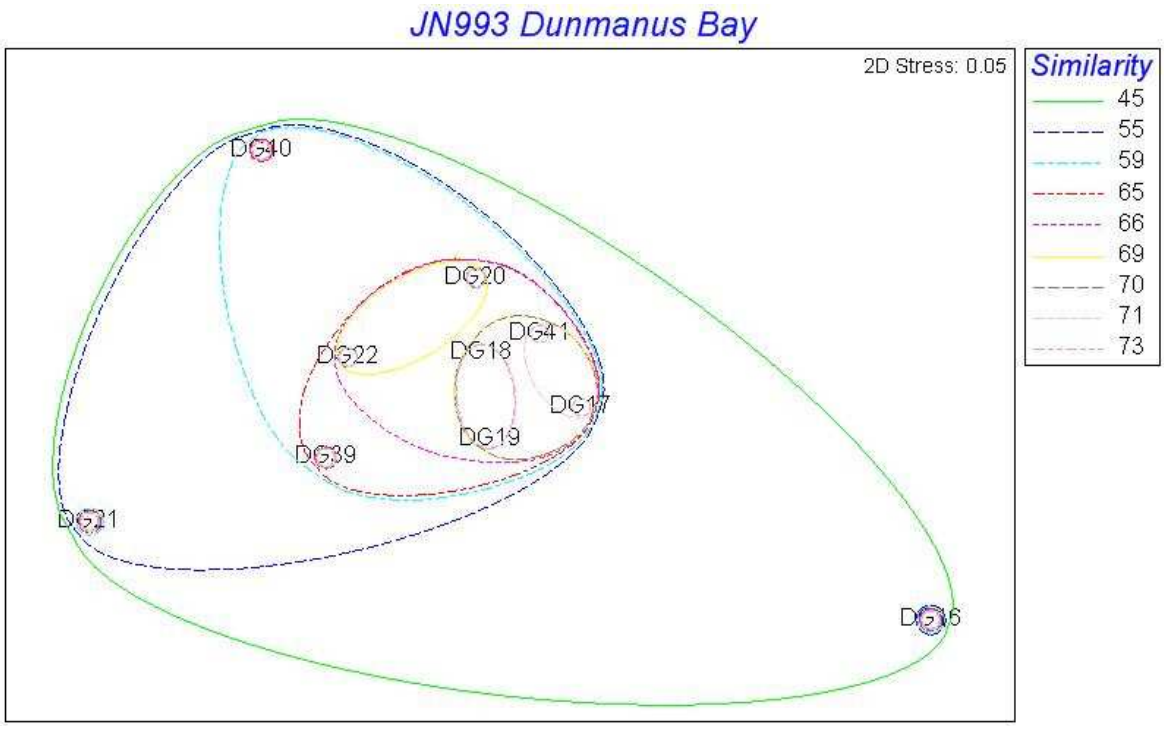

Figure 9: MDS plot of all 10 Dunmanus Bay stations.

Stations DG18 and DG19 formed a group at a similarity level of 73.94%. There were 53 species found at these 2 stations accounting for 3340 individuals. Of the 53 species present, 28 were present twice or less. Three species accounted for 90% of the faunal abundance within this group: the sea cucumber *Leptopentacta elongata* (52.7%), the polychaete *Scalibregma inflatum* (31.9%) and the polychaete *Diplocirrus glaucus* (5.4%). These 3 species accounted for 28% of the similarity within this group. Both of these stations had low richness, evenness and diversity due to the fact that 3 species accounted for 90% of the faunal abundance.

Stations DG17 and DG41 formed a group at a 71.15% similarity level. There were 57 species found at these 2 stations accounting for 1211 individuals. Of the 57 species present, 35 were present twice or less. Four species accounted for 78.5% of the faunal abundance within this group: the brittlestar *Amphiura filiformis* (25.8%), the sea cucumber *Leptopentacta elongata* (24%), the polychaete *Diplocirrus glaucus* (14.7%) and the polychaete *Scalibregma inflatum* (14%). These 4 species accounted for 28% of the similarity within this group. Both of these stations had reasonable richness, evenness and diversity levels, while 3 species did dominate, their dominance was not as extreme as in other stations.

Stations DG20 and DG22 formed a group at a 69.1% similarity level. There were 51 species found at these 2 stations accounting for 1168 individuals. Of the 51 species present, 31 were present twice or less. Three species accounted for 80.4% of the faunal abundance within this group: the sea cucumber *Leptopentacta elongata* (53.3%), the polychaete *Scalibregma inflatum* (21.9%) and the polychaete *Diplocirrus glaucus* (5.2%). These 3 species accounted for 23% of the similarity within this group. Station 20 had the lowest number of individuals and therefore when compared to the number of species present, had the highest evenness value. Station 22 had a reasonable richness level but low evenness and diversity values.

Station DG39 joined the above mentioned stations at a 65.4% similarity level. There were 35 species found at this station accounting for 929 individuals. Of the 35 species present, 18 were present twice or less. Three species accounted for 88.9% of the faunal abundance within this group: the sea cucumber *Leptopentacta elongata* (46.9%), the polychaete *Scalibregma inflatum* (34.6%) and the polychaete *Diplocirrus glaucus* (7.4%). This station had low richness, evenness and diversity due to the fact that 3 species accounted for approximately 90% of the abundance.

Station DG40 joined the above mentioned stations at a 59.92% similarity level. There were 32 species found at this station accounting for 741 individuals. Of the 32 species present, 20 were present twice or less. Three species accounted for 87.6% of the faunal abundance within this group: the polychaete *Scalibregma inflatum* (58.7%), the sea cucumber *Leptopentacta elongata* (25%), and the polychaete *Diplocirrus glaucus* (3.9%). This station had low richness, evenness and diversity due to the fact that 3 species accounted for approximately 88% of the abundance.

Station DG21 joined the above mentioned stations at a 55.49% similarity level. There were 23 species found at this station accounting for 568 individuals. Of the 23 species present, 12 were present twice or less. Three species accounted for 89% of the faunal abundance within this group: the sea cucumber *Leptopentacta elongata* (74.5%), the polychaete *Scalibregma inflatum* (11.4%) and the oligochaete *Tubificoides amplivasatus* (3.2%). This station had the lowest species numbers, richness, evenness and diversity. This was all due to the fact that 3 species accounted for approximately 90% of the abundance.

Station DG16 joined the above mentioned stations at a 47.35% similarity level. There were 77 species found at this station accounting for 908 individuals. Of the 77 species present, 48 were present twice or less. Four species accounted for 75% of the faunal abundance within this group: the polychaete *Scalibregma inflatum* (27.9%) the sea cucumber *Leptopentacta elongata* (16.2%), the brittlestar *Amphiura filiformis* (25.8%) and the polychaete *Diplocirrus glaucus* (15%). This station had the highest species numbers, richness and diversity. While four species did dominate this group, their dominance was not as extreme as in some of the other stations.

While all of these stations grouped somewhat differently due mainly to the percentage similarity that each species contributed to the group, it is clear that the assemblage as a whole is dominated by four species: the sea cucumber *Leptopentacta elongata* (43.6%), the polychaete *Scalibregma inflatum* (28.9%), the polychaete *Diplocirrus glaucus* (7.5%) and the brittlestar *Amphiura filiformis* (6.1%). *Leptopentacta elongata* is a sublittoral benthic species found buried in sandy or muddy sediment down to a depth of 70m. It is a burrowing sea cucumber, which lives in U-shaped burrows. *Amphiura filiformis* is a small brittle star which lives buried in fine muddy sands in water depths typically greater than 15m, although it can be found at extreme low water. It feeds on suspended material in flowing water, but will change to deposit feeding in stagnant water or areas of very low water flow (Ockelmann & Muus, 1978). *Scalibregma inflatum* is found around low water mark and in the shallow sublittoral, buried deep in sand or mud. It is an active burrower and feeds on detritus in sediment and never form tubes. *Diplocirrus glaucus* is a selective deposit feeding polychaete found on muddy sandy substrates.

2.3 Sediment

The results from the traditional granulometric analysis can be seen in Table 5. The sediment sampled in Dunmanus Bay ranged from coarse sand to sandy mud with varying degrees of coarse material. All stations were dominated by silt-clay, with the exception of DG39, which was dominated by coarse sand. Station DG41 contained the highest percentage of gravel (19.2%), station DG17 contained the highest percentage of very coarse sand (13%). Station DG39 contained the highest percentage of coarse sand (39%). Station DG19 contained the highest percentage of medium sand (11.7%). Station DG16 contained the highest percentage

of fine sand (14.3%) and very fine sand (31.1%). Station DG18 contained the highest proportion of silt-clay (38.6%). Figure 10 shows the sediment type at each station sampled.

Table 5: Granulometric results for the 10 Dunmanus stations.

Station	Gravel	Very Coarse Sand	Coarse Sand	Medium Sand	Fine Sand	Very Fine Sand	Silt-Clay
DG16	2.2	5.5	5.8	4.7	14.3	31.1	36.4
DG17	14.9	13	10.4	8.9	8.9	11.2	32.7
DG18	7.4	9.9	9.7	8.1	9.2	17.1	38.6
DG19	6.3	12.3	14.1	11.7	10.8	12.5	32.3
DG20	12.3	9.8	8.7	7.9	6.9	15.7	36
DG21	15.1	10.9	9.1	7.6	9.3	14	33.8
DG22	6	12.1	12.4	11	10.8	13.6	34.1
DG39	5.3	6.9	39	5.1	6.9	12.1	24.7
DG40	15.4	12.8	9.7	8.4	9.3	11.6	32.8
DG41	19.2	10.2	10.2	9.4	9	15.6	26.4

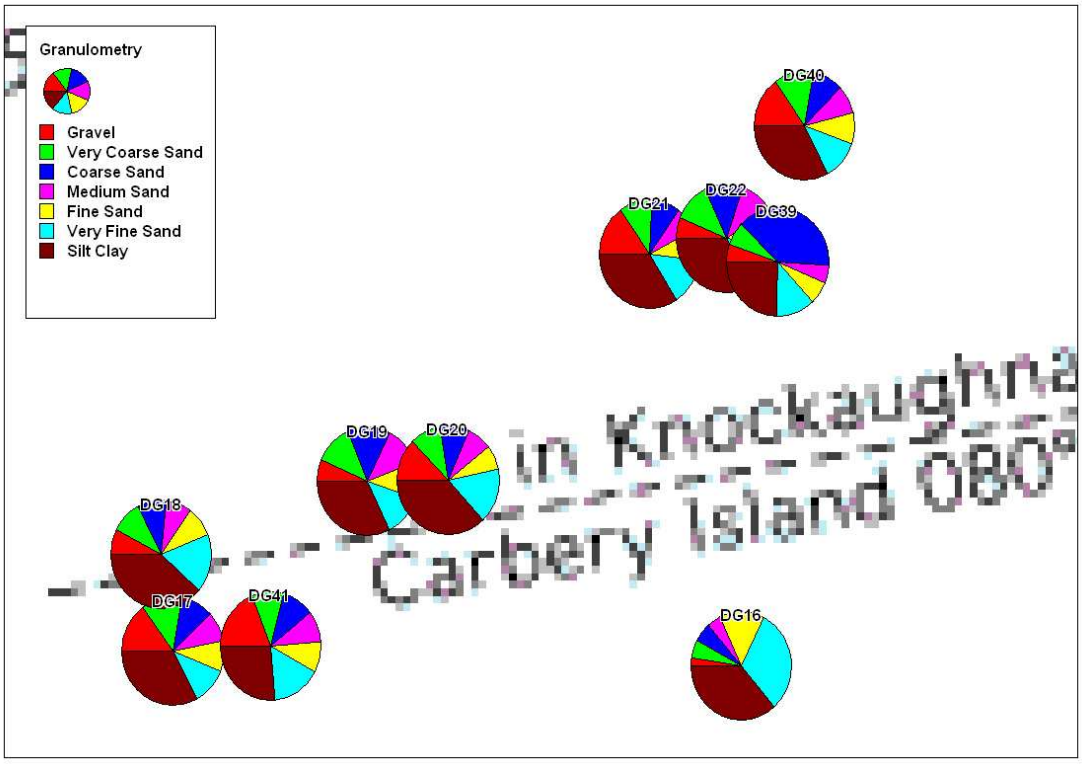

Figure 10: Granulometric results for the 10 Dunmanus Bay stations.

Figure 11 shows the PCA ordination of the sediment data analysed from the Dunmanus Bay stations. The variation seen in this 2-D ordination accounted for 78% of the overall variation, PC1 accounted for 45.5% of the variation, whereas PC2 accounted for 32.5% of the variation. The station characterised by coarse sand (DG39) can be seen as clearly distinct from the

other stations, as can the station characterised by fine sand, very fine sand and silt-clay (DG16). The remaining stations all grouped together based on their relatively high gravel, very coarse sand or medium sand contents.

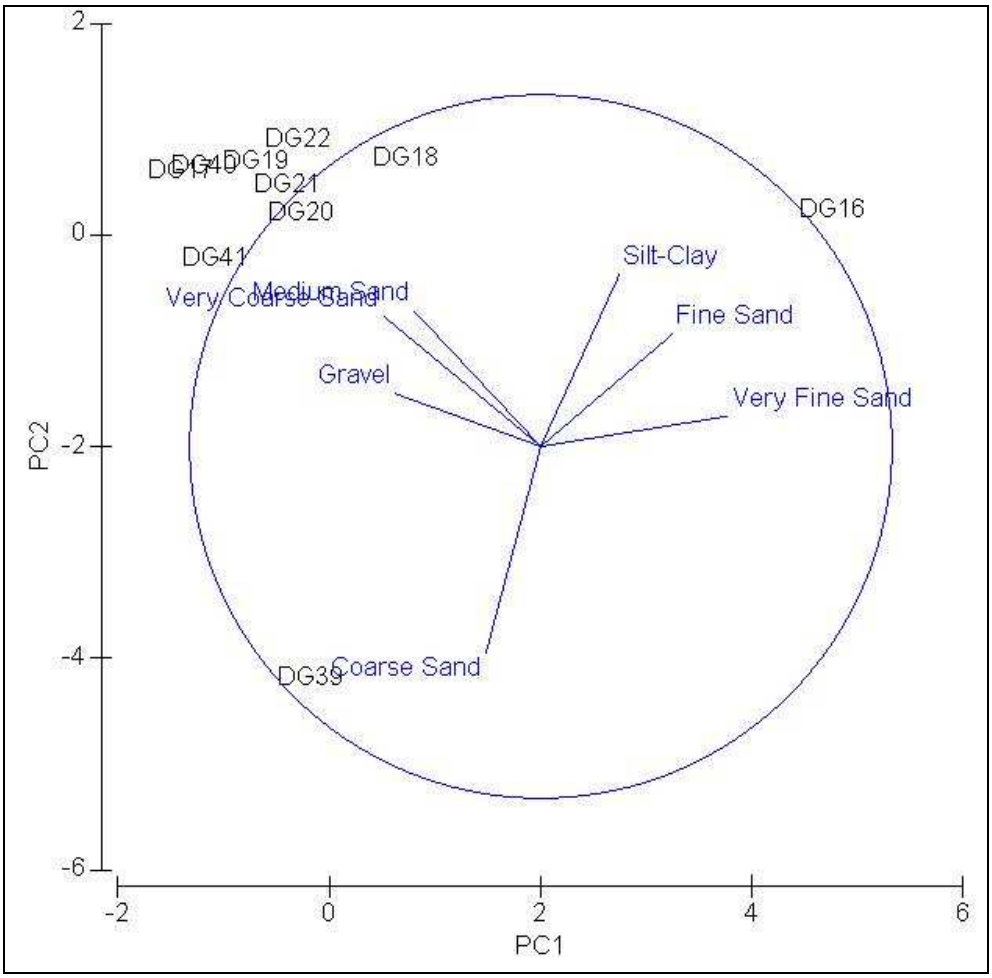

Figure 11: PCA plot for all 10 Dunmanus Bay stations.

2.4 SPI

2.4.1 Station DG16

Figure 12 shows a SPI image from Station DG16. Maximum and minimum penetration depths were 21.74 and 20.48cm respectively. The substrate consisted of very fine sand. The aRPD was patchy/streaky at the surface. Burrows were present down to a depth of 17.44cm and voids were present between depths of 4.55 and 19.04cm.

Figure 12: SPI Image from Station DG16.

2.4.2 Station DG17

Figure 13 shows a SPI image from Station DG17. Maximum and minimum penetration depths were 22.5 and 21.96cm respectively. The substrate consisted of very fine sand. The aRPD was patchy/streaky at the surface. Numerous voids and burrows were present from 9.67 cm to 22.28cm depth.

Figure 13: SPI Image from Station DG17.

2.4.3 Station DG18

Figure 14 shows a SPI image from Station DG18. This station over penetrated and therefore maximum and minimum penetration depths could not be calculated. The substrate consisted of very fine sand. There was evidence of burrowing fauna, with voids and fauna captured in the image.

Figure 14: SPI Image from Station DG18.

2.4.4 Station DG19

Figure 15 shows a SPI image from Station DG19. Maximum and minimum penetration depths were 22.46 and 20.18cm respectively. The substrate consisted of very fine sand. The aRPD was streaky and ranged in depth from 5.44cm to 13.19cm. There were voids present between 1.94cm and 6.87 cm depth.

Figure 15: SPI Image from Station DG19.

2.4.5 Station DG20

Figure 16 shows a SPI image from Station DG20. Maximum and minimum penetration depths were 22.46 and 21.95cm respectively. The substrate consisted of fine sand. The aRPD was streaky and there were numerous feeding voids.

Figure 16: SPI Image from Station DG20.

2.4.6 Station DG21

Figure 17 shows a SPI image from Station DG21. Maximum and minimum penetration depths were 22.5 and 20.04cm respectively. The substrate consisted of very fine sand. The aRPD was streaky due to bioturbation ranging in depth from 0.00cm to 18cm. There was vermiform infauna and subsurface voids from 18.88 to 19.8cm deep.

Figure 17: SPI Image from Station DG21.

2.4.7 Station DG22

Figure 18 shows a SPI image from Station DG22. Maximum and minimum penetration depths were 22.5 and 20.19cm respectively. The substrate consisted of very fine sand with some silt-clay. The aRPD was shallow (2.53cm maximum, 0.00cm minimum). The subsurface was void of life to a depth of 14.16cm.

Figure 18: SPI Image from Station DG22.

2.4.8 Station DG39

Figure 19 shows a SPI image from Station DG39. Maximum and minimum penetration depths were 21.53 and 20.06cm respectively. The substrate consisted of fine sand and very fine sand. The aRPD was streaky ranging in depth from 0.00cm to 6.15cm. There were subsurface voids/infauna at depths ranging from 16.9cm to 18.46cm depth.

Figure 19: SPI Image from DG39.

2.4.9 Station DG40

Figure 20 shows a SPI image from Station DG40. Maximum and minimum penetration depths were 21.74 and 20.27cm respectively. The aRPD was streaky. There was a reduced cast at the sediment surface. Feeding voids/fumaroles were present also.

Figure 20: SPI Image from DG40.

2.4.10 Station DG41

Figure 21 shows a SPI image from Station DG41. Maximum and minimum penetration depths were 22.5 and 21.99cm respectively. The substrate consisted of very fine sand. The aRPD was streaky and there was large void present.

Figure 21: SPI Image from Station DG41.

Chapter 3. Geochemical and microbiological characteristics

3.1 Introduction

Geochemical and microbiological (phylogenetic) analysis is on-going. Here we present initial results and interpretation for the analysis of: 1. the organic component of core and grab sediment samples (organic biomarkers [DCU] and 3D Excitation–emission matrix fluorescence spectroscopy [Dr Carlos Rocha, Trinity College Dublin]), 2. the microbiology of core profiles (molecular biology, Dr Chris Allen, QUB)) and 3. the inorganic characteristics of sediment and water samples (redox potential, elemental analysis, CTD profiles, and methane concentrations in overlying water, [DCU and TCD). On-going work also includes methane concentration analysis in the pore waters of core sediments.

3.2 Lipid Biomarkers

Marine sediments are sinks for organic carbon produced by marine organisms and terrestrially derived natural organic matter. Rivers provide the major conduits for the transport of terrestrial organic matter from land to sea. Lipid biomarkers can provide valuable information regarding the origin, transport pathways and alteration and transformation processes of organic matter due to their recalcitrance in aquatic environments (Wakeham et al 2007, Marcos et al, 2008). In addition, the diversity of molecular structures makes it possible to match specific organisms with specific compounds (Volkman, 2006). Lipid profiles in ancient sediments can be used as proxies for paleoenvironmental and paleoclimatic reconstruction (Dahl et al, 2004). Lipids represent a major organic carbon pool in phytoplankton and, although they represent only a small fraction of sedimentary organic carbon, they are widely applied to evaluate biogeochemical and diagenetic processes in marine sediments (Belicka et al, 2004). Coastal upwelling systems provide environments well suited to the analysis and utilization of biomarker tracers owing to elevated primary productivity and high rates of sedimentation of labile autochthonous organic-rich material (Marlow et al, 2001) . Allochthonous lipids (e.g. higher plant waxes) can, on the other hand, be transported to the oceanic realm via several mechanisms, including freshwater runoff or eolian supply (Hedges et al, 2007).

Our aim is to apportion the main organic matter sources in the surface and core sediments of Dunmanus Bay. Comparisons between pockmark and non-pockmark areas will also be made such that the influence, if any, of pockmark formation on organic constituents can be investigated. Major lipid classes (fatty acids, alcohols, sterols, alkenones) are being used as a

tool for identifying the processes involved in the production, transport and alteration of sedimentary organic OM and the formation of pockmarks in the area.

3.2.1 **Methods**

3.2.1.1 Free lipids extraction and partitioning:

The sediment samples (~12-44g) are sequentially extracted in a pressured solvent extractor (ASE 200, Dionex) modified after Wiesenberg et al., 2004. Briefly an aliquot of sediment is extracted twice at 70^{o}C and 140^{o}C at elevated pressure with dichloromethane/methanol (93/7; v/v). Extracts are combined and the solvents rotary evaporated (bath temp. <37^{o}C). Dried extract residues are hydrolysed with 1N methanolic KOH for 30 min in an ultrasonic bath at 50^{o}C. Neutral and acidic lipids are partitioned according to modified protocol after Belicka et al., 2002. Briefly base hydrolysis products are diluted and extracted three times with hexane/diethyl ether (9/1; v/v). The combined organic phase is concentrated on the rotary evaporator. The retained aqueous phase is acidified with diluted HCl and re-extracted and concentrated in a similar manner to obtain a fatty acids fraction. Samples are transferred to 2ml vials, dried in a stream of nitrogen and stored in -80^{o}C until analysis.

3.2.1.2 Base hydrolysis

Solvent-extracted sediment is hydrolysed according to Otto et al., 2005 to release ester-bound lipids. Briefly aliquots (~9-20g) of extracted sediment are refluxed for 3h with 50ml of 1N methanolic KOH solution. The cooled suspension is acidified with 6N HCl to pH 1 and filtered on pre-extracted glass fibre filters (Whatman GF/A). Hydrolysed sediment residue is oven-dried and extracted twice with dichloromethane/methanol (1/1; v/v) for 15 min in an ultrasonic bath. Combined filtrate and solvent extracts are concentrated on a rotary evaporator. Bound lipids are re-suspended in Nanopure water and extracted three times with diethyl ether. The solvent is removed by rotary evaporation and the lipid residue transferred to 2ml vials and dried in a stream of nitrogen. Samples are then stored in -80^{o}C until analysis.

3.2.1.3 CuO oxidation

Aliquots of solvent extracted sediment are oxidized with CuO to release monomers of non-extractable material modified after Hedges and Ertel, 1982 and Otto et al., 2005. Briefly an aliquot of solvent extracted sediment (~1-2g) is loaded to a Teflon lined bomb (Parr

Instruments, p/n 4744) alongside 1g of dichloromethane extracted CuO, 100mg of Mohr's Salt ($FeH_{20}N_2O_{14}S_2$) and 15ml of 2M NaOH solution. The suspension is sparged with nitrogen and incubated at 170^{o}C for 2.5h. Post reaction residue is filtered and the CuO oxidation products recovered by diethyl ether extraction. The solvent is removed by rotary evaporation and the lipid residue transferred to 2ml vials and dried in a stream of nitrogen. Samples are stored in -80^{o}C until analysis.

3.2.1.4. Derivatization and GC-MS; GC-IRMS analysis

Free lipid fractions are re-dissolved in 1000µl of hexane/diethyl ether (9/1; v/v) , base hydrolysis and CuO oxidation products are re-dissolved in 1000µl of diethyl ether. Sulphur was removed by addition of activated copper. 500ul aliquot of extracts are subsequently dried in a stream of nitrogen. Neutral lipids and CuO products are derivatized with BSTFA (N,O-bis-(trimethylsilyl) trifluoroacetamide) and pyridine (9/1; v/v) for 3h at 70^{o}C while fatty acids and base hydrolysis products are methylated with BF_3 in methanol (14%) for 30min at 70^{o}C and subsequently silylated with BSTFA and pyridine under the same conditions. Derivatization products are dried in a stream of nitrogen, redissolved in 100µl of hexane/chloroform (4/1; v/v) and immediately analysed using Agilent 6890 gas chromatograph (GC) coupled to Agilent 5973 N quadropole mass selective detector (MSD) and IsoPrime stable isotope mass spectrometer (IRMS). The GC is fitted with a HP-5MS capillary column (30 m X 0.25 mm X 0.25µm). Splitless injection mode is used while other GC and MSD operating conditions are as described in Otto et al., 2005. The detector output is processed with Agilent Chemstation and ACD/Labs MS Processor.

Analytes are identified through mass spectra interpretation, NIST and Wiley spectral library data comparison and literature comparison. Quantitation is based on internal standards: perdeuterated tetracosane (n-$C_{24}D_{50}$) for neutral lipids and CuO oxidation products, perdeuterated octadecanoic acid (n-$C_{24}D_{50}$; as methyl ester) for fatty acids and both for base hydrolysis products. Effluent is simultaneously fed into the MSD and IsoPrime combustion furnace through 1:1 fixed outlet splitter (Agilent, p/n 0101-0594). This custom built system allows simultaneous GC-MS and GC-IRMS analysis. The IsoPrime system is calibrated with a mixture of 15 hydrocarbons (Indiana University) and reference gas pulses of known δ^{13} values. Corrections for additional carbon atoms introduced during drivatization steps are made according to mass balance equations based on standard/standard-TMS(Me) experiment (n=4). Selected samples are run in triplicate to assess precision which is 0.5‰ for peaks above 1nA.

3.3 Sample results:

Figures 22 and 23 show free lipids (top) and fatty acid (bottom) profiles from the GC-03 core revealing an abundance of lipids such us: homologous C_{13}-C_{36} n-alkanes, C_{12}-C_{34} alkanoic acids and C_{12}-C_{34} alkanols. Molecular distribution of n-alkanes shows strong odd-chain carbon number predominance with a maximum at $C_{31,}$ while alkanoic acids and alkanols display even-chain carbon number predominance with a maximum at C_{28}. Other identified components are long-chain, C_{30} and C_{32} mid-chain diols and ketols, secondary alcohols, traces of long-chain aldehydes and methyl ketones, mono and diacyloglycerides and a suite of sterols: cholest-5-en-3β-ol ($C_{27}\Delta^5$, cholesterol), 5α-cholestan-3β-ol (cholestanol), ergost-5,22-dien-3β-ol ($C_{28}\Delta^{5,22}$, crinosterol/brassicasterol), ergost-5-en-3β-ol ($C_{28}\Delta^5$, campesterol), stigmast-5,22-dien-3β-ol ($C_{29}\Delta^{5,22}$, stigmasterol), stigmast-5-en-3β-ol ($C_{29}\Delta^5$, sitosterol), 5α-stigmastan-3β-ol (sitostanol), 4α,23,24-trimethyl-5α-cholest-22-en-3β-ol ($C_{30}\Delta^{22}$, dinosterol) and one terpenoid: friedelan-3-one. The fatty acid fraction also contains monounsaturated C_{14}-C_{22} alkanoic acids, branched *iso*, *antiso* and multimethyl alkanoic acids C_{14}-C_{17}, ω- and (ω-1)-hydroxy C_{14}-C_{30} alkanoic acid, and traces of α and β hydroxyl C_{12}-C_{26} alkanoic acids. Ester bound lipids are dominated by similar sterols to those observed in neutral fractions accompanied by alkanoic acids and alkanols. Initial analysis and interpretation reveals an abundance of terrestrial lipids, confirmed by stable isotope data. There are also indications of a higher plant input and signals derived from microalgae, possibly flora and phytoplankton.

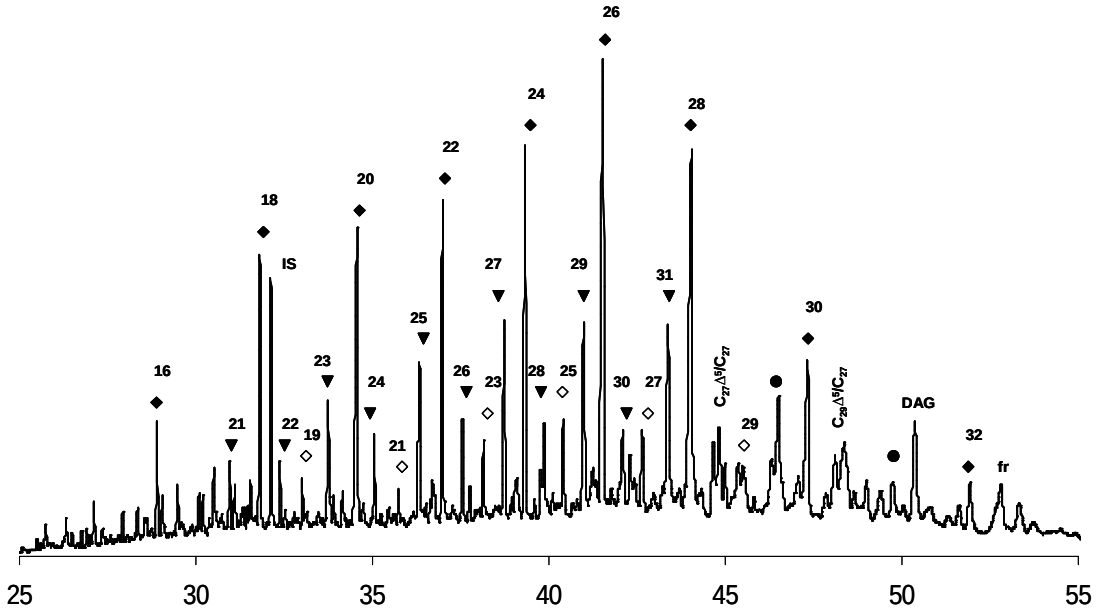

Figure 22. Free lipids profile from the GC-03 core

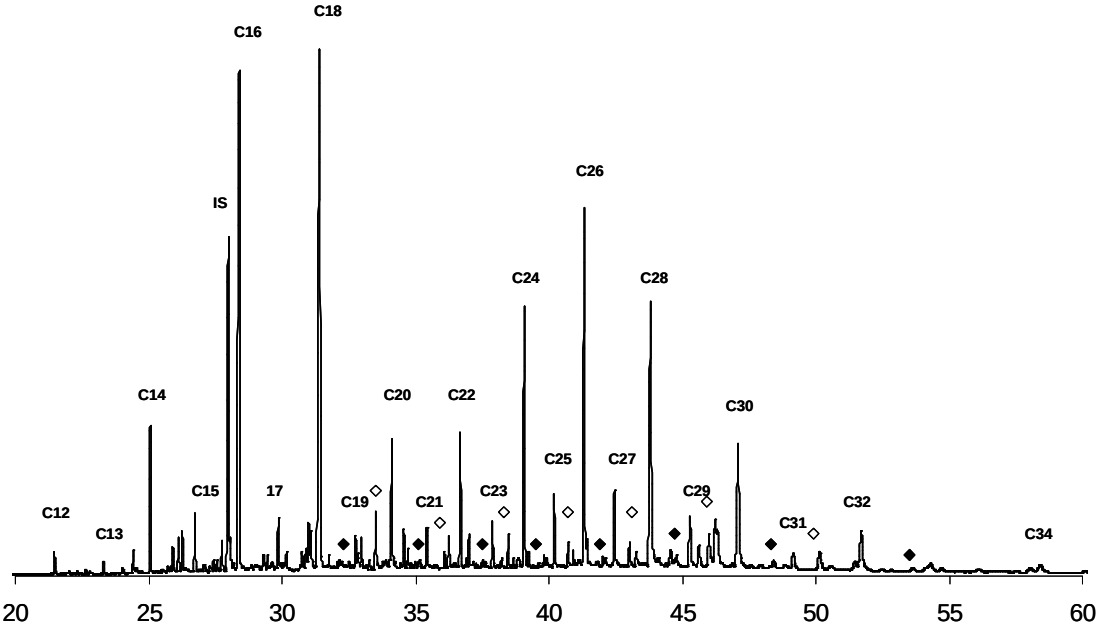

Figure 23. Fatty acid profile from the GC-03 core.

The superimposed chromatograms in Figure 24 shows the input and fate of fresh organic carbon that can be observed through base hydrolysis experiments which target ester-bound lipids. Lipids derived from fresh organic detritus are deposited as esters (black profile) and are very abundant in the uppermost layers of the sediment since benthic organisms did have enough time to consume them. Looking a little bit deeper into the sediment (gray profile) we can see that ester-bound lipids are completely removed from the system.

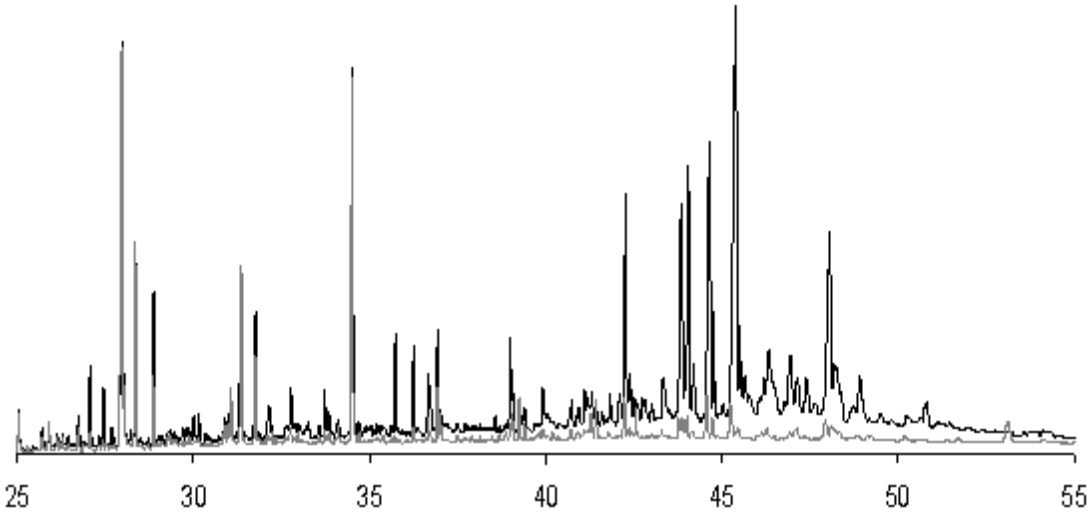

Figure 24 Lipid profile depicting depth changes in biomarker composition down the GC-03 core.

3.4 Redox potential - introduction

Redox potential (E_h), also known as oxidation-reduction potential or ORP is a bulk parameter that describes the ability of a studied system to acquire electrons - reduce its oxidation state. It is an important but troublesome parameter often used in determination of biogeochemical zonation of marine sediment systems.

The dynamics of organic matter diagenesis on the seafloor, which is directly or indirectly linked with almost all biogeochmical processes that take place in the sediment, is controlled by the availability of different electron acceptors. Succession of these electron acceptors is directly linked with energy yields of the diagenetic redox reactions such as:

- oxidation by O_2 (yield: -3190 kJ/mol)
- oxidation by manganese oxides (-3090)
- oxidation by nitrate (-2750)
- oxidation by iron oxides (-1410)
- oxidation by sulphate (-380)
- methane fermentation (-350)

Despite the abundance of information, redox potential is difficult to measure since oxygen exposure (which is difficult to control in the field) changes the state of the equilibrium in the sediment. Therefore all material handling and measurements have to be conducted in a protective atmosphere (argon or nitrogen, rarely helium). Moreover the electrode cannot be calibrated and the solutions used for checking if the electrode is working can 'shock' it causing memory effects. Additionally sulphide poisoning has to be controlled by frequent polishing of the electrode surface or using multiple electrodes. Generally an error of ±50mV is an accepted spread in the results (only if they make sense of course).

3.4.1 Methods

A Broadley James ORP Process Probe with double junction and Ag/AgCl reference was used to measure redox potential. The electrode was cleaned with deionized water and the Pt band was inspected for signs of poisoning. While not in use the electrode was stored in KCl solution. The electrode was checked before use by immersion in pH buffers (pH 4.0 and 7.0) saturated with quinhydrone powder (Sigma-Aldrich). It was ready to use when the ΔE_h was within 172±4mV; values outside this range indicate an electrode problem. Measurements were taken under a protective atmosphere of high purity argon (Air Products) in portable glove box (Sigma-Aldrich).

3.4.2 Results

- 5 gravity cores and 9 box cores were analysed
- The depths of two major zones were determined: post-oxic: blue (from -150 to +200mV) and anoxic: yellow (from -200 to -250mV)
- post-oxic zone ranges from 5cm to 35cm
- processes such as nitrate, manganese and iron reduction take place in this zone
- the anoxic zone was discovered to be very shallow and in the depth of the recovered cores was dominated by sulphide/sulphate redox couplings,

- shallow anoxic zones are typical in areas of high productivity with substantial amounts of organic carbon reaching the seabed and also ofintensive benthic activity
- methanic zone (methane/carbonate redox couple) was not reached
- oxic zone (green, from +200 to +450mV) was not preserved in the recovered gravity cores. Box and grab coring revealed that well oxygenated top centimetres of the sediment are a mixture of phytodetrital drift and loose fine sands,
- this layer was analysed in samples collected with box corers
- box coring also allowed analysis of the top 15cm of the seafloor with greater resolution

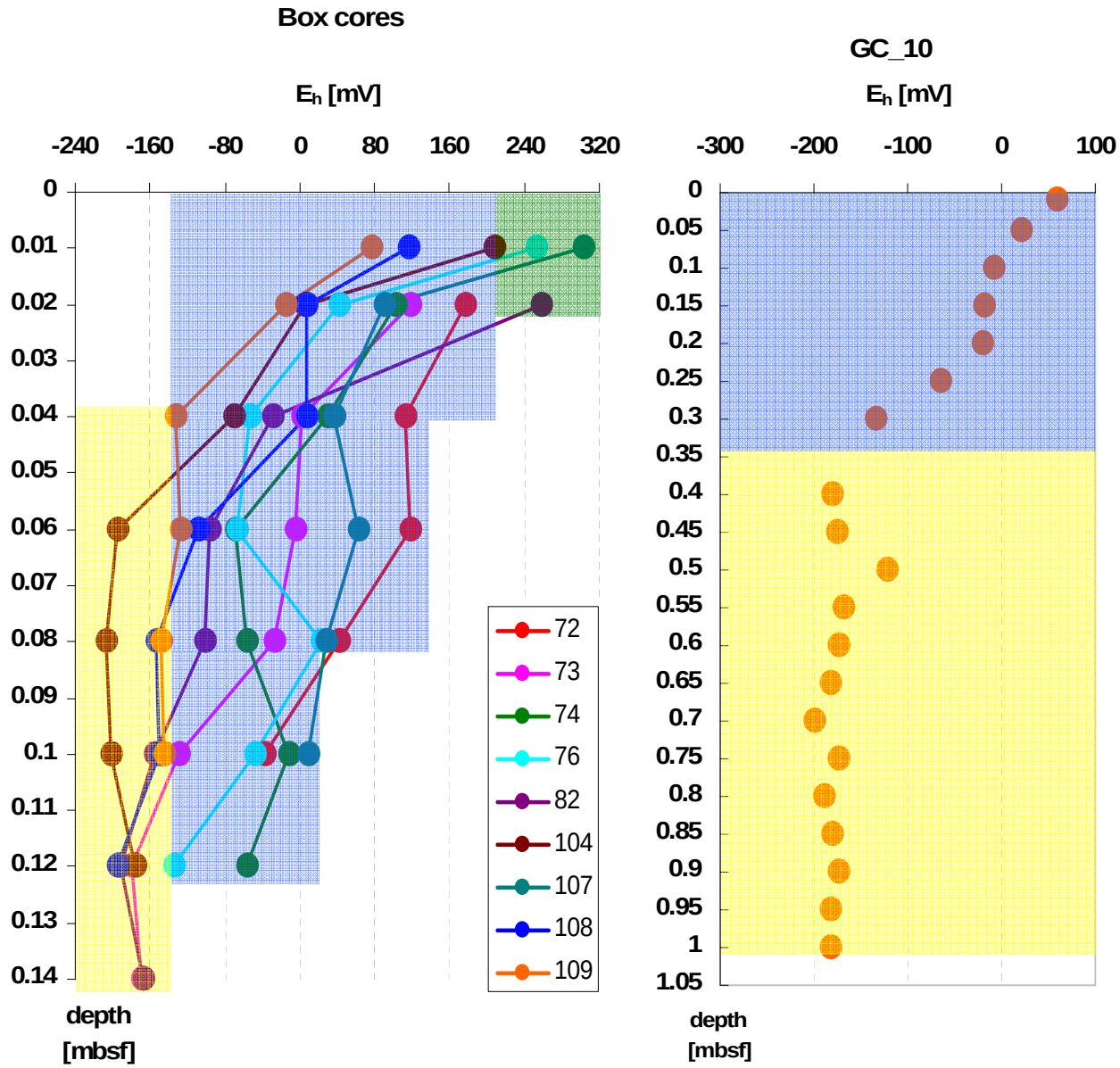

Figure 25. An example of a redox potential profile down a Dunmanus Bay box core (left) and gravity (right) core.

3.5 Excitation–emission matrix fluorescence spectroscopy of pore water.

Excitation–emission matrix fluorescence spectroscopy (EEMF) provides detailed information about the fluorescence properties of dissolved organic matter (DOM) within sediment pores. With this technique, a three-dimensional picture (3D-EEMF) is generated of fluorescence intensity as a function of excitation and emission wavelength. 3D-EEMF spectra has been generated for several cores and work is on-going on those remaining. For example, the scans of the GC_03 core shown in Fig 26 tell us that there is a smooth transition from protein-like marine DOM to humic and fulvic like terrestrial-derived DOM with depth, suggesting a mixing gradient between the two end-members (ie, land and sea). This is compounded by the data on bulk C:N (Fig. 27) ratios from the same core, and from the data on the SO_4:Cl ratio (Fig. 28), which taken together, strongly indicate that there is a potential source of land-based material at the sea bottom in Dunmanus bay, and not a simple diagenetic depth gradient. This source might be seasonal, or driven by other abiotic forcing functions (including the buildup and release of biogenic methane and other gases). However, further analysis is required and planned interpretation of other techniques will also allow a strong hypothesis to be formed.

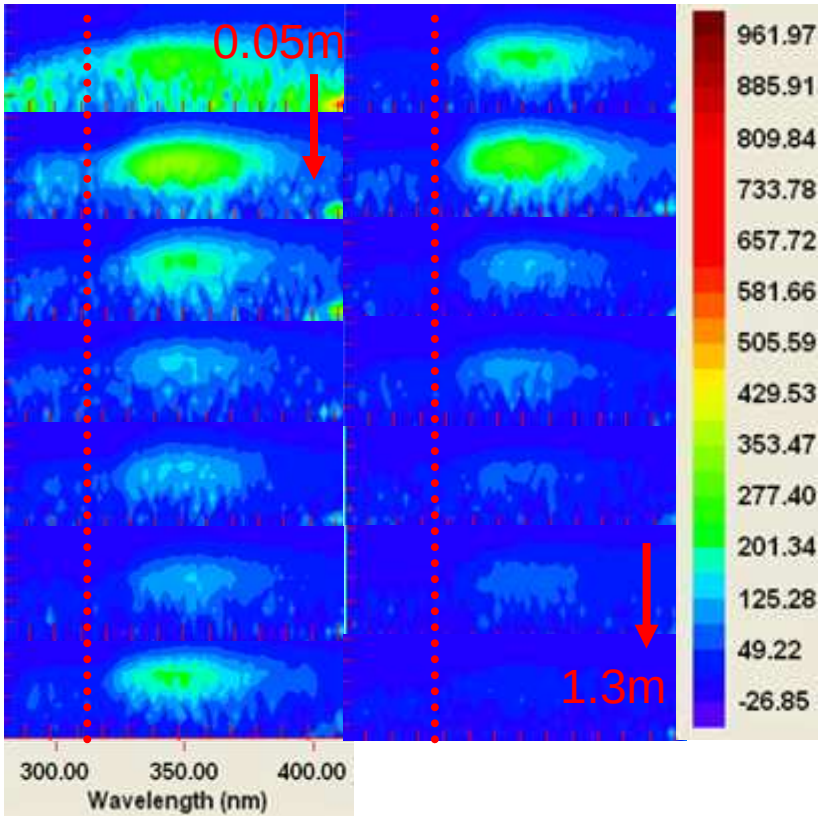

Figure26. EEM 3D profile of the GC-03 core. Red dotted line separates protein-like material (left) from humic-like material (right).

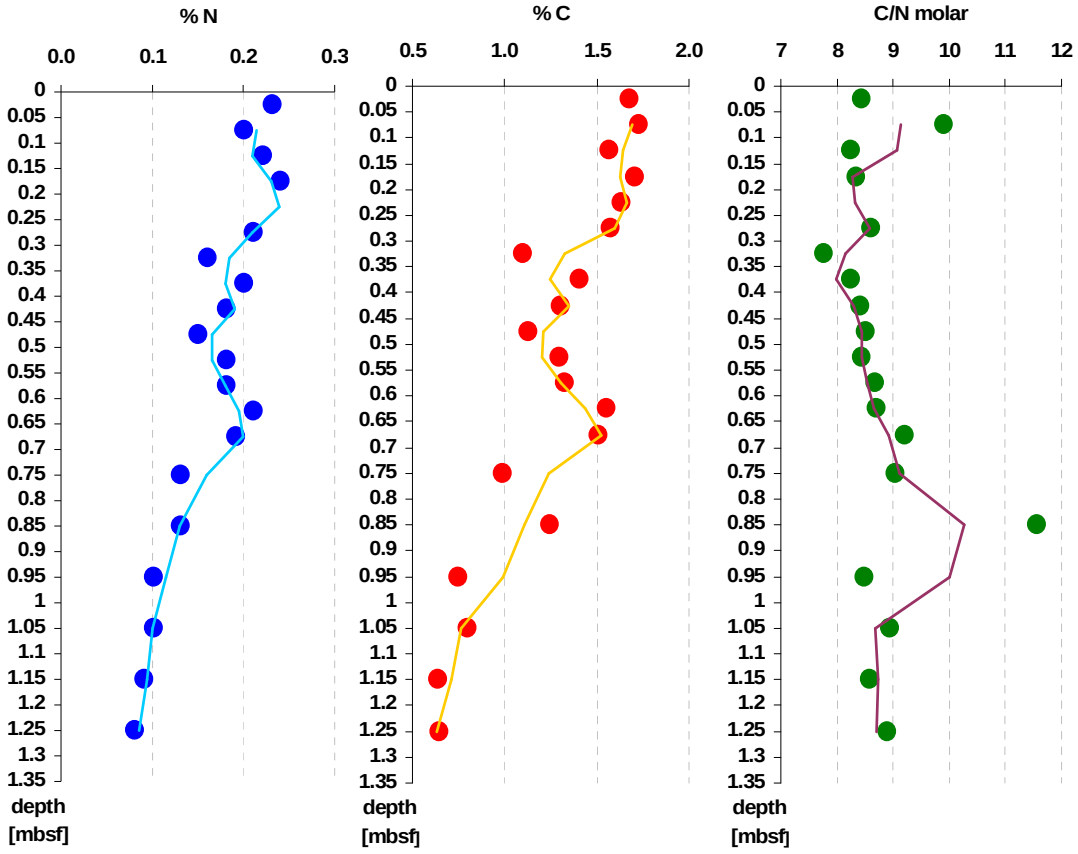

Figure 27. Carbon, nitrogen and C/N ratios down the GC-03 core

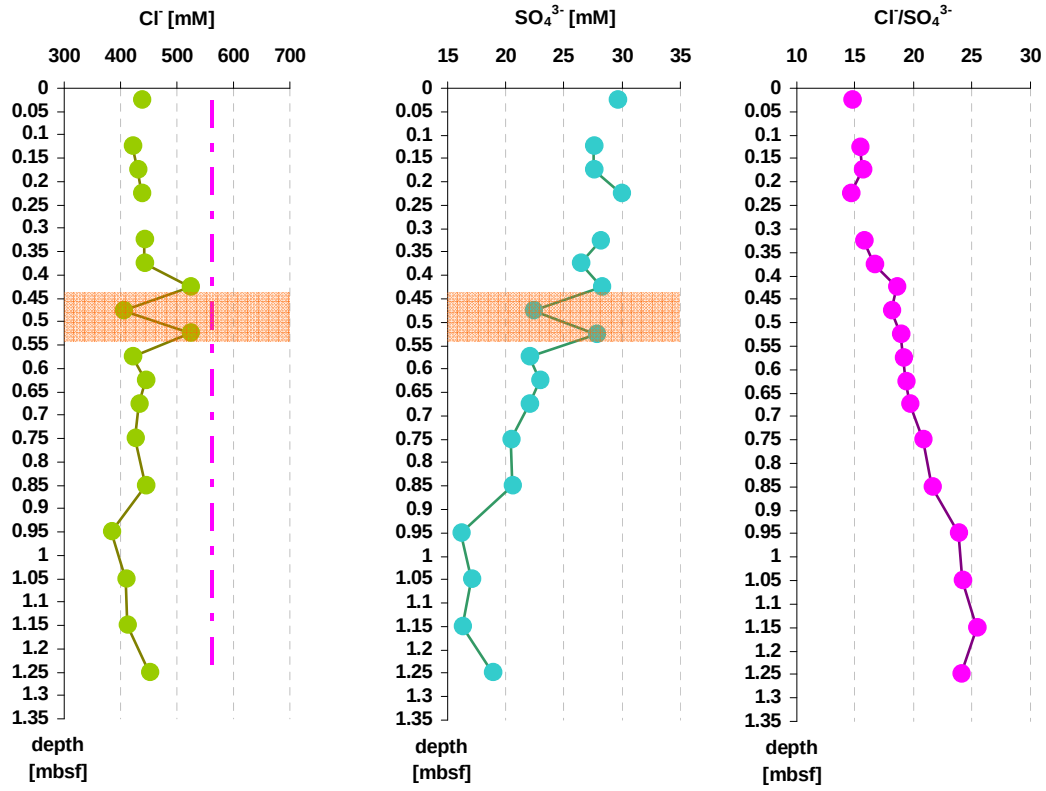

Figure 28. Chlorine, sulphate and Cl^-/SO_4^{3-} ratios down the GC-03 core.

Additional points on Figures 26, 27 and 28:

- straight sulphate profile may indicate high methane flux and that anaerobic oxidation of methane (AOM) is a dominating process in the deeper sections of the sediment rather than organic matter oxidation which results with concave-like profiles
- sulphate has not been depleted therefore a sulphate-methane transition zone (place of AOM) has not been reached,
- sulphate profiles can be used to calculate methane fluxes,
- coloured areas in the sulphate/chlorinity profiles is a sandy layer, possibly responsible for result scatter

3.6 Microbiology (Phylogenetic analysis)

Through our collaboration with Dr Chris Allen of Queens University in Belfast, we are beginning to find evidence for the presence of catabolic gene clusters for anaerobic benzoate degradation in the top sections of cores from the pockmark area of Dunmanus Bay (Figure 29. Such clusters are usually found in freshwater bacteria so this discovery demonstrates the ubiquity of this catabolic capacity. Furthermore, in the bottom section of this core, we have found evidence for the biogeochemically important microbial process of anaerobic methane oxidation through the presence of a consortia consisting mainly of archaea.

Following cloning of the benzoyl coa reductase fragment two sequences were obtained from the sea core DNA. The first sequence obtained showed 95% homology to an uncultured bacterium clone CT1 putative benzoyl coa reductase (Accession no. AY956883.1). The second sequence showed 100% homology, over a shorter stretch, to an Ensifer sp 2FB8 putative benzoyl coa reductase (accession no. AY956848.1).

From initial DGGE work two preliminary sequences have been obtained. The first sequence shows 96% homology to an uncultured *Oceanspirillales* marine organism partial 16s sequence (accession no. EU167290.1). The second sequence shows 93% homology to a *Marionobacterium* sp PY97E partial 16s sequence. (Accession no. EU660510.1).

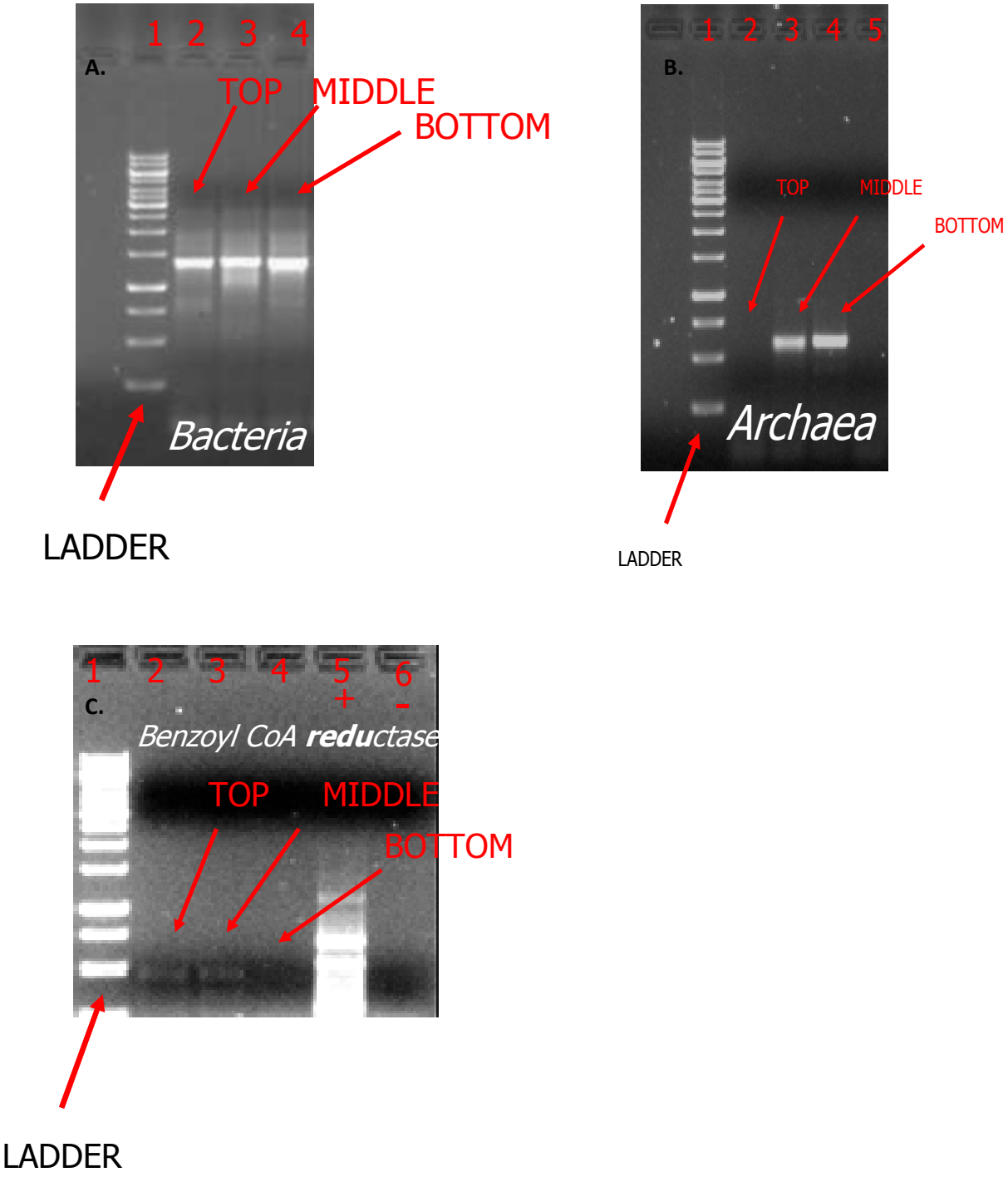

Figure 29. A. Eubacterea16s PCR products obtained from GC-03 core samples after purification. B. Archea 16s PCR products. C. Benzoyl coa reductase PCR fragment.

Further points:

i) That pcr products for both 16S archael and eubactereal strains have been isolated from top, middle and bottom fractions of the core. Note that preliminary sequence analysis of eubacteria suggests marine organisms are present and therefore supports the view that the sampling regime is effective. Full population analysis using a combination of DGGE and cloning/sequencing can now proceed.

ii) Benzoate CoA reductase pcr products have been obtained and sequenced. This is important – as it suggests we may use the presence/analysis of catalytic genes here to show effective removal of organic cpds. This work is in progress. We have also isolated pcr products for methyl CoA reductase (though not sequenced yet).

3.7 ITRAX

The Itrax Core Scanner is a unique new instrument designed to obtain optical, micro-radiographic and µ-X-Ray fluorescence spectrometry (µXRF) elemental profiles for sediment cores of up to 1800mm in length and 120mm in diameter.

Preliminary work has begun on Dunmanus Cores (Figure 30) and results from the solid phase Fe profile from the GC-03 core reveal changes in the concentration of iron-minerals down-core, possibly illustrating diagenetically induced dissolution and precipitation processes, but particle size effects cannot yet be ruled out.

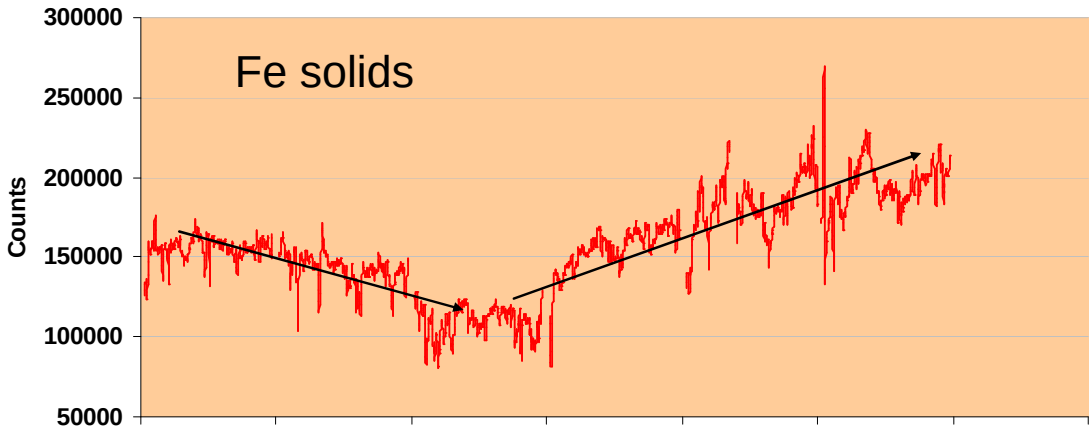

Figure 30. ITRAX solid phase Fe profile from the GC-03 core.

3.8 **Methane concentrations in water.**

A Franatech "METS" methane sensor (Figure 31) was hired for the research cruise to quantify methane concentrations in the water column over pockmark areas and in areas without pockmarks. The METS is a unique underwater methane sensor that can measure in-situ CH_4 concentrations.

The detector room is protected against water and pressure by a silicone membrane. The gas molecules diffuse through the membrane, following the partial pressure gradient between water and detector room, according to the Law of Henry. Hence, the concentration in the detector room is directly correlated to the concentration in the outside water. The correlation is expressed by the calibration formula.

Figure 31. The METS detector.

3.8.1 Methods

The sensor performed very well even though it was not designed for use with CTDs. Interesting and scientifically sound data were collected. To achieve full potential of such instrumentation we recommend combining the METS sensor with the ROV. This would allow continuous methane monitoring with an unprecedented resolution.

The sensor was prepared for use according to the manufacturers recommendations:

- The sensor was powered up for a minimum of 24 hours before deployment, and never switch off until the end of the cruise,
- The sensor's membrane was conditioned for a minimum of 24 hours before deployment by immersion in site seawater,
- between uses the sensor was kept in seawater,
- if cruising time was longer than an hour, the sensor was dismounted from the CTD and stored in seawater
- during casts, the sensor was maintained at a depth of a maximum of 4 m above seabed for the time necessary to stabilize its reading.

3.8.2 Results

Differences in methane concentration were observed and are presented in Figure 32. Southern casts recorded higher methane concentrations and stations to the east from the pockmark cluster recorded lower methane concentrations which may indicate that higher levels of methane in the bottom water are linked with the features. To investigate this hypothesis bottom current dynamics and discrete samples analysis must be performed. Yet even if these facts are linked the concentration range observed is well within average for estuarine waters therefore we can speculate that possible venting may be subtle in nature. This speculation is additionally supported by the fact that pockmarks in Dunmanus Bay are very small features.

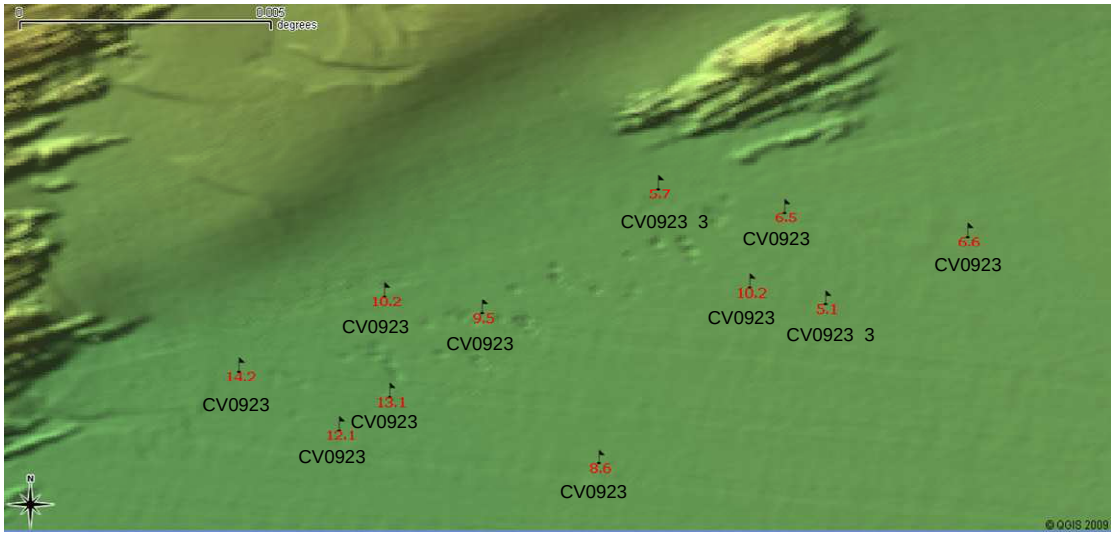

Figure 32. Methane concentrations in and station descriptions.**

3.9 CTDs

CTD (conductivity, temperature, and depth) profiles of the water column were measured for all sampling stations as were turbidity and fluorescence values (Figure 33). Interpretation is on-going.

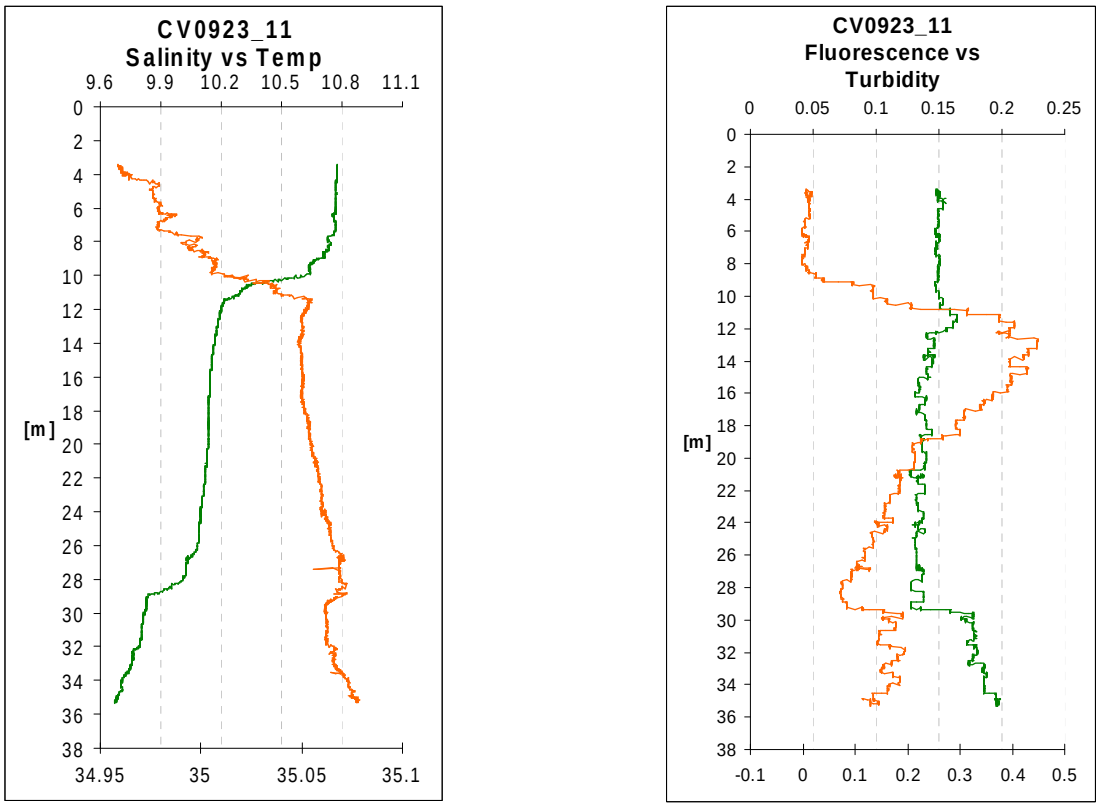

Figure 33. Examples of CTD and Fluorescence vs turbity profiles for Dunmanus Bay cores.

References

Belicka, L.L., R.W. Macdonald and H.R. Harvey, Sources and transport of organic carbon to shelf, slope, and basin surface sediments of the Arctic Ocean, *Deep-Sea Research Part I – Oceanographic Research Papers* 49 (2002), pp. 1463–1483.

Belicka, L.L., Macdonald, L.W., Yunker, M.B., Harvey, H.R., 2004. Marine Chemistry 86, 65–88.

Berkson JM, Clay CS (1973) Possible syneresis marine seismic study of late Quaternary sedimentation origin of valleys on the floor of Lake Superior, Nature 245:89-91

Boe R, Rise L, Ottesen D (1998) Elongate depressions on the southern slope of the Norwegian Trench (Skagerrak): morphology and evolution. Marine Geology 146:191-203

Bondarev VN, Rokos SI, Kostin DA, Dlugach AG, Polyakova NA (2002) Underpermafrost accumulation of gas in the upper part of the sedimentary cover of the Pechora Sea. Russian Geology and Geophysics 43:545-56

Boulton GS, Slot T, Blessing K et al. (1993) Deep circulation of groundwater in overpressured subglacial aquifiers and its geological consequences. Quaternary Science Reviews 12:739-745

Cole D, Stewart SA, Cartwright JA (2000) Giant irregular pockmark craters in the Palaeogene of the Outer Moray Firth Basin, UK North Sea. Marine Petroleum Geology 17:563-577

Dahl, K.A., Repeta, D.J., Goericke, R., 2004. Paleoceanography 19, PA1006. doi:10.1029/2003PA00090.

Danto PR, Austen MC, Burke RA jr, et al, (1991) Ecology of a North Sea pockmark with an active methane seep. Marine Ecology Progress Series, 70:49-63

Fader GBJ (1991) Gas-related sedimentary features from the eastern Canadian continental shelf. Continental Shelf Research 11:1123-1153

Hakan Hosgörmez (2006) Origin of the natural gas seep of Çirali (Chimera), Turkey: Site of the first Olympic fire. Journal of Asian Earth Sciences, 30:131-141

Hedges, J. I., and J. R. Ertel. 1982. Characterization of lignin by gas capillary chromatography of cupric oxide oxidation products. Anal. Chem. 54: 174-178.

Hedges, J.I., Keil, R.G., Benner, R., 1997. Organic Geochemistry 27, 195–212.

Hovland M (1981) Characteristics of pockmarks in the Norwegian Trench. Marine Geology 39:103-117

Hovland M (1981a) A classification of pockmark related features in the Norwegian Trench. Continental Shelf Institute

Hovland M (1982) Pockmarks and the recent geology of the central section of the Norwegian Trench. Marine Geology 47:283-301

Hovland M, Judd AG, King LH (1984) Characteristic features of pockmarks on the Morth Sea Floor and Scotian Shelf. Sedimentology 31:471-480

Hovland M, Judd AG (1988) Seabed pockmarks and seepages. Impact on geology, biology and marine environment. Graham and Trotman, London

Hovland M, Gallagher JW, Clennell MB et al (1997) Gas hydrate and free gas volumes in marine sediments: example from the Niger Delta front. Marine and Petroleum Geology 14:245-255

Hovland M (2003) Geomorphological, geophysical, and geochemical evidence of fluid flow through the seabed. Journal of Geochemical Exploration 78-79:287-291

Josenhans HW, King LH, Fader GBJ (1978) A side scan sonar mosaic of pockmarks on the Scotian Shelf. Canadian Journal of Earth Science 15:831-841

Judd AG (1981) Evaluating the hazard potential of pockmarks. Oceans 13:694-698

Judd AG, Hovland M (2007) Seabed fluid flow. The impact on geology, biology, and the marine environment. Cambridge University Press

Kelley JT, Dickson SM, Belknap DF, et al, (1994) Giant seabed pockmarks: Evidence for gas escape from Belfast Bay, Marine Geology 22:59-62

King LH, MacLean B (1970) Pockmarks of the Scotian Shelf. Geological Society of America Bulletin 81:3141-3148

Komatsu G, Kargel VR, Baker RG, Strom RG, Ori GG, Mosangini C, Tanaka KL (2000) A chaotic terrain formation hyphotesis: explosive outgas and outflow by dissociation of clathrate on Mars. Lunar and Planetary Science XXXI Conference Materials, Poster 1434

Kvenvolden KA, Lilley MD, Lorenson TD, Barnes PW, McLaughlin E (1993) The Beaufort Sea continental shelf as a seasonal source of atmospheric methane. Geophysical Research Letters 20:2459-2462

Marcos Y. Yoshinaga, Paulo Y.G. Sumida and Stuart G. Wakeham. Organic Geochemistry 39 (2008) 1385–1399.

Marlow, J.R., Farrimond, P., Rosell-Melé, A., 2001. In: Wefer, G., Berger, W.H., Richter, C. (Eds.), Proceedings of the Ocean Drilling Program, Scientific Results, vol. 175, pp. 1–26.

MacDonald IR, Guinasso NL jr, Sassen R, et al, (1994) Gas hydrate that breaches the sea floor on continental slope of the Gulf of Mexico. Geology, 22:699-702

McQuillin R, Fannin NGT (1979) Explaining the North Sea's lunar floor. New Scientist 83:90-92.

Otto A, Shunthirasingham C, Simpson MJ (2005) A comparison of plant and microbial biomarkers in grassland soils from the Prairie Ecozone of Canada. Organic Geochemistry 36:425-448

Paull C, Ussler W III, Maher N, et al., (2002) Pockmarks of Big Sur, California. Marine Geology 181:323-335

Pilcher R, Argent J (2007) Mega-pockmarks and linear pockmark trains on the West African continental margin. Marine Geology 244:15-32

Schumm SA (1970) Experimental studies on the formation of lunar surface featuresby fluidization. Geological Society of America (Bulletin) 81:2539-2552

Solheim A, Elverhoi A (1993) Gas-related sea floor craters in the Barents Sea. Geo-Marine Letters 13:235-243

Stoker MS (1981) Pockmark morphology: a preliminary description. Evidence for slumping and doming. Institute of Geological Sciences, Marine Geophysics Unit, Report 81/10

Taniguchi M, Burnett WC, Cable JE, Turner JV (2002) Investigation of submarine groundwater discharge. Hydrological Processes 16:2115-2129

Taylor DI (1992) Nearshore shallow gas around the UK coast. Continental Shelf Research 19:70-116

Volkman, J.K., 2006. Lipid markers for marine organic matter. In: Hutzinger, O. (Ed.-in-Chief), The Handbook of Environmental Chemistry. Vol 2: Reactions and Processes. In: Volkman, J.K. (Ed.) Part N: Marine Organic Matter: Biomarkers, Isotopes and DNA. Springer, Berlin, pp. 27–70.
Wakeham, S.G., Lee, C., Hedges, J.I., Hernes, P.J., Peterson, M.L., 1997a. Geochimica et Cosmochimica Acta 61, 5363–5369.

Wiesenberg, G.L.B., L. Schwark and M.W.I. Schmidt, Improved automated extraction and separation procedure for soil lipid analyses, *Eur. J. Soil Sci.* 55 (2004), pp. 256–349.

Chapter 4.

4.1 Conclusions and Further Work.

The results of both the faunal analyses, particle size distribution, combined faunal and sediment analyses and the SPI survey show the area sampled in Dunmanus to be quite uniform throughout. Even though Station 16 was furthest away from pock mark fields, it had a species list and sediment type that was generally similar to the other sites sampled. This high level of similarity indicates that any effect of escaping gasses on assemble type and sediment is at a low level and is not discernible using standard benthic sampling devices such as grabs.

On-going organic analysis appears to indicate that there is a smooth transition from protein-like marine dissolved organic matter (DOM) to humic and fulvic like terrestrial-derived DOM with depth, suggesting a mixing gradient between the two end-members (ie, land and sea). Elemental analysis also strongly indicates that there is a potential source of land-based material at the sea bottom in Dunmanus Bay, and not a simple diagenetic depth gradient. Further analysis is required and planned interpretation of other techniques will also allow a strong hypothesis to be formed. Straight sulphate profiles may indicate high methane flux and that anaerobic oxidation of methane (AOM) is a dominating process in the deeper sections of the sediment rather than organic matter oxidation which results with concave-like profiles. This is interesting as we are also finding evidence for the biogeochemically important microbial process of anaerobic methane oxidation through the presence of a consortia consisting mainly of archaea in the bottom section of this core. Different catabolic gene clusters for anaerobic benzoate degradation have been found in the top sections of Dunmanus Bay cores. Such clusters are usually found in freshwater bacteria so this discovery demonstrates the ubiquity of this catabolic capacity.

Differences in methane concentration in overlying water were observed which may indicate that higher levels of methane are linked with pockmarks. The concentration range observed was within those expected therefore we can speculate that possible venting may be subtle in nature. Work is on-going to detect and quantify methane concentrations in the sediment cores. Extensive biomarker, metals and organic analysis is also planned with the support of INFOMAR and we are aiming for a peer reviewed publication by the end of the year.

Appendix I
Sample Log

Station	Longitude		Latitude		Time	Date	Rep	Sediment Type	Fauna	Colour	Smell	Photo	Sample Depth	Sub sample	Comment
	Deg	DM	Deg	DM											
DG39	9	42.60	51	33.62	17:45	25/04/09	A-E	Muddy sand	Cucumbers, Pectinaria, tube worms (mud tubes), Shrimp, Bivalve, Brittlestars	Grey brown	-	Y	Full	Meio	Retook sediment grab. Did not match (had a lot of rotting plant material (& H2S smell)
DG22	9	42.63	51	33.63	22:08	24/04/09	A-E	Compact mud (clayey)	Cucumbers, tubeworms, glycerids	-	-	Y	Full		
DG21	9	42.68	51	33.62	21:05	24/04/09	A-E	Muddy sand	Cucumbers, Pectinaria, Shrimp	Grey	-	Y	Full	Meio	& Sed
DG20	9	42.82	51	33.52	19:43	24/04/09	A-E	Muddy sand	Cucumbers, brittlestars	Grey	-	Y	Full	Meio	& Sed
DG19	9	42.88	51	33.52	18:57	24/04/09	A-E	Muddy sand	Terebellids, Pectinaria, Cucumbers, Brittlestars, Nephtys	Grey	-	Y	Full	Meio	& Sed
DG18	9	43.02	51	33.49	17:41	24/04/09	A-E	Muddy sand	Sea cucumbers, brittlestars, Pectinaria	Grey	-	Y		Meio	& Sed

Station	Longitude		Latitude		Time	Date	Rep	Sediment Type	Fauna	Colour	Smell	Photo	Sample Depth	Sub sample	Comment
DG17	9	43.01	51	33.45	16:07	24/04/09	A-E	Muddy sand	Sea cucumbers, brittlestars, Pectinaria	Grey	-	Y		Meio	& Sed
DG16	9	42.62	51	33.44	15:24	24/04/09	A-E	Muddy sand	Cucumbers, ophiuroids		-	Y		Meio	& Sed
DG40	9	42.58	51	33.68	19:21	25/04/09	A-E	Muddy sand	Cucumbers, worms, Nephtys, Decapod (Jaxea), Scalibregmids	Grey	-	Y	Full	Meio	& Sed
DG41	9	42.94	51	33.45	21:17	25/04/09	A-E	Muddy sand	Cucumbers, Nephtys, Brittlestars, tube worms (mud tube Melinna like)	Grey	-	Y	Full	Meio	& Sed

Appendix II
SPI Apparatus
and Data Analysis

SEDIMENT PROFILE IMAGERY:

APPARATUS AND DATA ANALYSES

APPARATUS AND DEPLOYMENT

A remotely operated sediment profile camera is used to obtain *in situ* digital profile images of up to 20 cm of the top layers of sediment on the seafloor. It differs from other underwater cameras in that it vertically slices through the sediment-water interface and images the sediment section in profile. Functioning like an inverted periscope, it consists of a wedge-shaped prism with a plexiglass face plate. Light is provided internally by a flash strobe and the back of the prism has a mirror mounted at a 45° angle. This reflects the image of the sediment-water interface at the face plate up to the camera, which is housed on top of the prism. The camera - prism assembly is supported by an inner frame or cradle which can move relative to an outer supporting frame under control of a 'passive' hydraulic piston (see Figure 1).

The camera prism assembly cradle can be moved up and down by producing tension or slack on the winch wire. As the camera is lowered to the seafloor, tension on the winch wire keeps the prism in the up position. The supporting frame lands on the bottom first, leaving the area directly under the prism undisturbed. As the winch wire is slackened, the prism cradle descends toward the bottom at a controlled rate of fall (Figure 2). The wedge-shaped prism enters the bottom and is driven into the sediment by its weight. The piston ensures that the prism enters the bottom slowly and does not disturb the sediment - water interface. Additional lead weights can be attached to the prism cradle to assist prism penetration if required.

On impact with the bottom, a trigger activates a time delay on the camera shutter release and a digital photograph is taken when the prism comes to rest. Because the sediment is photographed directly against the face plate, turbidity of the ambient seawater does not affect image quality. After the photograph or image is taken, tension on the winch wire raises the prism cradle to the up position, a wiper blade cleans off the face plate, the strobe is recharged and the camera can be lowered for another image. In this manner the SPI assembly can be rapidly 'hopped' over the seabed and a series of images obtained at any one sampling location. After the camera is taken back on board a rubber ring records the

depth the camera had penetrated and a counter records the number of successful image shots taken. Specific measurement techniques and interpretive considerations for the analysis of a range of parameters from the SPI images are presented below.

A compact, equally effective diver operated sediment profile camera apparatus (Figure 3) has been developed for operation in shallow waters and shallow areas generally inaccessible by the larger remotely operated machine. As with the remotely operated SPI camera, the camera prism is mounted on a supporting stabiliser frame which can be moved up and down in an action controlled by a hydraulic system. Once the camera's frame touches the bottom, the scientific diver exerts pressure on the prism housing causing it to penetrate the sediment fabric under control of the hydraulic piston. This allows the optical prism to enter the bottom at approximately 6 cm sec^{-1}. The slow fall rate ensures that the descending prism does not impact the bottom at a high rate and therefore minimizes disturbance of the sediment-water interface. The prism is driven several centimeters into the seafloor and the camera trigger is tripped so that a photograph is taken. The diver ensures that the SPI frame is not moved or disturbed in any way while the camera is taking a picture so that any physical disturbance of the sediment detected in a SPI image is not an artifact caused by the instrument itself.

DATA ANALYSIS

Images are captured using Canon EOS 450D digital SLR cameras (12 megapixel) and Nikkor optics and are stored on SD (secure digital) memory cards. They are downloaded to a laptop computer before being analysed in detail. The image analysis system used can discriminate a wide range of different grey scales, so subtle features can accurately be digitised and measured.

Customised software in conjunction with an image analysis system is used for the analysis of a series of 21 physical, chemical and biological parameters on each image. Before all measurements from each SPI image are stored on disk, a summary display is made on the screen so the operator can verify if the values stored in memory for each variable are within expected range; if anomalous values are detected, software options allow re-measurement before storage on disk. All data stored on disks are printed out on data sheets for editing by the principal investigator and as a hard-copy backup of the data stored on disk; a separate

data sheet is generated for each SPI image. Disk storage of all SPI parameters allows any variable of interest to be compiled, sorted, graphed, or compared statistically.

A great deal of information about benthic processes is available from sediment profile images. Measurable parameters, many of which are calculated directly by image analysis, include physical / chemical parameters (i.e. sediment type measured as grain size major mode, prism penetration depth providing a relative indication of sediment shear strength, sediment surface relief, condition of mud clasts, redox potential discontinuity depth and degree of contrast, sediment gas voids) and biological parameters (i.e. infaunal successional stage of a well documented successional paradigm for soft marine sediments (see Pearson and Rosenberg, 1978), degree of sediment reworking, dominant faunal type, epifauna and infauna, apparent species richness, depth of faunal activity, presence of microbial aggregations).

A multi- parameter organism-sediment index (OSI) is calculated on the basis of the measured physical and biological parameters. This index characterises habitat quality and has been found to be an excellent parameter for mapping disturbance gradients and the health status of the seabed. Specific analytical and interpretative aspects of the parameters measured from the SPI images are outlined below.

SEDIMENT TYPE DETERMINATION

The sediment grain-size major mode and range are visually estimated from the photographs by overlaying a grain-size comparator, which is at the same scale. This comparator was prepared by using the SPI camera to photograph a series of pre-prepared sediments which were graded according to the Udden-Wentworth size classification scheme. The classes of sediment used ranged from mud to granule. There are seven grain-size classes are on the comparator, i.e. < 0.063mm (≥ 4ø) (i.e. silt clay), 0.063 -0.125mm (4-3ø) (i.e. very fine sand), 0.0125 - 0.25mm (3-2ø) (i.e. fine sand), 0.025- 0.5mm) (2-1 ø) (i.e. medium sand), 0.5 - 1.0mm (1-0ø) (i.e. coarse sand), 1.0 -2.0mm (0 to –(-)1ø) (i.e. very coarse sand), > 2.0mm (< -1ø) (i.e. gravel). Seven grain-size classes are on this comparator: ≥ 4ø, 4-3ø, 3-2ø, 2-1ø, 1-0ø, 0-(-)1ø, < -1ø. The lower limit of optical resolution of the photographic system is about 0.062mm, allowing recognition of grain sizes equal to or greater than coarse silt. The accuracy of the method has been documented by comparing the SPI estimates with grain-size statistics determined from laboratory sieve analyses.

PRISM PENETRATION DEPTH

The SPI prism penetration depth is determined by measuring both the largest and smallest linear distance between the sediment-water interface and the bottom of the digital image frame. The SPI analysis software automatically averages these maximum and minimum values to determine the average penetration depth. All three values, (maximum, minimum, and average penetration depth) are included on the data sheets. Prism penetration is potentially a noteworthy parameter; if the number of weights used in the camera is held constant throughout a survey, the camera functions as a static-load penetrometer. Comparative penetration values from sites of similar grain-size give an indication of the relative sediment bearing capacity or shear strength.

SEDIMENT BOUNDARY ROUGHNESS

Sediment boundary roughness is determined by measuring the vertical distance (parallel to the digital image border) between the highest and lowest points of the sediment-water interface. In addition, the likely origin (e.g. physical or biogenic) of this small-scale topographic relief is indicated when it is evident. In sandy sediments, boundary roughness can be a measure of sand wave height. On silt-clay bottoms, boundary roughness values often reflect biogenic features such as faecal mounds or surface burrows.

MUD CLASTS

When fine-grained, cohesive sediments are disturbed, either by physical bottom scour or faunal activity (e.g. decapod foraging), intact clumps of sediment are often scattered about the seafloor. These mud clasts can be seen at the sediment-water interface in SPI images. During analysis, the number of clasts is counted, the diameter of a typical clast is measured, and their oxidation state is assessed. Depending on their place of origin and the depth of disturbance of the sediment column, mud clasts can be reduced or oxidised (in SPI images, the oxidation state is apparent from their reflectance value; see 'Apparent redox potential discontinuity depth' section below). Also, once at the sediment-water interface, these sediment clumps are subject to bottom-water oxygen levels and bottom currents. Based on laboratory microcosm observations of reduced sediments placed within an aerobic environment, oxidation of reduced surface layers by diffusion alone is quite rapid, occurring within 6-12 hours. Consequently, the detection of reduced mud clasts in an obviously aerobic setting suggests a recent origin. The size and shape of mud clasts, e.g. angular versus rounded, is also considered. Mud clasts may be moved about and broken up by

bottom currents and/or animals (macro- or meiofauna) (Germano, 1983). Over time, large angular clasts become small and rounded. Overall, the abundance, distribution, oxidation state, and appearance of mud clasts are used to make inferences about the recent pattern of seafloor disturbance in an area.

APPARENT REDOX POTENTIAL DISCONTINUITY (ARDP) DEPTH

In fine-grained coastal areas, when there is oxygen in the overlying water column, the near surface sediment will have a higher reflectance value relative to hypoxic or anoxic sediment underlying it. This is because the oxidised surface sediment contains particles coated with ferric hydroxide (an olive colour when associated with particles), while the suphidic sediments below this oxygenated layer are grey to black. The boundary between the coloured ferric hydroxide surface sediment and underlying grey to black sediment is defined here as the apparent redox potential discontinuity (abbreviated as the RPD). This 'apparent' depth may, or may not, be equivalent to the actual RPD depth, which is defined as the depth at which the Eh = 0 as measured by microelectrodes. As explained below, in most cases, the depth of Eh = 0 potential in the sediment differs from the 'apparent' RPD as imaged by SPI.

The difference between the depth of the true RPD (Eh = 0) and the imaged apparent RPD can be explained as follows. As dissolved oxygen diffuses into sediment pore water, it is consumed by a variety of biological and geo-chemical reactions. One of these reactions involves the oxidation of iron, which is precipitated onto mineral grains located at, or near, the sediment surface. Once oxidised, these ferric hydroxide-coated particles are bioturbated downward into pore-waters, which lack free molecular oxygen (negative Eh). However, the ferric hydroxide coatings are meta-stable, and reduction of the iron is a slow process relative to the rate of bioturbation. This explains the presence of oxidised grain coatings (high optical reflectance sediment) in reducing pore waters. In the presence of bioturbating infauna, the thickness of the RPD directly reflects the particle bioturbation depth.

The areal extent of the RPD is determined by digitising its unique reflectance value. This oxidised, high-reflectance area is digitised, measured to scale, and divided by the prism window width to obtain a mean depth for the RPD (or particle bioturbation depth). The RPD depth is given special attention in these analyses, because it is a sensitive indicator of

the biological mixing depth, infaunal successional status, and within-station sediment patchiness. In the absence of bioturbating infauna, the RPD will achieve a maximum depth of up to 5 mm solely by diffusion depending on the concentration gradient of dissolved oxygen, reducing substrates within the sediment, water temperature (reaction rates), and sediment permeability.

The configuration of the RPD boundary is also of significance. In sandy sediments, physical forces dominate surface relief and RPD depth, which tends to be constant or uniform and does not necessarily follow the surface contours provided by bed-forms. In muddy sediments, the RPD is more complex and convoluted. Here, the RPD layers tend to be broadly uniform and more or less follow the contours of surface sediments. However, smaller scale convolutions are superimposed on this pattern in response to biogenic reworking by a resident infauna. Biogenic structures are regions of enhanced biological and geo-chemical activity where the activities of infaunal organisms can increase flux across the oxic-anoxic sediment interface (Diaz and Schaffner, 1988). Consequently, the RPD boundary is a complicated surface much greater in actual area than a simple aerial measurement would estimate and with a greater effect on sediment-water interface flux rates than is initially apparent (Diaz and Schaffner, 1988).

Another important characteristic of the RPD is the degree of contrast in reflectance values at this boundary. This contrast is related to the interactions among the amount of organic-loading and bioturbational activity in the sediment, and the levels of bottom water dissolved oxygen in an area. High inputs of labile organic material increase sediment oxygen demand, and subsequently sulphate reduction rates (and the abundance of sulphide end-products). This results in more highly reduced (lower-reflectance) sediments at depth and higher RPD contrasts. Although the SPI image analysis system quantifies the degree of contrast, this value can vary as a function of light intensity controls on the image analysis system, which are adjusted by the operator when a wide range of sediment types (e.g. silt-clay to coarse sand) is encountered. As a result, the quantified RPD contrast level may not be a meaningful parameter. However, a qualitative (visual) assessment of the RPD contrast (i.e. high versus low) is often considered in the interpretive process.

SEDIMENTARY METHANE

At extreme levels of organic-loading, pore-water sulphate is depleted, and methanogenesis occurs. The process of methanogenesis is detected by the appearance of methane bubbles in the sediment column. These gas-filled voids are readily discernible because of their irregular, generally circular aspect and glassy texture (due to the reflection of the strobe off the gas). If present, the number and total aerial coverage of all methane pockets is measured.

INFAUNAL SUCCESSIONAL STAGE

The mapping of successional stages is based on the theory that organism-sediment interactions follow a predictable sequence after a major seafloor perturbation. This theory states that primary succession results in the predictable appearance of macrobenthic invertebrates belonging to specific functional types following a benthic disturbance. These invertebrates interact with sediment in specific ways. Because functional types are the biological units of interest, this definition does not demand a sequential appearance of particular invertebrate species or genera. This theory is now well established in the scientific literature (see Pearson and Rosenberg, 1978; Rhoads and Boyer, 1982; Rhoads and Germano, 1986).

The term disturbance is used here to define natural processes, such as seafloor erosion, changes in seafloor chemistry, foraging disturbances which cause major reorganisation of the resident benthos, or anthropogenic impacts, such as dredged material or sewage sludge dumping, thermal effluents from power plants, pollution impacts from industrial discharge, etc. An important aspect of using this successional approach to interpret benthic monitoring results is relating organism-sediment relationships to the dynamical aspects of end-member seres. This involves deducing dynamics from structure, a technique pioneered by Johnson (1972) for marine soft-bottom habitats. The application of an inverse methods approach to benthic monitoring requires the *in situ* measurements of salient structural features of the organism-sediment relationships measured through SPI technology.

Pioneering (Stage 1) species are the first to colonise a new or newly disturbed bottom and reach high densities in a short time. Pioneering (Stage I) assemblages usually consist of dense aggregations of tubicolous or otherwise sedentary organisms that live near the sediment surface and feed at the surface or from the water column (Pearson and Rosenberg,

1978; Rhoads and Germano, 1986). *Capitella capitata, Malacoceros fuliginosus* and Spionidae species are typical forms. These functional types are usually restricted to the near surface of the bottom and their sedimentary effects include (i) the construction of dense tube aggregations which can influence sedimentation/erosion, (ii) deepening of the redox boundary by fluid bioturbation, and (iii) the occlusion of the sediment surface with faecal pellets. These associations are typically characterised by a shallow redox boundary and shallow bioturbation depths, particularly in the earliest stages of colonisation.

In the absence of further physical, chemical or biological disturbance, the pioneering assemblages are replaced by deposit feeders. This is progressive and can be arbitrarily divided into an intermediate and an equilibrium phase (Stages II and III, respectively). Typical Stage II species are shallow dwelling bivalves, tubicolous amphipods and some polychaete species.

Stage III taxa, in turn, represent high-order successional stages typically found in low disturbance regimes. A Stage III or equilibrium assemblage is persistent and is dominated by a bioturbating infauna, which feed at depth within the sediment. Sedimentary effects are distinctive and include (i) the transfer of water and particles over vertical distances of 10 - 20 cm, (ii) the production of homogeneously mixed fabrics by intensive reworking, with faecal pellets at and below the sediment surface, (iii) the creation of void feeding spaces at depth within the bottom, (iv) the extension of the redox boundary to c. 20 cm, and (v) the production of a distinctive surface microtopography unless smoothed over by tidal resuspension. Such deep-dwelling species as the polychaetes, *Pectinaria* sp., Maldanidae sp., the echinoderm, *Trachythyone elongata, Amphiura sp*. and *Echinocardium sp*. and the crustaceans *Lysiosquilla* sp., *Nephrops* sp. and *Upogebia* sp. These invertebrates are infaunal, and many feed at depth in a head-down orientation. The localised feeding activity results in distinctive excavations called feeding voids. Diagnostic features of these feeding structures include: a generally semicircular shape with a flat bottom and arched roof, and a distinct granulometric change in the sediment particles overlying the floor of the structure. This relatively coarse-grained material represents particles rejected by the head-down deposit-feeder. These deep-dwelling infaunal taxa preferentially ingest the finer sediment particles. In the retrograde transition of Stage III to Stage I, it is sometimes possible to recognise the presence of relict (i.e. collapsed and inactive) feeding voids. (It should be

added to the above generalisations that pioneering and higher successional species may coexist, if disturbance involves only the superficial sediment layers).

These end-member stages (Stages I and III) are easily recognised in SPI images by the presence of dense assemblages of near-surface polychaetes and/or the presence of subsurface feeding voids. Both types of assemblages may be present in the same image.

ADDITIONAL BIOLOGICAL PARAMETERS

Several additional biological parameters are measured from the digital images using the computer image analysis system. These include: the density per linear cm of polychaete and/or amphipod tubes at the sediment water interface; the minimum and maximum depth of faecal pellet layers and the minimum and maximum depth of feeding voids. Dominant faunal type (i.e. epifauna or infauna) and apparent species richness are also estimated.

SPI ORGANISM-SEDIMENT INDEX (OSI)

A multi-parameter SPI Organism-Sediment Index (OSI) has been constructed to characterise habitat quality and the method of its calculation is shown in Table 1.

The OSI is the sum of values allocated to the various physical/chemical and biological SPI parameters measured and it has a potential value range of -10 to +11. The Organism-Sediment Index is calculated automatically from the software after completion of all measurements from each digital image. This index has been found to be an excellent parameter for mapping disturbance gradients in an area and documenting eco-system recovery after disturbance.

Habitat quality is defined relative to two end-member standards. The lowest value is given to those bottoms which have low or dissolved oxygen in the overlying bottom water, no apparent macrofaunal life, and methane gas present in the sediment. The SPI OSI value for such a condition is minus 10. At the other end of the scale, an aerobic bottom with a deeply depressed RPD, evidence of a mature macrofaunal assemblage, and no apparent methane gas bubbles at depth will have a SPI OSI value of plus 11.

Chemical parameters	Index value	Biological parameters	Index value
Mean apparent RPD depth (cm)		**Successional stage (Primary succession)**	
0	**0**		
>0 - 0.75	**1**	Azoic	**-4**
0.76 - 1.50	**2**	Stage 1	**1**
1.51 - 2.25	**3**	Stage 1-2	**2**
2.26 - 3.00	**4**	Stage 2	**3**
3.01 - 3.75	**5**	Stage 2-3	**4**
>3.75	**6**	Stage 3	**5**
Methane Present	**-2**	**(Secondary succession)**	
No / low oxygen	**-4**	Stage 1 on Stage 2	**5**
		Stage 2 on Stage 3	**5**

Table 1. Method of calculating the Organism - Sediment Index (OSI) value.

From experience with mapping this parameter, values of +7 to +11 are typical of undisturbed sediments while values ≤ 6 tend to be found at sites which have experienced recent physical disturbance (e.g. bottom erosion by currents or disturbance of the bottom by scavenging fish or crustaceans) or are chemically stressed, organically loaded, sulphidic or contaminated in some way. In dealing with areas which are subject to organic enrichment (which may have a variety of origins ranging from natural runoff to anthropogenic inputs), OSI values in the range +6 to +1 generally indicate an overload situation where inputs exceed the capacity of the system and organic matter accumulates on the bottom. Index values which fall in the range +1 to -10 identify varying degrees of habitat degradation associated with a continual accumulation of organic matter and an oxygen depletion on the bottom. At the upper end of the scale, it has been found that OSI values of the order of +11 may reflect a productivity enhancement stage of organic enrichment where natural plant and animal production is increase in response to the ready availability of particulate organic material.

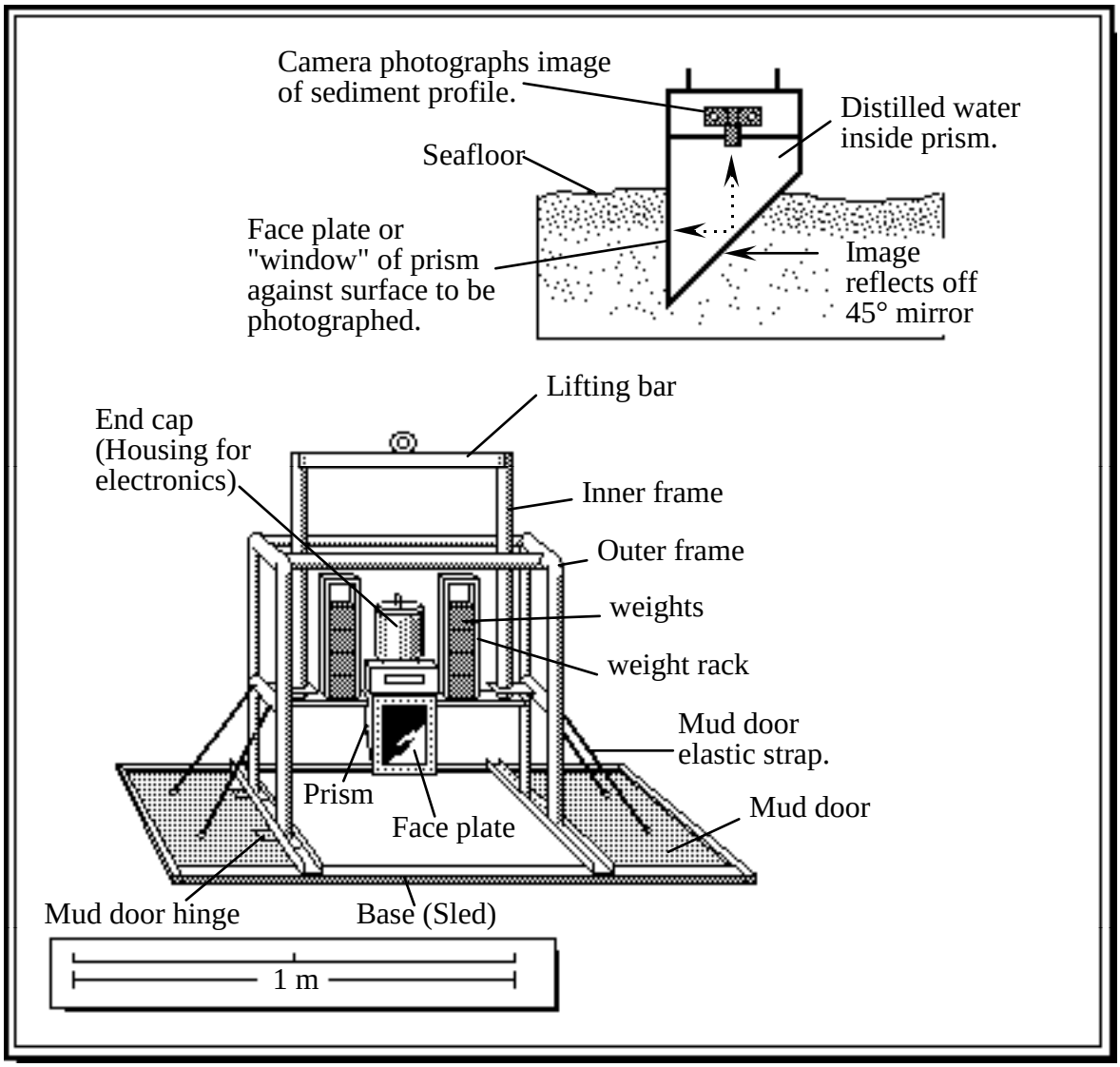

Figure 1. Representation of the remotely operated **S**ediment **P**rofile **I**magery camera.

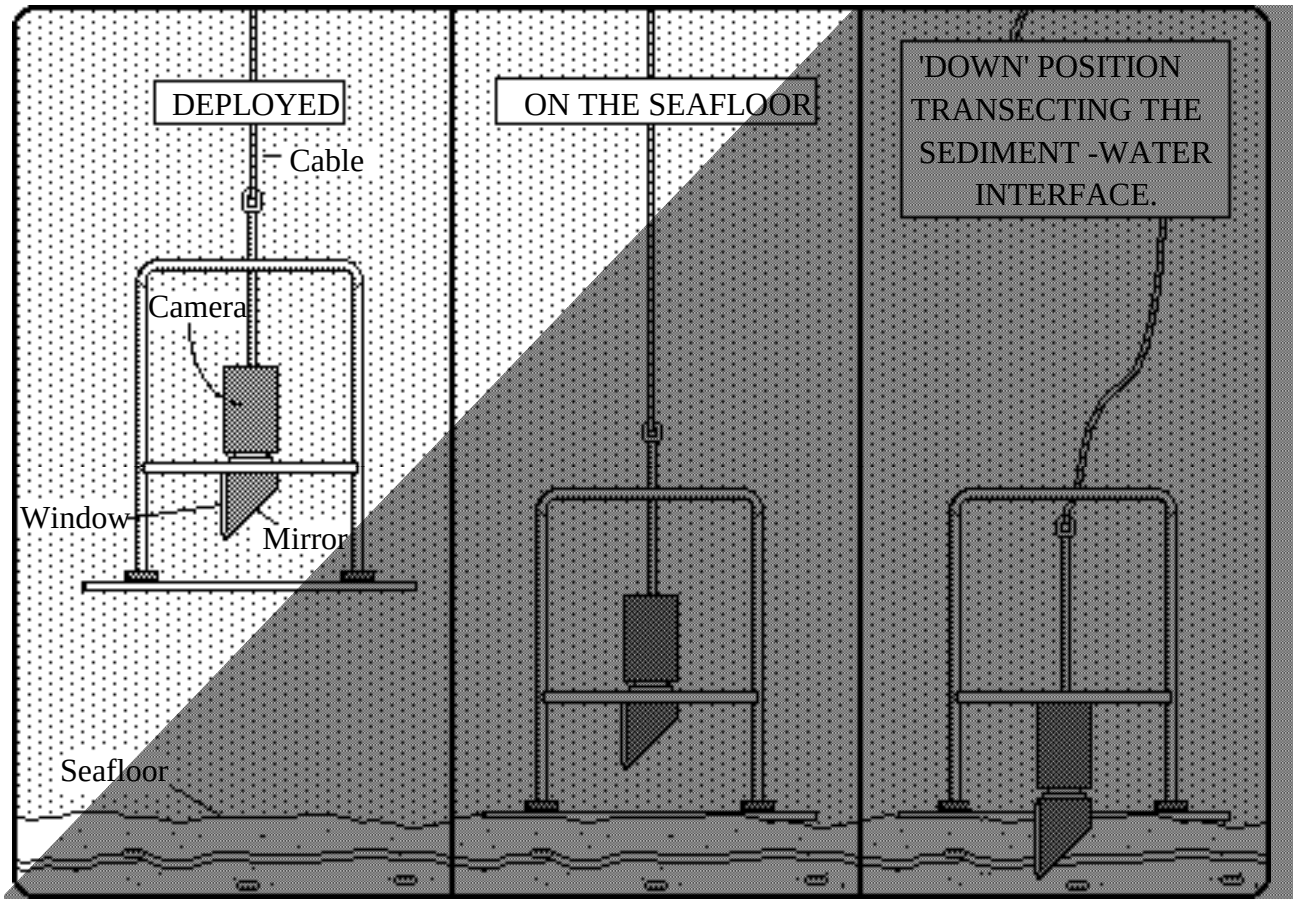

Figure 2. **S**ediment **P**rofile **I**magery (SPI): camera deployment on the seafloor.

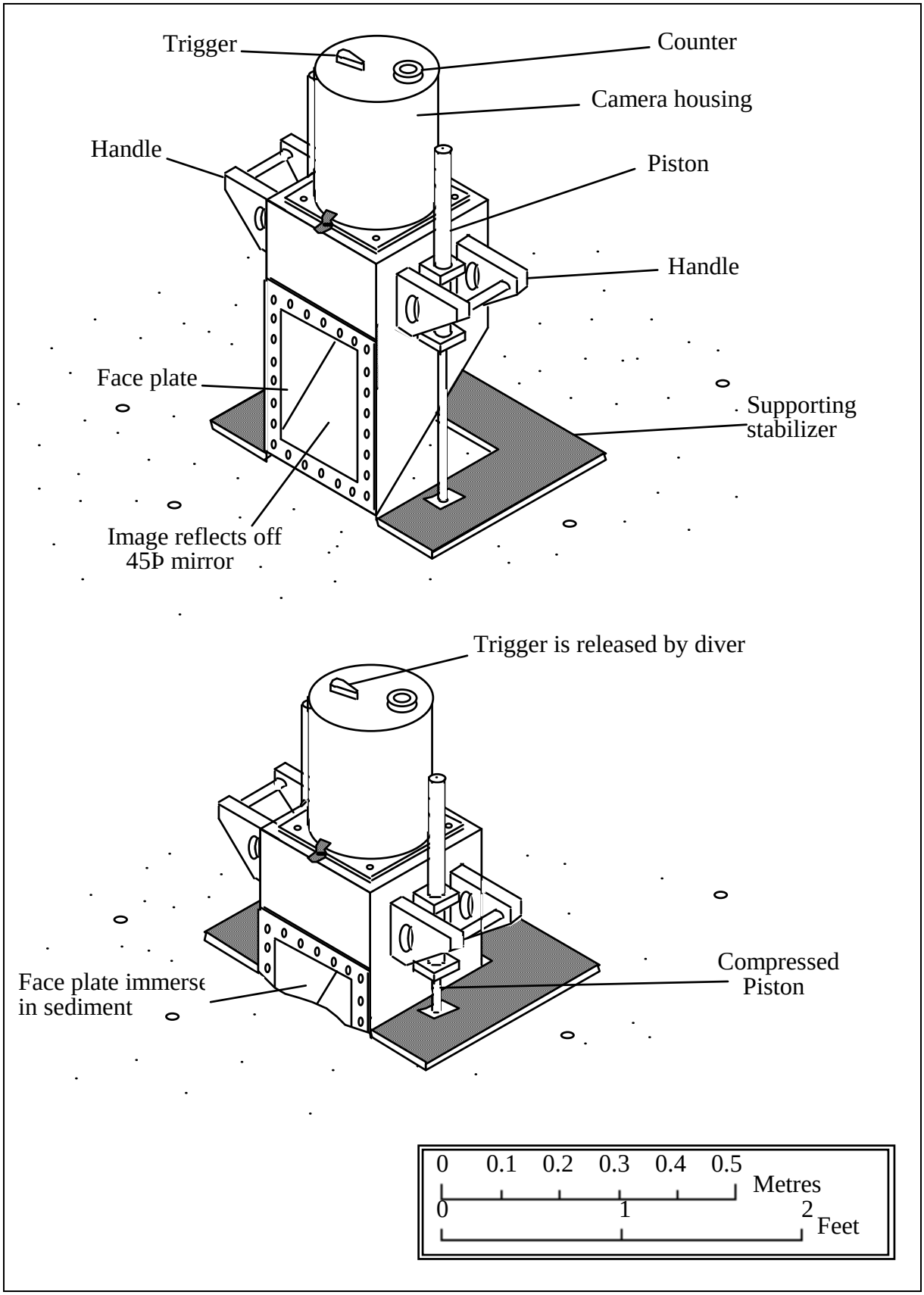

Figure 3. Details of the diver operated **S**ediment **P**rofile **I**magery (SPI) camera.

Appendix III
Faunal Abundance
Species List

Station			DG16	DG17	DG18	DG19	DG20	DG21	DG22	DG39	DG40	DG41
CNIDARIA	D	1	0	0	0	0	0	0	0	0	0	0
ACTINIARIA	D	662	0	0	0	0	0	0	0	0	0	0
Actiniaria sp.	D	662	0	0	0	0	0	0	1	0	0	0
Sagartia troglodytes	D	715	2	0	0	0	0	0	0	0	0	0
Edwardsia claparedii	D	766	0	0	0	1	0	0	0	0	0	0
PLATYHELMINTHES	F	1	0	0	0	0	0	0	0	0	0	0
Turbellaria	F	2	0	0	0	0	0	0	0	0	0	0
Turbellaria sp.	F	2	2	1	1	1	1	0	0	0	2	0
NEMATODA	HD	1	0	0	0	0	0	0	0	0	0	0
Nematoda sp.	HD	1	2	0	0	0	5	0	1	1	2	0
ENDOPLINA	HD	5	0	0	0	0	0	0	0	0	0	0
Thoracostomopsidae	HD	13	0	0	0	0	0	0	0	0	0	0
Mesacanthion cf. diplechma	HD	32	2	0	0	0	0	0	0	0	0	0
CHROMADORINA	HD	178	0	0	0	0	0	0	0	0	0	0
Comesomatidae	HD	247	0	0	0	0	0	0	0	0	0	0
Dorylaimopsis punctata	HD	249	2	0	0	2	0	0	1	1	0	1
Comesoma sp.	HD	250	0	0	0	0	0	1	0	0	0	0
Sabatieria sp.	HD	254	2	0	0	0	0	0	0	0	0	0
Sabatieria praedatrix	HD	262	0	0	1	1	0	1	4	3	0	2
NEMERTEA	G	1	0	0	0	0	0	0	0	0	0	0
Nemertea sp.	G	1	8	8	6	7	4	3	5	7	4	5
PRIAPULIDA	J	1	0	0	0	0	0	0	0	0	0	0
Priapulus caudatus	J	7	0	2	0	1	0	0	2	2	4	1
SIPUNCULA	N	1	0	0	0	0	0	0	0	0	0	0
GOLFINGIIFORMES	N	10	0	0	0	0	0	0	0	0	0	0
Golfingiidae	N	11	0	0	0	0	0	0	0	0	0	0
Golfingia vulgaris	N	17	0	1	0	0	0	0	0	0	0	0
Thysanocardia procera	N	28	0	1	2	10	2	0	3	4	6	1
Phascolion strombus strombus	N	34	1	0	0	0	0	0	0	0	0	0

Station			DG16	DG17	DG18	DG19	DG20	DG21	DG22	DG39	DG40	DG41
ANNELIDA	P	1	0	0	0	0	0	0	0	0	0	0
PHYLLODOCIDA	P	3	0	0	0	0	0	0	0	0	0	0
Polynoidae	P	25	0	0	0	0	0	0	0	0	0	0
Polynoidae sp.	P	25	0	0	0	0	1	0	0	0	0	0
Harmothoe andreapolis	P	51	1	0	0	1	0	0	0	0	0	0
Pholoidae	P	90	0	0	0	0	0	0	0	0	0	0
Pholoe sp.	P	91	1	0	0	0	0	0	0	0	0	0
Pholoe inornata	P	92	0	1	2	0	0	0	0	0	0	2
Phyllodocidae	P	114	0	0	0	0	0	0	0	0	0	0
Pseudomystides spinachia	P	137	0	0	0	0	0	0	1	0	0	0
Paranaitis kosteriensis	P	176	1	0	0	0	0	0	0	0	0	0
Phyllodoce sp.	P	178	1	0	0	0	0	0	0	0	0	0
Glyceridae	P	254	0	0	0	0	0	0	0	0	0	0
Glycera alba	P	256	0	2	1	1	1	0	1	1	0	1
Glycera rouxi	P	263	4	1	0	0	1	0	1	0	0	1
Goniadidae	P	266	0	0	0	0	0	0	0	0	0	0
Glycinde nordmanni	P	268	0	0	0	0	0	0	0	0	1	0
Goniada maculata	P	271	8	0	1	2	1	0	2	0	0	2
Hesionidae	P	293	0	0	0	0	0	0	0	0	0	0
Ophiodromus flexuosus	P	313	7	2	1	4	6	4	5	4	3	6
Ancistrosyllis groenlandica	P	338	5	5	4	5	2	2	5	8	13	5
Syllidae	P	346	0	0	0	0	0	0	0	0	0	0
Exogone hebes	P	421	1	2	0	0	0	0	0	0	0	0
Nereididae	P	458	0	0	0	0	0	0	0	0	0	0
Nereididae sp.	P	458	0	0	0	0	0	0	0	0	1	0
Nephtyidae	P	490	0	0	0	0	0	0	0	0	0	0
Nephtys sp.	P	494	1	1	1	1	0	0	0	0	1	1
Nephtys hombergii	P	499	6	0	0	0	0	0	0	0	0	0
Nephtys incisa	P	501	3	4	14	14	11	7	10	13	13	8
Lumbrineridae	P	569	0	0	0	0	0	0	0	0	0	0

Station			DG16	DG17	DG18	DG19	DG20	DG21	DG22	DG39	DG40	DG41
Lumbrineridae sp.	P	569	1	0	1	0	0	0	0	0	0	0
Lumbrineris sp.	P	572	0	0	0	0	0	0	0	2	0	1
Lumbrineris gracilis	P	579	31	3	1	4	2	0	3	0	0	1
Abyssoninoe hibernica	P	580	0	0	0	0	0	0	1	0	0	0
Lumbrineris latreilli	P	582	0	1	0	1	0	0	0	0	0	0
ORBINIIDA	P	654	0	0	0	0	0	0	0	0	0	0
Orbiniidae	P	655	0	0	0	0	0	0	0	0	0	0
Scoloplos armiger	P	672	1	1	0	0	0	0	0	0	0	0
SPIONIDA	P	707	0	0	0	0	0	0	0	0	0	0
Poecilochaetidae	P	716	0	0	0	0	0	0	0	0	0	0
Poecilochaetus serpens	P	718	2	0	0	0	0	0	0	0	0	0
Spionidae	P	720	0	0	0	0	0	0	0	0	0	0
Spionidae sp.	P	720	1	1	1	0	0	0	0	1	0	0
Minuspio cf. multibranchiata	P	746	2	0	0	0	1	0	0	0	0	0
Spio sp.	P	787	1	1	3	1	1	0	1	2	2	1
Spiophanes sp.	P	793	0	2	0	0	0	2	0	1	0	0
Spiophanes bombyx	P	794	3	1	0	0	0	0	0	2	0	0
Spiophanes cf. kroyeri	P	795	0	0	3	0	1	0	1	0	1	2
Magelonidae	P	802	0	0	0	0	0	0	0	0	0	0
Magelona alleni	P	804	11	17	25	14	16	6	23	14	11	21
Magelona minuta	P	806	7	1	1	7	5	4	1	3	0	3
Chaetopteridae	P	810	0	0	0	0	0	0	0	0	0	0
Spiochaetopterus typicus	P	820	0	0	0	1	0	0	0	0	0	0
Cirratulidae	P	822	0	0	0	0	0	0	0	0	0	0
Aphelochaeta sp.	P	823	0	1	4	3	3	0	3	3	0	1
Aphelochaeta marioni	P	824	0	0	0	0	0	0	1	0	0	0
Cirratulus caudatus	P		1	0	0	0	0	0	0	0	0	0
Tharyx killariensis	P	846	2	1	1	3	1	0	1	1	0	2
FLABELLIGERIDA	P	872	0	0	0	0	0	0	0	0	0	0
Flabelligeridae	P	873	0	0	0	0	0	0	0	0	0	0

Station			DG16	DG17	DG18	DG19	DG20	DG21	DG22	DG39	DG40	DG41
Diplocirrus glaucus	P	878	136	115	66	114	36	11	25	69	29	63
CAPITELLIDA	P	902	0	0	0	0	0	0	0	0	0	0
Capitellidae	P	903	0	0	0	0	0	0	0	0	0	0
Capitella capitata	P	907	0	0	0	0	0	0	1	0	0	0
Notomastus latericeus	P	921	6	0	0	2	0	1	1	1	0	0
Maldanidae	P	938	0	0	0	0	0	0	0	0	0	0
Maldanidae sp.	P	938	1	1	0	0	0	0	0	0	0	0
Clymenura tricirrata	P		5	0	0	0	0	0	0	0	0	0
Praxillella affinis	P	971	2	0	0	0	0	0	0	0	0	0
Scalibregmatidae	P	1020	0	0	0	0	0	0	0	0	0	0
Scalibregma inflatum	P	1027	253	32	561	503	160	65	96	321	435	137
OWENIIDA	P	1089	0	0	0	0	0	0	0	0	0	0
Oweniidae	P	1090	0	0	0	0	0	0	0	0	0	0
Myriochele oculata	P		4	0	0	1	0	0	0	0	0	0
Owenia fusiformis	P	1098	1	0	0	1	0	0	1	0	0	1
TEREBELLIDA	P	1099	0	0	0	0	0	0	0	0	0	0
Pectinariidae	P	1100	0	0	0	0	0	0	0	0	0	0
Amphictene auricoma	P	1102	1	0	0	0	0	0	0	0	0	0
Pectinaria sp.	P	1106	2	0	0	0	0	0	0	0	0	0
Pectinaria belgica	P	1109	0	3	3	3	0	2	1	3	2	1
Ampharetidae	P	1118	0	0	0	0	0	0	0	0	0	0
Melinna palmata	P	1124	5	12	4	5	2	0	2	1	0	7
Ampharetinae sp.	P	1125	1	0	0	0	0	0	0	0	0	0
Ampharete sp.	P	1133	0	0	0	0	0	0	1	0	0	0
Trichobranchidae	P	1171	0	0	0	0	0	0	0	0	0	0
Terebellides stroemi	P	1175	0	0	0	0	0	0	0	0	0	1
Terebellidae	P	1179	0	0	0	0	0	0	0	0	0	0
Terebellidae indet.	P	1179	0	0	1	1	0	0	0	0	0	0
Polycirrinae	P	1227	0	0	0	0	0	0	0	0	0	0
Polycirrus sp.	P	1235	0	0	0	0	0	0	0	0	0	1

Station			DG16	DG17	DG18	DG19	DG20	DG21	DG22	DG39	DG40	DG41
Polycirrus medusa	P	1242	1	0	0	0	0	0	0	0	0	0
OLIGOCHAETA	P	1402	0	0	0	0	0	0	0	0	0	0
Oligochaeta sp.	P	1402	0	0	0	1	0	0	0	0	0	0
TUBIFICIDA	P	1403	0	0	0	0	0	0	0	0	0	0
Tubificinae	P	1473	0	0	0	0	0	0	0	0	0	0
Tubificoides amplivasatus	P	1489	4	23	10	37	11	18	7	6	10	10
CRUSTACEA	R	1	0	0	0	0	0	0	0	0	0	0
COPEPODA	R	142	0	0	0	0	0	0	0	0	0	0
CENTROPAGOIDEA	R	284	0	0	0	0	0	0	0	0	0	0
Candaciidae	R	308	0	0	0	0	0	0	0	0	0	0
Candacia armata	R	310	0	0	0	0	0	0	0	1	0	0
AMPHIPODA	S	97	0	0	0	0	0	0	0	0	0	0
Oedicerotidae	S	118	0	0	0	0	0	0	0	0	0	0
Westwoodilla caecula	S	140	0	0	1	0	0	0	0	0	0	0
Leucothoidae	S	175	0	0	0	0	0	0	0	0	0	0
Leucothoe lilljeborgi	S	178	1	2	2	2	0	0	2	0	1	0
Urothoidae	S	245	0	0	0	0	0	0	0	0	0	0
Urothoe elegans	S	248	4	0	0	0	0	0	0	0	0	0
Phoxocephalidae	S	252	0	0	0	0	0	0	0	0	0	0
Harpinia antenaria	S	254	3	0	0	0	0	0	0	0	0	0
Harpinia crenulata	S	255	1	1	1	0	0	0	0	0	0	1
Ampeliscidae	S	422	0	0	0	0	0	0	0	0	0	0
Ampelisca sp.	S	423	0	0	0	0	1	0	1	0	0	0
Ampelisca brevicornis	S	427	2	0	0	0	0	0	0	0	1	1
Ampelisca spinipes	S	438	2	1	0	0	0	0	0	0	0	1
Gammaridae	S	464	0	0	0	0	0	0	0	0	0	0
Gammaridae sp.	S	464	0	0	0	0	0	0	1	0	0	0
Melitidae	S	495	0	0	0	0	0	0	0	0	0	0
Melitidae sp.	S	495	1	0	0	0	0	0	0	0	0	0
Phtisicidae	S	655	0	0	0	0	0	0	0	0	0	0

Station			DG16	DG17	DG18	DG19	DG20	DG21	DG22	DG39	DG40	DG41
Pseudoprotella phasma	S	659	1	0	0	0	0	0	0	0	0	0
TANAIDACEA	S	1099	0	0	0	0	0	0	0	0	0	0
Leptognathiinae	S	1130	0	0	0	0	0	0	0	0	0	0
Leptognathia gracilis	S	1133	4	1	0	2	0	0	0	3	1	0
CUMACEA	S	1183	0	0	0	0	0	0	0	0	0	0
Bodotriidae	S	1184	0	0	0	0	0	0	0	0	0	0
Iphinoe serrata	S	1201	7	2	1	0	0	0	0	0	0	2
Leuconiidae	S	1204	0	0	0	0	0	0	0	0	0	0
Eudorella truncatula	S	1208	1	1	0	0	1	0	1	0	1	1
Diastylidae	S	1244	0	0	0	0	0	0	0	0	0	0
Diastylis sp.	S	1224	1	0	0	0	0	0	0	0	0	0
Diastylis bradyi	S	1248	3	1	0	1	0	0	0	0	0	0
Diastylis lucifera	S	1252	0	0	1	0	0	0	0	0	0	0
DECAPODA	S	1276	0	0	0	0	0	0	0	0	0	0
Decapoda sp.	S	1276	0	0	0	0	0	1	0	0	0	0
Decapoda larvae	S	1276	2	0	0	0	0	0	0	1	0	0
ALPHEOIDEA	S	1327	0	0	0	0	0	0	0	0	0	0
Processidae	S	1361	0	0	0	0	0	0	0	0	0	0
Processa nouveli holothuisi	S	1367	0	0	0	0	0	1	0	0	0	0
THALASSINOIDEA	S	1404	0	0	0	0	0	0	0	0	0	0
Lemidiidae	S	1410	0	0	0	0	0	0	0	0	0	0
Jaxea nocturna	S	1412	0	1	1	0	1	1	1	3	1	0
Callianassidae	S	1413	0	0	0	0	0	0	0	0	0	0
Callianassa subterranea	S	1415	0	1	0	0	0	0	0	2	0	0
BRACHYURA	S	1485	0	0	0	0	0	0	0	0	0	0
Brachyura sp.	S	1485	0	0	0	0	0	0	0	0	1	0
Goneplacidae	S	1603	0	0	0	0	0	0	0	0	0	0
Goneplax rhomboides	S	1606	0	0	0	0	0	0	0	1	0	0
MOLLUSCA	W	1	0	0	0	0	0	0	0	0	0	0
CAUDOFOVEATA	W	2	0	0	0	0	0	0	0	0	0	0

Station			DG16	DG17	DG18	DG19	DG20	DG21	DG22	DG39	DG40	DG41
Chaetoderma nitidulum	W	9	2	0	0	0	0	0	0	0	0	0
MESOGASTROPODA	W	256	0	0	0	0	0	0	0	0	0	0
RISSOACEA	W	319	0	0	0	0	0	0	0	0	0	0
Rissoinae	W	325	0	0	0	0	0	0	0	0	0	0
Rissoa sp.	W	326	0	0	0	0	0	0	0	0	0	1
Epitoniidae	W	541	0	0	0	0	0	0	0	0	0	0
Epitonium clathrus	W	549	1	0	0	0	0	0	0	0	0	0
NEOGASTROPODA	W	670	0	0	0	0	0	0	0	0	0	0
CEPHALASPIDEA	W	1002	0	0	0	0	0	0	0	0	0	0
Cylichnidae	W	1024	0	0	0	0	0	0	0	0	0	0
Cylichna cylindracea	W	1028	3	1	0	1	2	1	0	0	0	0
NUCULOIDA	W	1561	0	0	0	0	0	0	0	0	0	0
Nuculidae	W	1563	0	0	0	0	0	0	0	0	0	0
Nucula sp.	W	1565	1	0	0	0	0	0	0	0	0	0
Nucula hanleyi	W	1568	1	0	0	0	0	1	1	0	2	0
Nucula nitidosa	W	1569	1	0	0	0	0	0	0	0	0	0
Nucula nucleus	W	1570	4	0	0	0	0	0	1	0	0	0
VENEROIDA	W	1815	0	0	0	0	0	0	0	0	0	0
Thyasiridae	W	1833	0	0	0	0	0	0	0	0	0	0
Thyasira flexuosa	W	1837	0	0	0	0	2	0	0	0	1	0
Montacutidae	W	1888	0	0	0	0	0	0	0	0	0	0
Mysella bidentata	W	1906	1	0	0	0	0	0	1	0	0	0
Semelidae	W	2057	0	0	0	0	0	0	0	0	0	0
Abra alba	W	2059	2	1	2	1	2	0	0	2	0	0
Abra nitida	W	2061	0	0	0	0	0	0	0	0	1	0
Veneridae	W	2086	0	0	0	0	0	0	0	0	0	0
Mysia undata	W	2139	1	0	0	0	0	0	0	0	0	0
PHORONIDA	ZA	1	0	0	0	0	0	0	0	0	0	0
Phoronidae	ZA	2	0	0	0	0	0	0	0	0	0	0
Phoronidae sp.	ZA	2	2	0	0	0	0	0	0	0	1	0

Station			**DG16**	**DG17**	**DG18**	**DG19**	**DG20**	**DG21**	**DG22**	**DG39**	**DG40**	**DG41**
Phoronis sp.	ZA	3	2	4	14	11	3	6	7	5	3	13
ECHINODERMATA	ZB	2	0	0	0	0	0	0	0	0	0	0
OPHIUROIDEA	ZB	105	0	0	0	0	0	0	0	0	0	0
OPHIURIDA	ZB	121	0	0	0	0	0	0	0	0	0	0
Amphiuridae	ZB	148	0	0	0	0	0	0	0	0	0	0
Amphiura sp. juvenile	ZB	149	15	21	4	3	3	0	0	0	1	3
Amphiura chiajei	ZB	152	0	3	5	1	2	0	0	0	0	7
Amphiura filiformis	ZB	154	143	192	10	42	21	5	6	1	1	120
Ophiuridae	ZB	165	0	0	0	0	0	0	0	0	0	0
Ophiura sp. juvenile	ZB	166	0	0	1	0	0	0	0	0	0	0
DENDROCHIROTIDA	ZB	249	0	0	0	0	0	0	0	0	0	0
Phyllophoridae	ZB	258	0	0	0	0	0	0	0	0	0	0
Thyone fusus	ZB	262	0	0	0	0	0	0	0	0	0	1
Cucumariidae	ZB	266	0	0	0	0	0	0	0	0	0	0
Leptopentacta elongata	ZB	280	147	152	700	1059	70	423	552	436	185	139
APODIDA	ZB	289	0	0	0	0	0	0	0	0	0	0
Synaptidae	ZB	290	0	0	0	0	0	0	0	0	0	0
Leptosynapta sp.	ZB	291	1	0	0	0	0	0	0	0	0	0
Leptosynapta bergensis	ZB	292	3	0	0	2	0	2	0	0	0	0

Appendix IV
Grab Sample Log

Project: Pockmark ground-truthing survey in Dunmanus Bay, Co. Cork

Curise: CV09_23

Date: 22-28 April 2009

Vessel: Celtic Voyager

To meet the scientific objectives of the project various sampling instruments were used. Surficial sediment collection for the purpose of biological sampling and sedimentological investigations was performed with a Day Grab sampler. A Reineck Box Corer was employed to gain an insight into the first 20cm of sediment without disturbing the surface. Also several sediment cores were collected with a Gravity Corer fitted with a 2m long barrel. Performance of the sampling instruments varied between different seabed types. The Day Grab and Reineck Box Corer were most reliable on soft fine-grained sediments and underperformed slightly on coarser sands with a high percentage of shell hash. The Gravity Corer performance was less than optimal since even in very soft sediment full recovery was not achieved. Highest recovery was 1.3m with an average recovery around 1.0m

Sample label	CV09_23_001	Station	001	Type	Grab	Date	23/04/09
Instrument	Day Grab	Depth	40.0m	Lat	51 33.5380' N	Long	9 42.7750' W
Description	Very fine smooth and sticky mud. Gelatinous structure and very homogeneous. Very well sorted. Dark green/grey in colour. There is a very fine sand matrix but this was hard to see due to the sticky nature of the mud.						
Anticipated testing	CNS analysis (DCU), heavy metals (DCU, UL), bulk stable carbon (DCU)						

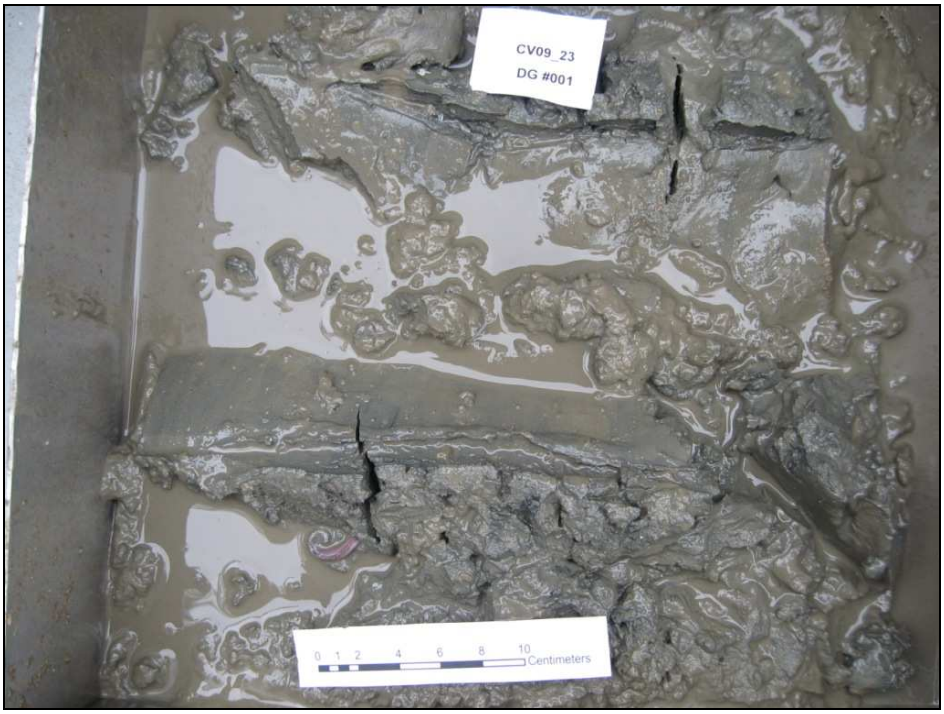

Sample label	CV09_23_002	Station	002	Type	Grab	Date	23/04/09
Instrument	Day Grab	Depth	41.0m	Lat	51 33.6000' N	Long	9 42.7500' W
Description	Sample is very similar to the previous one. Very fine sticky med. Dark green/grey in colour. No in fauna present (visible). Homogeneous and smooth.						
Anticipated testing	CNS analysis (DCU), heavy metals (DCU, UL), bulk stable carbon (DCU)						

Sample label	CV09_23_003	Station	003	Type	Grab	Date	23/04/09
Instrument	Day Grab	Depth	41.3m	Lat	51 33.5740’ N	Long	9 42.7380’ W
Description	Very fine sticky mud as in previous sample						
Anticipated testing	CNS analysis (DCU), heavy metals (DCU, UL), bulk stable carbon (DCU)						

Sample label	CV09_23_004	Station	004	Type	Grab	Date	23/04/09
Instrument	Day Grab	Depth		Lat	51 33.6090’ N	Long	9 42.7050’ W
Description	Very fine sticky mud. Slight change in colour from previous sample. Black bands redox layering throughout the sample (Running parallel) Dark green/grey and black in colour						
Anticipated testing	CNS analysis (DCU), heavy metals (DCU, UL), bulk stable carbon (DCU)						

Sample label	CV09_23_005	Station	005	Type	Grab	Date	23/04/09
Instrument	Day Grab	Depth	41.0m	Lat	51 33.6250’ N	Long	9 42.6370’ W
Description	Sample is similar in composition as previous sample and the black 'banding' redox layer is also clear throughout the sample. Very sticky texture (quite dry compared to previous sample)						
Anticipated testing	CNS analysis (DCU), heavy metals (DCU, UL), bulk stable carbon (DCU)						

Sample label	CV09_23_006	Station	006	Type	Grab	Date	23/04/09
Instrument	Day Grab	Depth	41.5m	Lat	51 33.6680’ N	Long	9 42.6290’ W
Description	A very fine sticky mud with slightly less black 'banding' within the sample. Similar in colour (main sample). No in fauna visible.						
Anticipated testing	CNS analysis (DCU), heavy metals (DCU, UL), bulk stable carbon (DCU)						

Sample label	CV09_23_007	**Station**	007	**Type**	Grab	**Date**	23/04/09
Instrument	Day Grab	**Depth**	41.6m	**Lat**	51 33.6220' N	**Long**	9 42.5640' W
Description	A very fine mud. This sample is a lot stiffer than in previous samples. Very obvious and clear black redox layer throughout the sample. Dark grey/green in colour. There were also 2 strands of a grassy nature in the sample.						
Anticipated testing	CNS analysis (DCU), heavy metals (DCU, UL), bulk stable carbon (DCU)						

Sample label	CV09_23_008	**Station**	008	**Type**	Grab	**Date**	23/04/09
Instrument	Day Grab	**Depth**	41.6m	**Lat**	51 33.6590' N	**Long**	9 42.5620' W
Description	A similar mud in composition to previous sample but the sample is a lot less sticky in nature and has a more fluid appearance. There is no odour in this sample						
Anticipated testing	CNS analysis (DCU), heavy metals (DCU, UL), bulk stable carbon (DCU)						

Sample label	CV09_23_009	**Station**	009	**Type**	Grab	**Date**	23/04/09
Instrument	Day Grab	**Depth**	41.6m	**Lat**	51 33.6780' N	**Long**	9 42.5560' W
Description	Moderately sticky mud (very fine sand matrix hard to see/feel). Black banding (redox layer) again very clear in sample.						
Anticipated testing	CNS analysis (DCU), heavy metals (DCU, UL), bulk stable carbon (DCU)						

Sample label	CV09_23_010	**Station**	010	**Type**	Grab	**Date**	23/04/09
Instrument	Day Grab	**Depth**	41.6m	**Lat**	51 33.6810' N	**Long**	9 42.5578' W
Description	Black sticky slightly rough textured mud with fine - medium sand in matrix c.10% (Hard to see but texture could be felt) Light -medium brown algae visible on top of sample Very intense odour						
Anticipated testing	CNS analysis (DCU), heavy metals (DCU, UL), bulk stable carbon (DCU)						

Sample label	CV09_23_011	**Station**	011	**Type**	Grab	**Date**	23/04/09
Instrument	Day Grab	**Depth**	41.7m	**Lat**	51 33.6820’ N	**Long**	9 42.5700’ W
Description	A dark green/grey smooth homogeneous mud. Slightly sticky in texture.						
Anticipated testing	CNS analysis (DCU), heavy metals (DCU, UL), bulk stable carbon (DCU)						

Sample label	CV_09_23_012	**Station**	012	**Type**	Grab	**Date**	23/04/09
Instrument	Day Grab	**Depth**	42.1m	**Lat**	51 33.6380’ N	**Long**	9 42.6660’ W
Description	Very slight coarser texture to the matrix of this mud - possibly fine sand (this could be easily felt). Green/grey in colour and very homogeneous. 2-3 red worms present						
Anticipated testing	CNS analysis (DCU), heavy metals (DCU, UL), bulk stable carbon (DCU)						

Sample label	CV09_23_013	**Station**	013	**Type**	Grab	**Date**	23/04/09
Instrument	Day Grab	**Depth**	42.0m	**Lat**	51 33.6850’ N	**Long**	9 42.6260’ W
Description	Sample is similar to previous one (012) with the same slightly coarser texture of a fine sand matrix. No in fauna visible						
Anticipated testing	CNS analysis (DCU), heavy metals (DCU, UL), bulk stable carbon (DCU)						

Sample label	CV_09_23_014	**Stationn**	014	**Type**	Grab	**Date**	23/04/09
Instrument	Day Grab	**Depth**		**Lat**	51 33.6370’ N	**Long**	9 42.6280’ W
Description	Very smooth fine sandy mud with a 'polished' texture and appearance. Sand matrix c. 5-10%, easier to see this matrix compared to previous samples. Quite sticky and very homogeneous. No in fauna visible.						
Anticipated testing	CNS analysis (DCU), heavy metals (DCU, UL), bulk stable carbon (DCU)						

Sample label	CV09_23_015	**Station**	015	**Type**	Grab	**Date**	23/04/09
Instrument	Day Grab	**Depth**	42.3m	**Lat**	51 33.6128' N	**Long**	9 42.5793' W
Description	This mud is very dry and stiff in composition. Very well sorted homogeneous dark grey/green mud. Little to none black bands visible.						
Anticipated testing	CNS analysis (DCU), heavy metals (DCU, UL), bulk stable carbon (DCU)						

Sample label	CV_09_23_023	**Station**	023	**Type**	Grab	**Date**	24/04/09
Instrument	Day Grab	**Depth**	39.7m	**Lat**	51 33.6860' N	**Long**	9 42.5500' W
Description	Profile almost visible - Black/grey mud on bottom with drift dark green/grey sand on top. Sample is quite stiff and sticky in nature.						
Anticipated testing	CNS analysis (DCU), heavy metals (DCU, UL), bulk stable carbon (DCU)						

Sample label	CV09_23_024	**Station**	024	**Type**	Grab	**Date**	24/04/09
Instrument	Day Grab	**Depth**	39.6m	**Lat**	51 33.6815' N	**Long**	9 42.5315' W
Description	This mud is more unconsolidated (fluid) than previous sample.						
Anticipated testing	CNS analysis (DCU), heavy metals (DCU, UL), bulk stable carbon (DCU)						

Sample label	CV_09_23_025	**Station**	025	**Type**	Grab	**Date**	24/04/09
Instrument	Day Grab	**Depth**	39.7m	**Lat**	51 33.6678' N	**Long**	9 42.5744' W
Description	Similar to previous sample some small consolidated fragments in the mud						
Anticipated testing	CNS analysis (DCU), heavy metals (DCU, UL), bulk stable carbon (DCU)						

Sample label	CV09_23_026	Station	026	Type	Grab	Date	24/04/09
Instrument	Day Grab	Depth	39.7m	Lat	51 33.6643' N	Long	9 42.5739' W
Description	Mud is sticky and stiff in composition. Contains a lot more sea cucumbers than in previous samples. Dark green/greyish black in colour.						
Anticipated testing	CNS analysis (DCU), heavy metals (DCU, UL), bulk stable carbon (DCU)						

Sample label	CV_09_23_027	Station	027	Type	Grab	Date	24/04/09
Instrument	Day Grab	Depth	39.6m	Lat	51 33.6761' N	Long	9 42.5863' W
Description	Stiff and sticky fine - very fine sandy mud.						

Anticipated testing	CNS analysis (DCU), heavy metals (DCU, UL), bulk stable carbon (DCU)

Sample label	CV09_23_028	**Station**	028	**Type**	Grab	**Date**	24/04/09
Instrument	Day Grab	**Depth**	39.7m	**Lat**	51 33.6796' N	**Long**	9 42.5570' W
Description	Very similar to previous sample. Stick and stiff in composition.						
Anticipated testing	CNS analysis (DCU), heavy metals (DCU, UL), bulk stable carbon (DCU)						

Sample label	CV_09_23_029	**Station**	029	**Type**	Grab	**Date**	24/04/09
Instrument	Day Grab	**Depth**	39.4m	**Lat**	51 33.6864' N	**Long**	9 42.6085' W
Description	This sample is more unconsolidated than previous with a slight sulphide odour. Visible redox layer within sample.						

Anticipated testing	CNS analysis (DCU), heavy metals (DCU, UL), bulk stable carbon (DCU)

Sample label	CV09_23_030	**Station**	030	**Type**	Grab	**Date**	24/04/09
Instrument	Day Grab	**Depth**	39.4m	**Lat**	51 33.6952' N	**Long**	9 42.5706' W
Description	Visible redox layer in sample. Very fluid and unconsolidated -a lot less sticky and stiff. Some small black globules of organic matter in the sample.						
Anticipated testing	CNS analysis (DCU), heavy metals (DCU, UL), bulk stable carbon (DCU)						

Sample label	CV_09_23_031	**Station**	031	**Type**	Grab	**Date**	24/04/09
Instrument	Day Grab	**Depth**	39.4m	**Lat**	51 33.6887' N	**Long**	9 42.5656' W
Description	No odour or redox layer. Sampler is quite unconsolidated and more fluid, little to none						

	stickiness.
Anticipated testing	CNS analysis (DCU), heavy metals (DCU, UL), bulk stable carbon (DCU)

Sample label	CV09_23_032	**Station**	032	**Type**	Grab	**Date**	24/04/09
Instrument	Day Grab	**Depth**	39.5m	**Lat**	51 33.6895' N	**Long**	9 42.5382' W
Description	Slightly stiff mud but relatively unconsolidated. Less of a sandy texture in this sample.						
Anticipated testing	CNS analysis (DCU), heavy metals (DCU, UL), bulk stable carbon (DCU)						

Sample label	CV_09_23_033	**Station**	033	**Type**	Grab	**Date**	24/04/09
Instrument	Day Grab	**Depth**	39.4m	**Lat**	51 33.6521' N	**Long**	9 42.5611' W
Description	Sticky mud with some consolidated fragments. A fine sandy matrix within sample.						

Anticipated testing	CNS analysis (DCU), heavy metals (DCU, UL), bulk stable carbon (DCU)

Sample label	CV09_23_062	**Station**	062	**Type**	Grab	**Date**	25/04/09
Instrument	Day Grab	**Depth**	22.0m	**Lat**	51 43.2365' N	**Long**	9 31.7926' W
Description	Fine grained mud minor shells and organics. Well sorted and homogeneous						
Anticipated testing	CNS analysis (DCU), heavy metals (DCU, UL), bulk stable carbon (DCU)						

Sample label	CV_09_23_063	**Station**	063	**Type**	Grab	**Date**	25/04/09
Instrument	Day Grab	**Depth**	27.3m	**Lat**	51 42.3885' N	**Long**	9 31.9985' W

Description	Fine silty mud
Anticipated testing	CNS analysis (DCU), heavy metals (DCU, UL), bulk stable carbon (DCU)

Sample label	CV09_23_064	**Station**	064	**Type**	Grab	**Date**	25/04/09
Instrument	Day Grab	**Depth**	25.3m	**Lat**	51 42.3426' N	**Long**	9 30.9576' W
Description							
Anticipated testing	CNS analysis (DCU), heavy metals (DCU, UL), bulk stable carbon (DCU)						

Sample label	CV_09_23_065	**Station**	065	**Type**	Grab	**Date**	25/04/09

Instrument	Day Grab	Depth	15.9m	Lat	51 42.3321’ N	Long	9 27.8217’ W
Description	Fine mud (silty) with minor white shell fragments. Some redox and colour change visible						
Anticipated testing	CNS analysis (DCU), heavy metals (DCU, UL), bulk stable carbon (DCU)						

Sample label	CV09_23_066	Station	066	Type	Grab	Date	25/04/09
Instrument	Day Grab	Depth	30.1m	Lat	51 42.0349’ N	Long	9 42.0518’ W
Description	Colour change visible black redox layering						
Anticipated testing	CNS analysis (DCU), heavy metals (DCU, UL), bulk stable carbon (DCU)						

Sample label	CV_09_23_067	Station	067	Type	Grab	Date	25/04/09
Instrument	Day Grab	Depth	33.0m	Lat	51 41.4661’ N	Long	9 34.5447’ W
Description	Very fine clay/mud, homogenous sediment sample.						
Anticipated testing	CNS analysis (DCU), heavy metals (DCU, UL), bulk stable carbon (DCU)						

Sample label	CV09_23_068	Station	068	Type	Grab	Date	25/04/09
Instrument	Day Grab	Depth	41.1m	Lat	51 40.4285’ N	Long	9 34.5212’ W
Description	Very fine grained clay sediment with some mud content. Less biological content. Some minor white shell fragments. Very homogeneous. Little colour change.						
Anticipated testing	CNS analysis (DCU), heavy metals (DCU, UL), bulk stable carbon (DCU)						

Sample label	CV_09_23_069	Station	069	Type	Grab	Date	25/04/09
Instrument	Day Grab	Depth	33.7m	Lat	51 33.0000’ N	Long	9 42.0000’ W
Description	Fine grained mud with clays, dark greenish grey, minor shell fragments, patches of dark/black colour change in sediment, slightly coarser sediment tubes constructed by worms within sample.						
Anticipated testing	CNS analysis (DCU), heavy metals (DCU, UL), bulk stable carbon (DCU)						

Sample label	CV09_23_070	Station	070	Type	Grab	Date	25/04/09
Instrument	Day Grab	Depth	35.0m	Lat	51 40.0791’ N	Long	9 37.0650’ W
Description	Predominantly fine mud with some clay and minor silt or fine sand fraction. Dark greenish grey with small brittle stars and large worms with sediment burrows. Patches of dark/black within sediment. Slight colour change brown to more greenish with depth, but no defined layer of change.						
Anticipated testing	CNS analysis (DCU), heavy metals (DCU, UL), bulk stable carbon (DCU)						

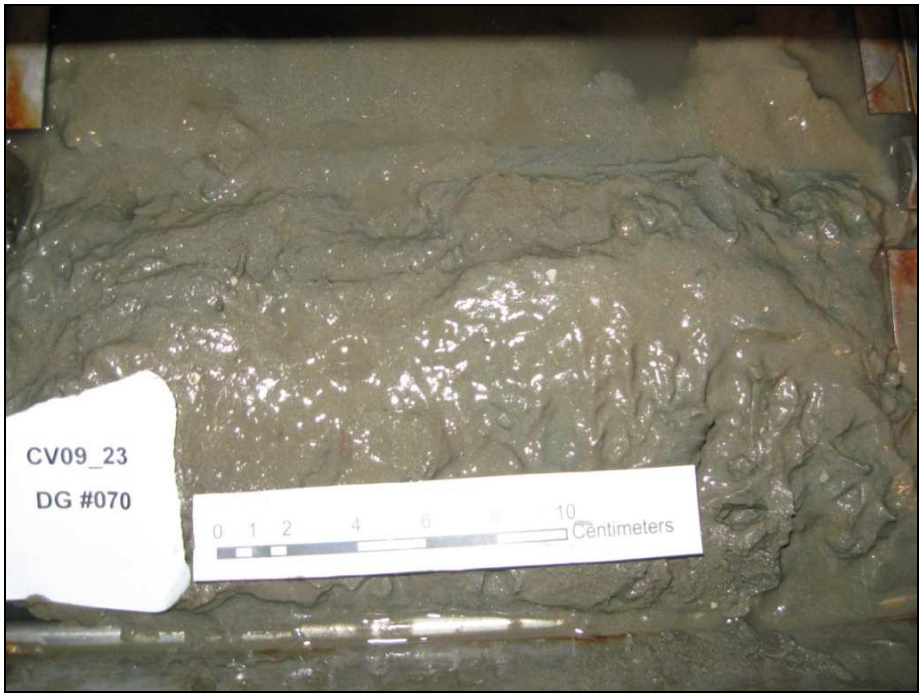

Sample label	CV_09_23_071	Station	071	Type	Grab	Date	25/04/09
Instrument	Day Grab	Depth	35.5m	Lat	51 39.9925' N	Long	9 38.0575' W
Description	Fine grained homogeneous mud with some clay. Dark green grey colour with colour variations through the sample.						
Anticipated testing	CNS analysis (DCU), heavy metals (DCU, UL), bulk stable carbon (DCU)						

Sample label	CV_09_23_050	Station	050	Type	Grab	Date	25/04/09
Instrument	Day Grab	Depth	26.8m	Lat	51 39.0926' N	Long	9 45.3703' W
Description	Well sorted shell hash and maerl. Brown/Black/Orange in colour. 1cm and less						
Anticipated testing	Sedimentology (GSI)						

(photograph missing)

Sample label	CV_09_23_059	Station	059	Type	Grab	Date	25/04/09

Instrument	Day Grab	Depth	43.9m	Lat	51 38.4205’ N	Long	9 44.7877’ W
Description	21cm recovery. Top and bottom similar in colour, top layer (Drift) is slightly browner in colour. Stickier towards the bottom. Some fine sand in the matrix						
Anticipated testing	Sedimentology (GSI)						

(photograph missing)

Sample label	CV_09_23_093	Station	093	Type	Grab	Date	26/04/09
Instrument	Day Grab	Depth	40.1m	Lat	51 39.8199’ N	Long	9 40.4192’ W
Description	Very fine grained, homogeneous mud with clay, dark greenish grey, no shell fragments, in faunal sea pen and worms						
Anticipated testing	Sedimentology (GSI)						

Sample label	CV_09_23_094	Station	094	Type	Grab	Date	26/04/09
Instrument	Day Grab	Depth	42.2m	Lat	51 38.3600’ N	Long	9 42.0824’ W
Description	Fine mud with minor silt/fine sand fraction. Very homogeneous with no colour change. Abundant worms with sediment walled burrows. Whole shells (minor) also.						
Anticipated testing	Sedimentology (GSI)						

Sample label	CV_09_23_095	**Station**	095	**Type**	Grab	**Date**	26/04/09
Instrument	Day Grab	**Depth**	46.7m	**Lat**	51 38.5384' N	**Long**	9 42.5020' W
Description	Homogeneous, fine mud with clay content, dark greenish grey, worms present, no shells.						
Anticipated testing	Sedimentology (GSI)						

Sample label	CV_09_23_096	**Station**	096	**Type**	Grab	**Date**	26/04/09
Instrument	Day Grab	**Depth**	16.7m	**Lat**	51 37.9665' N	**Long**	9 44.7544' W
Description	Fine grained mud with clay portion, dark greenish grey, homogeneous, no shells/fragments.						
Anticipated testing	Sedimentology (GSI)						

Sample label	CV_09_23_097	**Station**	097	**Type**	Grab	**Date**	26/04/09
Instrument	Day Grab	**Depth**	42.5m	**Lat**	51 33.1753’ N	**Long**	9 44.2262’ W
Description	Fine-grained, homogeneous, dark greenish grey sand with small silt/mud fraction.						
Anticipated testing	Sedimentology (GSI)						

Sample label	CV_09_23_098	**Station**	098	**Type**	Grab	**Date**	26/04/09
Instrument	Day Grab	**Depth**	37.8m	**Lat**	51 33.8390’ N	**Long**	9 41.6416’ W
Description	Fine mud with silt sample with some fine sand. Dark greenish grey, homogeneous with worms in sediment. Small shell fragments.						
Anticipated testing	Sedimentology (GSI)						

Sample label	CV_09_23_099	**Station**	099	**Type**	Grab	**Date**	26/04/09
Instrument	Day Grab	**Depth**	32.2m	**Lat**	51 33.9146' N	**Long**	9 40.5504' W
Description	Fine sand/silt with some mud. Homogeneous, dark greenish grey with small shell fragments. In faunal worms and brittle starfish.						
Anticipated testing	Sedimentology (GSI)						

Sample label	CV_09_23_100	**Station**	100	**Type**	Grab	**Date**	26/04/09
Instrument	Day Grab	**Depth**	31.4m	**Lat**	51 34.3010' N	**Long**	9 40.1761' W
Description	Predominantly fine sand/silt with minor mud fraction. Homogeneous, dark green grey with some patches of colour change to dark/black. Infonaut include Urchins, brittle starfish and worms with coarse sediment burrows. Whole shells ~ 10 mm diameter and shell fragments ~1mm diameter present.						

Anticipated testing	Sedimentology (GSI)

Sample label	CV_09_23_101	**Station**	101	**Type**	Grab	**Date**	26/04/09
Instrument	Day Grab	**Depth**	31.1m	**Lat**	51 34.5394’ N	**Long**	9 40.4192’ W
Description	Dark greenish grey mud with silt/fine sand. Shell fragments and worms present. Colour change 10 cm from surface.						
Anticipated testing	Sedimentology (GSI)						

Sample label	CV_09_23_102	**Station**	102	**Type**	Grab	**Date**	26/04/09
Instrument	Day Grab	**Depth**	28.5m	**Lat**	51 34.3124’ N	**Long**	9 39.0554’ W
Description	Medium to Fine Sand with fine silt mud fraction AND coarser shell/pebble clast portion. Dark greenish grey in colour with some dark/black and brown areas of colour change.						

	Many shell fragments. In faunal worms.
Anticipated testing	Sedimentology (GSI)

Sample label	CV_09_23_103	**Station**	103	**Type**	Grab	**Date**	26/04/09
Instrument	Day Grab	**Depth**	26.2m	**Lat**	51 34.3189’ N	**Long**	9 38.3809’ W
Description	Fine sand/silt sediment with mud fraction. Distinct colour change from green to brown ~ 6 cm below surface. Some small shell fragments. Worms.						
Anticipated testing	Sedimentology (GSI)						

Sample label	CV_09_23_128	**Station**	128	**Type**	Grab	**Date**	27/04/09
Instrument	Day Grab	**Depth**	31.1m	**Lat**	51 34.9220’ N	**Long**	9 38.8509’ W
Description	Mud with large portion of fine sand/silt. Dark green in colour very homogeneous. White shell fragments distributed throughout						
Anticipated testing	Sedimentology (GSI)						

Sample label	CV_09_23_129	**Station**	129	**Type**	Grab	**Date**	27/04/09
Instrument	Day Grab	**Depth**	29.3m	**Lat**	51 34.8855' N	**Long**	9 37.6215' W
Description	Dark patches in sediment. Mud with fine silt/sand fraction, homogeneous. Dark greenish gray in colour. White shell fragments						
Anticipated testing	Sedimentology (GSI)						

Sample label	CV_09_23_130	**Station**	130	**Type**	Grab	**Date**	27/04/09
Instrument	Day Grab	**Depth**	37.2m	**Lat**	51 32.8281' N	**Long**	9 40.8077' W
Description	Medium to coarse sand with shell hash. Pebbles up to 25mm. Large quantity of shell hash 1 - 25mm						
Anticipated testing	Sedimentology (GSI)						

Sample label	CV_09_23_131	**Station**	131	**Type**	Grab	**Date**	27/04/09
Instrument	Day Grab	**Depth**	31.2m	**Lat**	51 33.1200' N	**Long**	9 40.5054' W
Description	Fine grained sand with some silt. Shell fragments make up coarser fraction with fragments up to 5mm						
Anticipated testing	Sedimentology (GSI)						

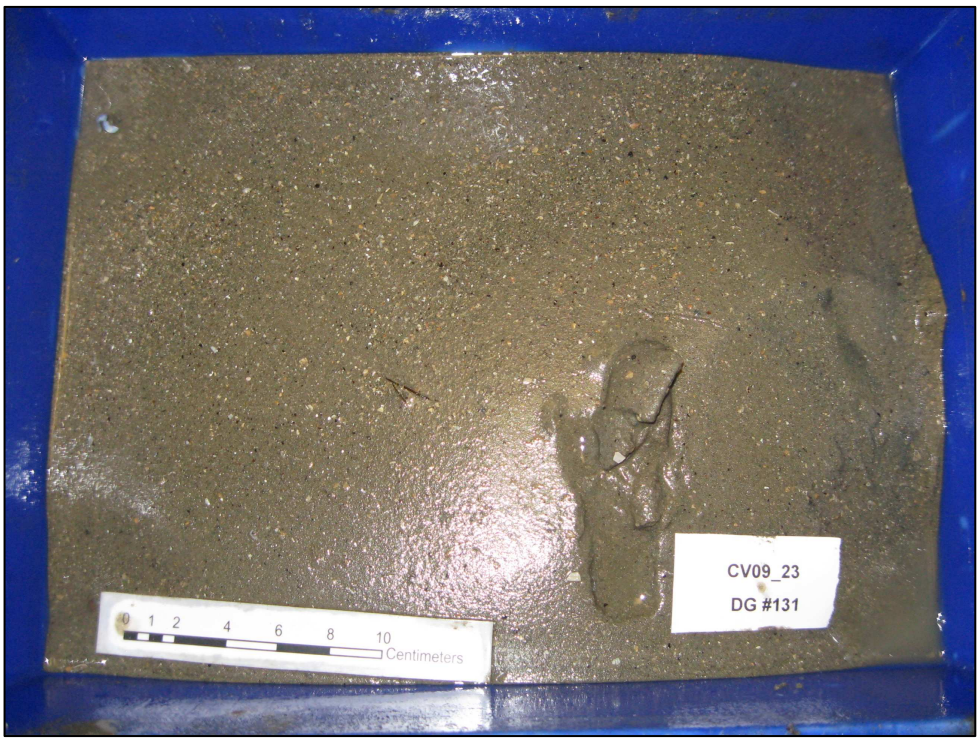

Appendix V
Box Sample Log

Project: Pockmark ground-truthing survey in Dunmanus Bay, Co. Cork

Curise: CV09_23

Date: 22-28 April 2009

Vessel: Celtic Voyager

To meet the scientific objectives of the project various sampling instruments were used. Surficial sediment collection for the purpose of biological sampling and sedimentological investigations was performed with a Day Grab sampler. A Reineck Box Corer was employed to gain an insight into the first 20cm of sediment without disturbing the surface. Also several sediment cores were collected with a Gravity Corer fitted with a 2m long barrel. Performance of the sampling instruments varied between different seabed types. The Day Grab and Reineck Box Corer were most reliable on soft fine-grained sediments and underperformed slightly on coarser sands with a high percentage of shell hash. The Gravity Corer performance was less than optimal since even in very soft sediment full recovery was not achieved. Highest recovery was 1.3m with an average recovery around 1.0m

Sample label	CV09_23_034	**Station**	34	**Type**	Box	**Date**	24/04/09
Instrument	Box Corer	**Depth**	39.8m	**Lat**	51 33.6876' N	**Long**	9 42.5434' W
Description	Box core sampling - taken from top bottom and bulk. Top - sandy mud as in previous samples. Bottom - dark grey sticky mud.						

Anticipated testing	Sedimentology (GSI)

Sample label	CV09_23_035	**Station**	35	**Type**	Box	**Date**	24/04/09
Instrument	Box Corer	**Depth**	39.8m	**Lat**	51 33.6876' N	**Long**	9 42.5434' W
Description	Box core sampling - taken from top bottom and bulk. Top - sandy mud as in previous samples. Bottom - dark grey sticky mud.						
Anticipated testing	Sedimentology (GSI)						

Sample label	CV09_23_036	**Station**	36	**Type**	Box	**Date**	24/04/09
Instrument	Box Corer	**Depth**	39.5m	**Lat**	51 33.6666' N	**Long**	9 42.5353' W
Description	Strong sulphide odour. Bottom 10B on GLEY2. Top 4/3 5Y. Very black on bottom of sample. Also holes within this section throughout the sample which may indicate fluid						

	flow. 1 angular-sub angular black pebble c. 2cm in length
Anticipated testing	Sedimentology (GSI)

Sample label	CV09_23_036	**Station**	36	**Type**	Box	**Date**	24/04/09
Instrument	Box Corer	**Depth**	39.6m	**Lat**	51 33.6811’ N	**Long**	9 42.5630’ W
Description	No blackness in this sample. 3/2 5Y in colour top and bottom						
Anticipated testing	Sedimentology (GSI)						

Sample label	CV09_23_038	**Station**	38	**Type**	Box	**Date**	24/04/09
Instrument	Box Corer	**Depth**	39.5m	**Lat**	51 33.6823’ N	**Long**	9 42.5611’ W
Description	Very similar to last core - no blackness. Too soft for tor-vane read.						

Anticipated testing	Sedimentology (GSI)

Sample label	CV09_23_042	**Station**	42	**Type**	Box	**Date**	24/04/09
Instrument	Box Corer	**Depth**	13.0m	**Lat**	51 38.8943' N	**Long**	9 48.5510' W
Description	Mud with very little fine sand. Shell hash and fragments in bottom of sample 3mm and less in size. Sticky in the bottom of the sample. Position taken on retrieval						
Anticipated testing	Sedimentology (GSI)						

Sample label	CV09_23_043	**Station**	43	**Type**	Box	**Date**	25/04/09
Instrument	Box Corer	**Depth**	15.2m	**Lat**	51 39.0736' N	**Long**	9 47.3757' W
Description	Recovery 14cm. Small shell fragments throughout the sample profile 4mm and less in						

	size
Anticipated testing	Sedimentology (GSI)

Sample label	CV09_23_044	**Station**	44	**Type**	Box	**Date**	25/04/09
Instrument	Box Corer	**Depth**	19.6m	**Lat**	51 38.1273’ N	**Long**	9 46.9166’ W
Description	15cm recovery. Rich in shell hash/fragments increasing towards the bottom. Full shells and fragments 5cm and less. Fine sand matrix in the mud						
Anticipated testing	Sedimentology (GSI)						

Sample label	CV09_23_045	**Station**	45	**Type**	Box	**Date**	25/04/09
Instrument	Box Corer	**Depth**	23.3m	**Lat**	51 39.0503’ N	**Long**	9 46.4958’ W
Description	12cm recovery. Sub sampling top bottom and push core. A much sandier sample - fine						

	to medium sandy mud with shell hash throughout
Anticipated testing	Sedimentology (GSI)

Sample label	CV09_23_046	**Station**	46	**Type**	Box	**Date**	25/04/09
Instrument	Box Corer	**Depth**	27.1m	**Lat**	51 39.1735’ N	**Long**	9 46.0558’ W
Description	13cm recovery. Medium sand with microscopic shell hash throughout. Some mud in the matrix - minimal max. 5%						
Anticipated testing	Sedimentology (GSI)						

Sample label	CV09_23_047	**Station**	47	**Type**	Box	**Date**	25/04/09
Instrument	Box Corer	**Depth**	27.0m	**Lat**	51 39.0717’ N	**Long**	9 46.0617’ W

Description	10 cm recovery. Fine to medium sand
Anticipated testing	Sedimentology (GSI)

Sample label	CV09_23_048	**Station**	48	**Type**	Box	**Date**	25/04/09
Instrument	Box Corer	**Depth**	28.6m	**Lat**	51 38.8813' N	**Long**	9 46.0137' W
Description	Well sorted shell hash. 7cm recovery						
Anticipated testing	Sedimentology (GSI)						

Sample label	CV09_23_049	Station	49	Type	Box	Date	25/04/09
Instrument	Box Corer	Depth	24.6m	Lat	51 39.2479' N	Long	9 45.6319' W
Description	Fine to medium sand with microscopic shell hash throughout						
Anticipated testing	Sedimentology (GSI)						

Sample label	CV09_23_050	Station	50	Type	Box	Date	25/04/09
Instrument	Box Corer	Depth	26.8m	Lat	51 39.0926' N	Long	9 45.3703' W
Description	Well sorted shell hash and maerl. Brown/Black/Orange in colour. 1cm and less						
Anticipated testing	Sedimentology (GSI)						

Sample label	CV09_23_051	Station	51	Type	Box	Date	25/04/09
Instrument	Box Corer	Depth		Lat	51 39.0121' N	Long	9 45.8282' W
Description	Fine to medium sand green/grey in colour with black mica specs throughout. Very well						

	sorted. 7cm recovery
Anticipated testing	Sedimentology (GSI)

Sample label	CV09_23_052	**Station**	52	**Type**	Box	**Date**	25/04/09
Instrument	Box Corer	**Depth**	29.5m	**Lat**	51 38.9206’ N	**Long**	9 45.9069’ W
Description	6cm recovery. Shell hash.						
Anticipated testing	Sedimentology (GSI)						

Sample label	CV09_23_053	**Station**	53	**Type**	Box	**Date**	25/04/09

Instrument	Box Corer	Depth	31.7m	Lat	51 38.9351’ N	Long	9 45.3842’ W
Description	Shell hash						
Anticipated testing	Sedimentology (GSI)						

Sample label	CV09_23_054	Station	54	Type	Box	Date	25/04/09
Instrument	Box Corer	Depth	33.1m	Lat	51 38.8214’ N	Long	9 45.2960’ W
Description	Shelly sandy mud. Shell fragments 50mm and less in size. Fine sandy matrix, slightly shelly texture. 8cm recovery						
Anticipated testing	Sedimentology (GSI)						

Sample label	CV09_23_055	Station	55	Type	Box	Date	25/04/09
Instrument	Box Corer	Depth	37.4m	Lat	51 38.7066' N	Long	9 45.6116' W
Description	8cm recovery. Fine to medium 'shelly' sand with shell hash. Some mud in the matrix						
Anticipated testing	Sedimentology (GSI)						

Sample label	CV09_23_056	Station	56	Type	Box	Date	25/04/09
Instrument	Box Corer	Depth	39.7m	Lat	51 38.5841' N	Long	9 45.7514' W
Description	Well sorted shell hash.						
Anticipated testing	Sedimentology (GSI)						

Sample label	CV09_23_057	Station	57	Type	Box	Date	25/04/09
Instrument	Box Corer	Depth	40.5m	Lat	51 38.7066' N	Long	9 45.6116' W
Description	Very clear difference in top to bottom. Redox layering on bottom very clear. Bottom						

	10BG GLEY2 Greenish Black. Top 4/2 5Y Olive Gray. Fine sand on top bottom is blacker muddier sand and a lot stickier. Soft structure (Push core)
Anticipated testing	Sedimentology (GSI)

Sample label	CV09_23_058	**Station**	58	**Type**	Box	**Date**	25/04/09
Instrument	Box Corer	**Depth**	42.8m	**Lat**	51 38.6852' N	**Long**	9 45.0350' W
Description	Muddy fine sand with a very soft structure. Difference in colour. Bottom 4/1 GLEY1. Dark greenish grey. Top 4/2 5Y Olive gray. Unconsolidated sample.						
Anticipated testing	Sedimentology (GSI)						

Sample label	CV09_23_059	**Station**	59	**Type**	Box	**Date**	25/04/09
Instrument	Box Corer	**Depth**	43.9m	**Lat**	51 38.4205' N	**Long**	9 44.7877' W
Description	21cm recovery. Top and bottom similar in colour, top layer (Drift) is slightly browner in						

	colour. Stickier towards the bottom. Some fine sand in the matrix
Anticipated testing	Sedimentology (GSI)

Sample label	CV09_23_060	**Station**	60	**Type**	Box	**Date**	25/04/09
Instrument	Box Corer	**Depth**	44.0m	**Lat**	51 38.4411' N	**Long**	9 44.4552' W
Description	20cm recovery. Dark greenish gray black mud - profile similar from top to bottom Slight (1cm) jelly like fluid layer on top which is browner in colour. Bottom is sticky and stiff mud						
Anticipated testing	Sedimentology (GSI)						

Sample label	CV09_23_061	**Station**	61	**Type**	Box	**Date**	25/04/09

Instrument	Box Corer	Depth	42.6m	Lat	51 38.9965' N	Long	9 43.6930' W
Description	Sample is similar to previous. 21cm recovery. Similar 1cm layer of jelly like lighter coloured drift mud on top. Shell fragments in bottom of sample						
Anticipated testing	Sedimentology (GSI)						

Sample label	CV09_23_072	Station	72	Type	Box	Date	26/04/09
Instrument	Box Corer	Depth	66.7m	Lat	51 31.0833' N	Long	10 01.2294' W
Description	13 cm recovery. Redox Layering. Silty Sand on top with sandy mud towards bottom Top Colour: 4/2 5Y Olive Grey. Bottom Colour: 3/2 5Y Dark Olive Grey. Shells and Shell Fragments on top. Smooth and homogeneous sediment						
Anticipated testing	Sedimentology (GSI)						

Sample label	CV09_23_073	Station	73	Type	Box	Date	26/04/09
Instrument	Box Corer	Depth	61.8m	Lat	51 34.4862' N	Long	9 58.5917' W
Description	23 cm recovery. Top => 12cm, Drift silty mud, unconsolidated, Gley 1 4/10Y Dark						

	greenish grey. Bottom => 11cm, Gley 1 3/10Y Very dark greenish grey, sticky sandy mud. Top silty mud - Less sticky, more viscous. Penetrometer Kg 0.5 (top) 1-1.2 (bottom)
Anticipated testing	Sedimentology (GSI)

Sample label	CV09_23_074	**Station**	74	**Type**	Box	**Date**	26/04/09
Instrument	Box Corer	**Depth**	57.2m	**Lat**	51 34.8282' N	**Long**	9 56.4544' W
Description	20 cm recovery. Top => 5Y 5/2 Olive Grey, Sticky silty mud, 0.5 kg penetrometer Bottom => Gley 1 4/1 Dark greenish grey, much stiffer mud, very slight very fine sand content. Bottom show redox layer 1-1.2 kg bottom						
Anticipated testing	Sedimentology (GSI)						

Sample label	CV09_23_075	**Station**	75	**Type**	Box	**Date**	26/04/09
Instrument	Box Corer	**Depth**	53.8m	**Lat**	51 35.9070' N	**Long**	9 55.5005' W

Description	14 cm recovery. Top => 5Y 4/2 Olive Grey, Silty Mud. Bottom => Gley 1 4/1 Dark Greenish Grey, Sticky, stiff mud with some fine sand. Bottom 10 cm shows redox layer
Anticipated testing	Sedimentology (GSI)

Sample label	CV09_23_076	**Station**	76	**Type**	Box	**Date**	26/04/09
Instrument	Box Corer	**Depth**	55.0m	**Lat**	51 35.5179' N	**Long**	9 54.5816' W
Description	16 cm recovery. Top => 5Y 4/2 Olive Grey, Fine sandy mud. Bottom => Gley 1 4/1 Dark greenish grey, very sticky mud, no sand - silty on bottom. Bottom 10 cm shows redox layering						
Anticipated testing	Sedimentology (GSI)						

Sample label	CV09_23_077	**Station**	77	**Type**	Box	**Date**	26/04/09
Instrument	Box Corer	**Depth**	54.5m	**Lat**	51 35.1067' N	**Long**	9 50.7617' W
Description	16 cm recovery. Top => 5Y 4/2 Olive grey, mud. Bottom => Gley 1 4/1 Dark greenish						

	grey, very stick mud (clay content)
Anticipated testing	Sedimentology (GSI)

Sample label	CV09_23_078	**Station**	78	**Type**	Box	**Date**	26/04/09
Instrument	Box Corer	**Depth**	39.5m	**Lat**	51 37.2883' N	**Long**	9 48.6236' W
Description	8 cm recovery. Fine to Medium sand						
Anticipated testing	Sedimentology (GSI)						

Sample label	CV09_23_079	**Station**	79	**Type**	Box	**Date**	26/04/09
Instrument	Box Corer	**Depth**	36.5m	**Lat**	51 37.5328' N	**Long**	9 48.2644' W
Description	Poor recovery. Fine to Medium sand						

Anticipated testing	Sedimentology (GSI)

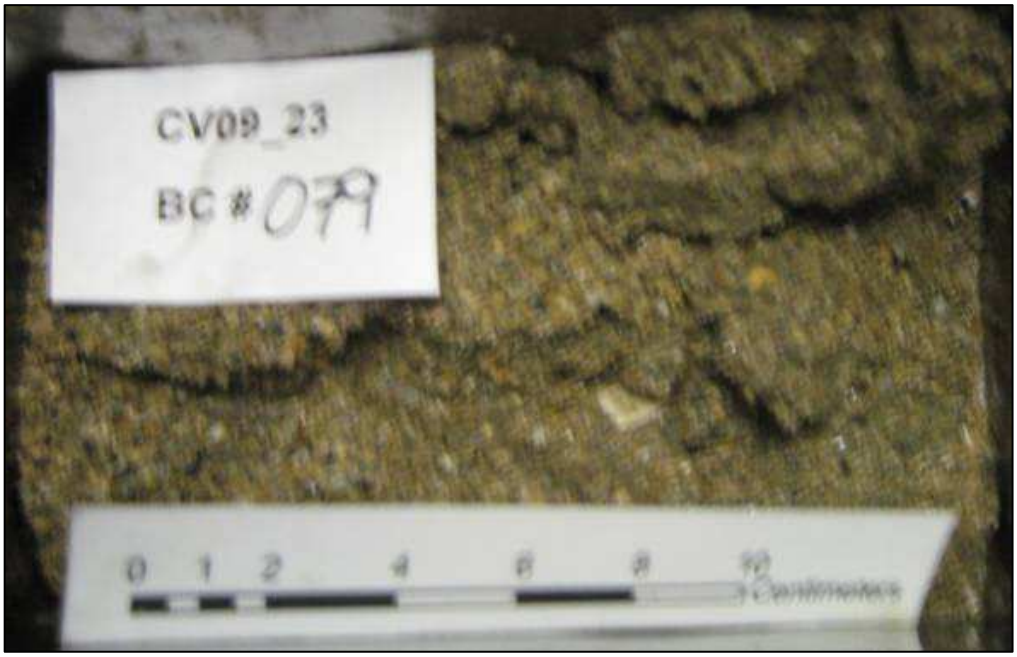

Sample label	CV09_23_080	**Station**	80	**Type**	Box	**Date**	26/04/09
Instrument	Box Corer	**Depth**	38.5m	**Lat**	51 37.8025' N	**Long**	9 47.4804' W
Description	15 cm recovery. Predominantly shell hash with c. 1% medium sand. Fragments 10 mm and smaller. Orange/Black/Brown shell fragments.						
Anticipated testing	Sedimentology (GSI)						

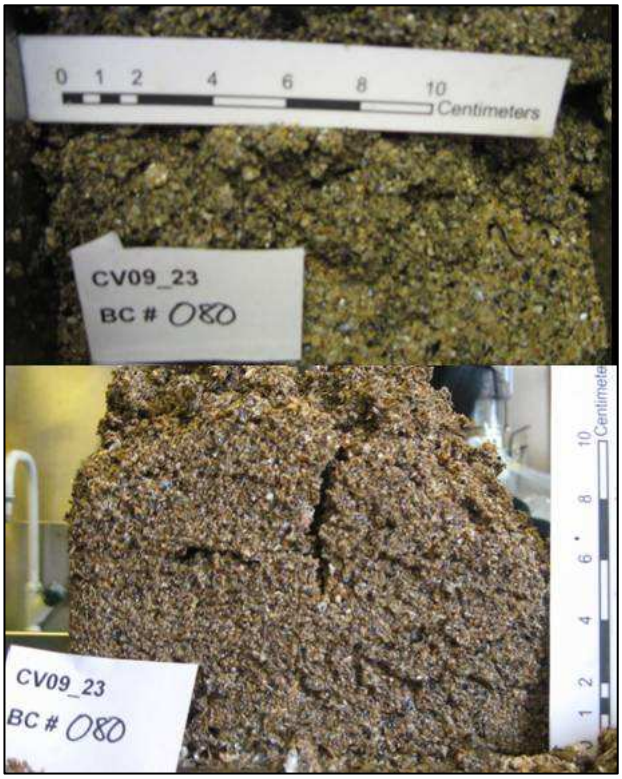

Sample label	CV09_23_081	**Station**	81	**Type**	Box	**Date**	26/04/09
Instrument	Box Corer	**Depth**	27.3m	**Lat**	51 38.1550' N	**Long**	9 47.2752' W
Description	4 cm recovery. Fine sand matrix of shell hash and clastic sediments, v. well sorted, smooth and homogeneous						

Anticipated testing	Sedimentology (GSI)

Sample label	CV09_23_082	**Station**	82	**Type**	Box	**Date**	26/04/09
Instrument	Box Corer	**Depth**	22.4m	**Lat**	51 39.0102' N	**Long**	9 46.7660' W
Description	16 cm recovery. Top => 5Y 5/2 Olive grey, mud. Bottom => Gley 1 3/1 Very dark greenish grey, very shelly sticky mud with large band of shell hash to the bottom of the sample						
Anticipated testing	Sedimentology (GSI)						

Sample label	CV09_23_083	**Station**	83	**Type**	Box	**Date**	26/04/09
Instrument	Box Corer	**Depth**	17.7m	**Lat**	51 38.9702' N	**Long**	9 47.0765' W
Description	20 cm recovery. Top => Gley 1 4/1 Dark greenish grey, sticky mud with some silt						

	Bottom => Similar colour but more clay content
Anticipated testing	Sedimentology (GSI)

Sample label	CV09_23_084	**Station**	84	**Type**	Box	**Date**	26/04/09
Instrument	Box Corer	**Depth**	16.2m	**Lat**	51 38.9835' N	**Long**	9 47.3142' W
Description	14 cm recovery. Top (9 to 14 cm) 5Y 4/2 Olive grey, silty mud. Bottom (0 to 9 cm) Gley 1 4/1 Dark greenish grey, shelly mud, some clay content. Shell hash increases to bottom. Redox layer also visible.						
Anticipated testing	Sedimentology (GSI)						

Sample label	CV09_23_085	**Station**	85	**Type**	Box	**Date**	26/04/09
Instrument	Box Corer	**Depth**	17.0m	**Lat**	51 38.9610' N	**Long**	9 47.5538' W
Description	Top => 2 cm of drift mud, slightly lighter in colour than bottom sediment, silty with no sand. Bottom => Gley 1 4/1 Dark greenish grey. Very soft mud. Small amount of shell						

	hash in the bottom 2 cm's of core
Anticipated testing	Sedimentology (GSI)

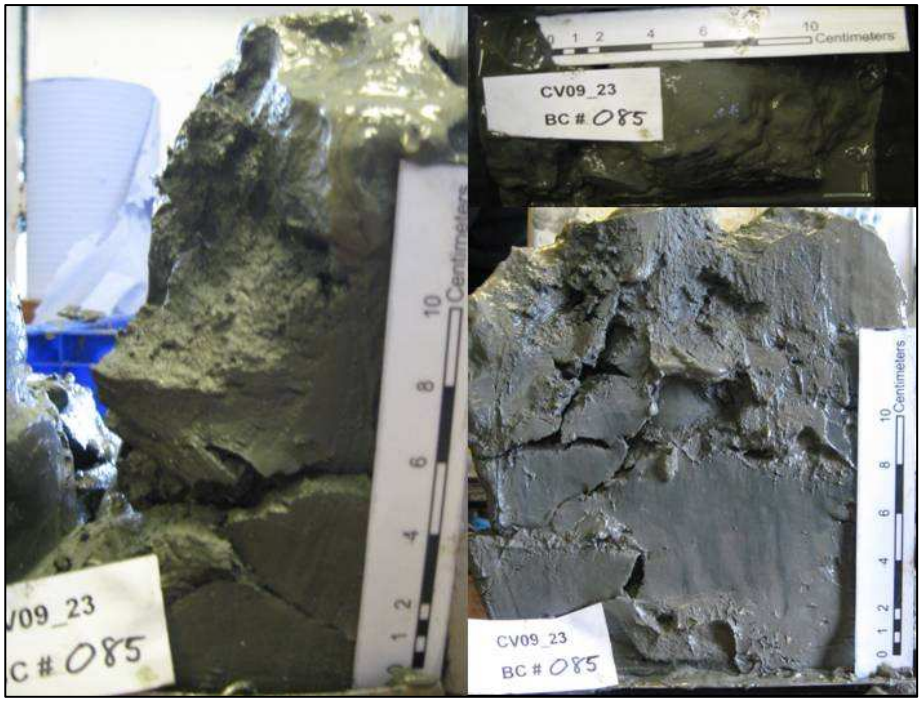

Sample label	CV09_23_086	**Station**	86	**Type**	Box	**Date**	26/04/09
Instrument	Box Corer	**Depth**	11.6m	**Lat**	51 38.8683' N	**Long**	9 47.7254' W
Description	13 cm recovery. Shelly throughout but increases to bottom, lots of fauna. Signs of bioturbation - sand around large burrow.						
Anticipated testing	Sedimentology (GSI)						

Sample label	CV09_23_087	**Station**	87	**Type**	Box	**Date**	26/04/09
Instrument	Box Corer	**Depth**	15.6m	**Lat**	51 38.8355' N	**Long**	9 47.8991' W
Description	19 cm recovery. Top => 5Y 4/2, Slightly silty mud, interpreted as drift. Bottom => Gley 1 4/1 Dark greenish grey, Sulphate odour, sticky but only slightly silty mud, small amount						

	of shell hash increasing to bottom, size of 3 mm or less
Anticipated testing	Sedimentology (GSI)

Sample label	CV09_23_088	**Station**	88	**Type**	Box	**Date**	26/04/09
Instrument	Box Corer	**Depth**		**Lat**	51 38.8176' N	**Long**	9 48.0431' W
Description	19 cm recovery. Top => Gley 1 5/1 greenish grey, fluid mud with shell hash and some silt, small amount of black organics on top. Bottom => Gley 1 4/1 dark greenish grey, sticky mud, slightly silty, small amount of shell hash. Shell hash visible from top to bottom						
Anticipated testing	Sedimentology (GSI)						

Sample label	CV09_23_089	**Station**	89	**Type**	Box	**Date**	26/04/09
Instrument	Box Corer	**Depth**		**Lat**	51 38.7287' N	**Long**	9 48.8100' W
Description	13 cm recovery. Top => Gley 1 5/1 greenish grey. Bottom => Gley 1 4/1 dark greenish						

	grey bottom is muddier and shell hash increases towards base
Anticipated testing	Sedimentology (GSI)

Sample label	CV09_23_090	**Station**	90	**Type**	Box	**Date**	26/04/09
Instrument	Box Corer	**Depth**	10.5m	**Lat**	51 38.7291' N	**Long**	9 48.8679' W
Description	13cm recovery. Top => Gley 1 5/1 greenish grey. Bottom => Gley 1 4/1 dark greenish grey bands/horizons of shell hash in centre large scallop/clam shells 6 to 7 cm, shell hash 10 mm and smaller. Drift mud on top, lighter in colour. Soft mud towards base with minor silt content						
Anticipated testing	Sedimentology (GSI)						

Sample label	CV09_23_091	**Station**	91	**Type**	Box	**Date**	26/04/09
Instrument	Box Corer	**Depth**	15.5m	**Lat**	51 39.2372' N	**Long**	9 47.5518' W
Description	Top => Gley 1 5/1 greenish grey. Bottom => Gley 1 4/1 dark greenish grey bands/horizons of shell hash in bottom. No large shell Fragments. Drift mud on top. Soft mud towards base, quite fluid						

Anticipated testing	Sedimentology (GSI)

Sample label	CV09_23_092	**Station**	92	**Type**	Box	**Date**	26/04/09
Instrument	Box Corer	**Depth**	19.0m	**Lat**	51 39.1685' N	**Long**	9 47.1242' W
Description	Mainly Mud. Small fragments of shell present. Increasing in density/stiffness downwards						
Anticipated testing	Sedimentology (GSI)						

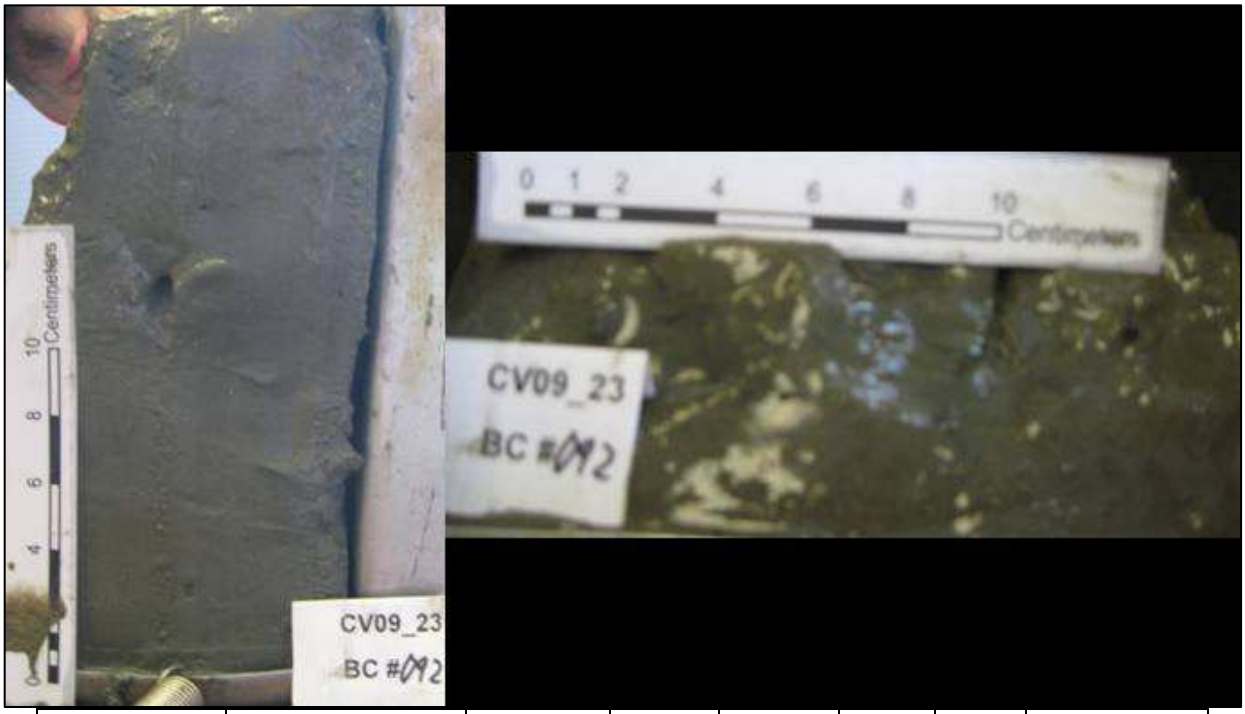

Sample label	CV09_23_104	**Station**	104	**Type**	Box	**Date**	27/04/09
Instrument	Box Corer	**Depth**	23.3m	**Lat**	51 35.5865' N	**Long**	9 36.3512' W
Description	15cm recovery. Top =>5Y 4/2 Olive Grey. Fine silty sand, homogeneous, 2 cm thick. Bottom = 5Y 3/2 Dark olive grey. Stiff mud with fine sand/silt, 13 cm thick. Redox visible in bottom. Top is drift sandy/silty mud on top has some worms and brittle stars. Sample						

	was v. stiff - indicting presence of clay?
Anticipated testing	Sedimentology (GSI)

Sample label	CV09_23_105	**Station**	105	**Type**	Box	**Date**	26/04/09
Instrument	Box Corer	**Depth**	31.6m	**Lat**	51 34.5524' N	**Long**	9 38.9764' W
Description	10 cm recovery. Top =>5Y 4/2 Olive Grey. 2 cm thick of silty sandy mud. Bottom = 2.5Y 3/2 V. Dark greyish brown. Muddy sand with gravel and shell hash at base. Shell fragments 10 mm and less in size .5 cm at very base of core has shell hash and some pebbles (40 mm diameter or less.						
Anticipated testing	Sedimentology (GSI)						

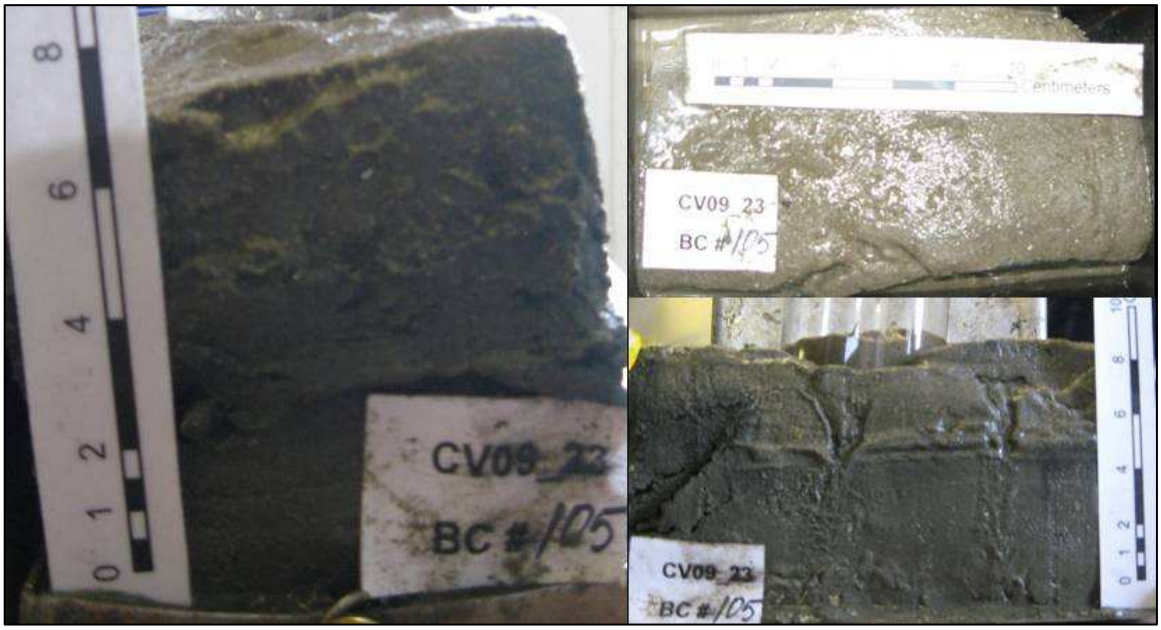

Sample label	CV09_23_106	**Station**	106	**Type**	Box	**Date**	27/04/09
Instrument	Box Corer	**Depth**		**Lat**	51 34.2155' N	**Long**	9 39.6039' W
Description	9 cm recovery. Top =>5Y 4/2 Olive Grey. Silty sandy mud - fluid drift, jelly like. Bottom => Gley 1 4/10Y Dark greenish grey. Shell hash at base						

Anticipated testing	Sedimentology (GSI)

Sample label	CV09_23_107	**Station**	107	**Type**	Box	**Date**	27/04/09
Instrument	Box Corer	**Depth**	31.5m	**Lat**	51 33.3892’ N	**Long**	9 40.0046’ W
Description	10 cm recovery. Top =>5Y 4/2 Olive Grey. Drift - Fine sand with some mud. Bottom => 5Y 3/2 Dark Olive grey slightly stiffer silty fine sand. Visible redox banding, small amount of shell hash towards bottom, shell fragments 3 mm or less in diameter						
Anticipated testing	Sedimentology (GSI)						

Sample label	CV09_23_108	**Station**	108	**Type**	Box	**Date**	27/04/09
Instrument	Box Corer	**Depth**	31.9m	**Lat**	51 34.4292’ N	**Long**	9 40.5250’ W
Description	19 cm recovery. Top =>5Y 4/2 Olive Grey. Drift material fine, silty mud, unconsolidated. Bottom => Gley 1 4/10Y Dark greenish Grey. Stiff mud, with some Fine silt, sticky. Clear						

	colour change with depth and redox layers. Band of shell hash in the very bottom.
Anticipated testing	Sedimentology (GSI)

Sample label	CV09_23_109	**Station**	109	**Type**	Box	**Date**	27/04/09
Instrument	Box Corer	**Depth**	32.3m	**Lat**	51 34.0523' N	**Long**	9 40.0535' W
Description	20 cm recovery. Top =>5Y 4/2 Olive Grey. Silty Mud, 1 cm of profile, drift sediment, very fluid. Bottom => Gley 1 4/10Y Dark greenish Grey. Sticky, silt mud Clear colour change and redox layers.						
Anticipated testing	Sedimentology (GSI)						

Appendix VI
Gravity Core Log

Project: Pockmark ground-truthing survey in Dunmanus Bay, Co. Cork

Curise: CV09_23

Date: 22-28 April 2009

Vessel: Celtic Voyager

To meet the scientific objectives of the project various sampling instruments were used. Surficial sediment collection for the purpose of biological sampling and sedimentological investigations was performed with a Day Grab sampler. A Reineck Box Corer was employed to gain an insight into the first 20cm of sediment without disturbing the surface. Also several sediment cores were collected with a Gravity Corer fitted with a 2m long barrel. Performance of the sampling instruments varied between different seabed types. The Day Grab and Reineck Box Corer were most reliable on soft fine-grained sediments and underperformed slightly on coarser sands with a high percentage of shell hash. The Gravity Corer performance was less than optimal since even in very soft sediment full recovery was not achieved. Highest recovery was 1.3m with an average recovery around 1.0m

Sample label	CV09_23_GC_01	**Station**	001	**Type**	Core	**Date**	24/04/09
Instrument	Gravity Corer	**Depth**	-	**Lat**	51 33.6552' N	**Long**	9 42.4416' W
Description	Sub sampled immediately for heavy metals analysis at 10cm interval. Dark green/grey in colour. Shell occurrences in layers, sandy mud. Stored fridge.						
Anticipated testing	Heavy metals (DCU, UL)						

Sample label	CV09_23_GC_02	Station	001	Type	Core	Date	24/04/09
Instrument	Gravity Corer	Depth	-	Lat	51 33.6552' N	Long	9 42.4416' W
Description	Not opened, stored at room temperature horizontally.						
Anticipated testing	Sedimentology (GSI)						

Sample label	CV09_23_GC_03	Station	002	Type	Core	Date	24/04/09
Instrument	Gravity Corer	Depth	-	Lat	51 33.6220' N	Long	9 42.6651' W
Description	Recovery: 1.3m. Split into sections: 1 (0.7m) and 2 (0.6m). Dark green/grey in colour, homogenous mud with sandy layers at 0.35, 0.9-95cm, air pocket at 0.55cm. Sub sampled for methane analysis at 5cm interval. Half cores stored in freezer. Redox potential measured.						
Anticipated testing	CNS analysis (DCU) Heavy metals (DCU, UL), bulk stable carbon (DCU), lipid analysis (DCU), methane (DCU)						

Sample label	CV09_23_GC_04	Station	003	Type	Core	Date	24/04/09
Instrument	Gravity Corer	Depth	-	Lat	51 33.6300' N	Long	9 42.5849' W
Description	Recovery: 1.13m. Split into sections: 1 (0.55m) and 2 (0.58m). Dark green/grey in colour. Shell occurrences in first 12cm and at 1.0m, homogenous mud enriched with sand at first 12cm and at 0.65-0.8cm. Sub sampled for methane analysis at 10cm interval. Half cores stored in freezer. Redox potential measured						
Anticipated testing	CNS analysis (DCU) Heavy metals (DCU, UL), bulk stable carbon (DCU), lipid analysis (DCU), methane (DCU)						

Sample label	CV09_23_GC_05	Station	004	Type	Core	Date	24/04/09
Instrument	Gravity Corer	Depth	30.7m	Lat	51 41.3250' N	Long	9 32.5332' W
Description	Recovery: 0.75m. Not opened, stored in freezer.						
Anticipated testing	CNS analysis (DCU), bulk stable carbon (DCU), lipid analysis (DCU)						

Sample label	CV09_23_GC_06	Station	005	Type	Core	Date	24/04/09
Instrument	Gravity Corer	Depth	-	Lat	51 33.6220' N	Long	9 42.6651' W
Description	Recovery: 1.0m. Not opened, stored in freezer.						
Anticipated testing	CNS analysis (DCU), bulk stable carbon (DCU), lipid analysis (DCU)						

Sample label	CV09_23_GC_09	Station	-	Type	Core	Date	27/04/09
Instrument	Gravity Corer	Depth	-	Lat	-	Long	-
Description	Recovery: 0.95m. Dark green/grey in colour. Shell occurrences at 5-10cm, homogenous mud with sandy layer at 0.5cm. Sub sampled for methane analysis at 10cm interval. Half cores stored in freezer. Redox potential measured.						
Anticipated testing	CNS analysis (DCU) Heavy metals (DCU, UL), bulk stable carbon (DCU), lipid analysis (DCU), methane (DCU)						

Sample label	CV09_23_GC_10	Station	-	Type	Core	Date	27/04/09
Instrument	Gravity Corer	Depth	-	Lat	51 33.5114' N	Long	9 42.8673' W
Description	Recovery: 1.0m. Dark green/grey in colour, homogenous sandy mud. Sub sampled for methane analysis at 10cm interval. Half cores stored in freezer. Redox potential measured.						
Anticipated testing	CNS analysis (DCU), Heavy metals (DCU, UL), bulk stable carbon (DCU), lipid analysis (DCU)						

Sample label	CV09_23_GC_11	Station	-	Type	Core	Date	27/04/09
Instrument	Gravity Corer	Depth	-	Lat	51 33.7002' N	Long	9 42.6372' W
Description	Not opened, stored at room temperature horizontally.						
Anticipated testing	Sedimentology (GSI)						

Sample label	CV09_23_GC_12	**Station**	-	**Type**	Core	**Date**	27/04/09
Instrument	Gravity Corer	**Depth**	-	**Lat**	51 33.6735' N	**Long**	9 42.3765' W
Description	Not opened, stored in fridge horizontally.						
Anticipated testing	High resolution heavy metal profiling (DCU, UCD)						

Sample label	CV09_23_GC_13	**Station**	-	**Type**	Core	**Date**	27/04/09
Instrument	Gravity Corer	**Depth**	-	**Lat**	51 33.0833' N	**Long**	9 43.9844' W
Description	Not opened, stored at room temperature horizontally.						
Anticipated testing	Sedimentology (GSI)						

Sample label	CV09_23_GC_14	**Station**	-	**Type**	Core	**Date**	27/04/09
Instrument	Gravity Corer	**Depth**	-	**Lat**	51 33.7941' N	**Long**	9 42.1240' W
Description	Recovery: 1.14m. Split into sections: 1 (0.64m) and 2 (0.50m). Dark green/grey in colour, homogenous sandy mud. Sub sampled for methane analysis at 10cm interval. Half cores stored in freezer. Redox potential measured.						
Anticipated testing	CNS analysis (DCU), Heavy metals (DCU, UL), bulk stable carbon (DCU), lipid analysis (DCU)						

Sample label	CV09_23_GC_16	**Station**	-	**Type**	Core	**Date**	27/04/09
Instrument	Gravity Corer	**Depth**	-	**Lat**	51 33.7941' N	**Long**	9 42.1240' W
Description	Recovery: 1.14m. Not opened, stored in freezer.						
Anticipated testing	CNS analysis (DCU), bulk stable carbon (DCU), lipid analysis (DCU)						